QUANTUM CORRECTIONS IN THE COMPUTER SIMULATION OF SIMPLE LIQUIDS AND SOLIDS.

NIGEL CORBIN

ROYAL HOLLOWAY COLLEGE;1982

A thesis submitted for the Ph.D. degree of the University of London.

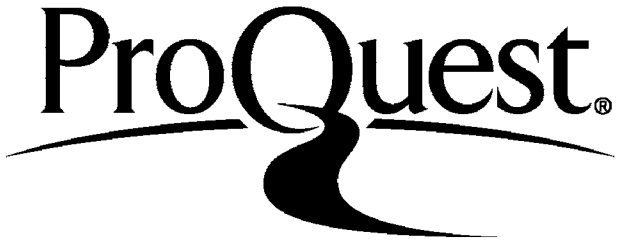

ABSTRACT

A number of methods for the inclusion of quantum effects in the computer simulation of simple systems have been studied. The systems principally studied are fluids such as neon or fluorine, (modelled by simple potentials such as the Lennard-Jones 12-6), for which quantum effects are small, in some sense. These methods all follow the structure of classical Monte Carlo or molecular dynamics methods, to a greater or lesser extent.

The Wigner expansion of the partition function in powers of Planck's constant allows quantum corrections to the free energy to be expressed in terms of classical ensemble averages, which (to order $\hbar^2$) can easily be estimated by classical simulation. The Wigner expansion can be derived from Feynman's path integral formulation of quantum mechanics, which also leads to a number of other methods, all resembling classical Monte Carlo methods. These range from effective, temperature dependent, potentials, to approximate schemes for estimating path integrals.

Since Monte Carlo methods can give no dynamical data, an attempt has been made to represent the solids and liquids of interest as systems of wavepackets, and to derive equations of motion for these using the time-dependent Schrodinger equation.

All of the Monte Carlo methods give results for neon that are in accord with all previous work, while attempts to simulate helium provide an insight into the range of validity of the methods. The wavepacket methods give excellent results for the solid and liquid states of neon.

CONTENTS

Tables:-

4.2 Results obtained by scaling data from Table 2.1 with effective Lennard-Jones parameters.

4.3 Results obtained for the 2-centre Gaussian model of fluorine, using an effective potential.

4.4 Results obtained for the Lennard-Jones fluid using the method of Stratt and Miller:

4.5 As 4.4, but using the Gaussian potential.

a) Neon, 32 atoms

b) Neon, 108 atoms

c) Helium, 32 atoms

4.6 Results obtained for the fourier series method.

5.1 Results obtained for a system of 108 harmonic oscillators using Heller's first method.

5.2 Results obtained for Lennard-Jones solids, using Heller's first method:

a) Argon, c.10 K

b) Neon, c. 2 K

c) Neon, c. 1 K

5.3 Results obtained for solid Neon, using the Gaussian potential, and Heller's second method.

5.4 As above, but using the first method.

5.5 Results obtained for the gaussian potential using the second method:.

a) Neon

b) Helium

6.1 Derivatives of the free energy correction, obtained from a least squares fit, and related thermodynamic properties.

a) Lennard-JonessNeon

b) Gaussian Neon

6.2 Quantum-classical differences obtained using effective and classical potentials.

6.3 Results obtained for Neon, using the Gaussian potential, by all of the methods described above.

List of Figures:-

5.2 Internal energy of neon crystal, as obtained by the first method for the Lennard-Jones potential, and the second method for the Gaussian potential.

5.3 Single particle density matrices for neon and helium, as obtained from the second method.

5.4 Radial distribution function for argon, as estimated by the second method.

5.5 As 5.4, but neon.

6.1 Temperature dependence of the quantum correction to pressure, as obtained by least squares fitting.

6.2 As 6.1, but volume dependence.

6.3 As 6.2, but internal energy.

6.4 Potential energy expectation for two atoms, obtained from Heller's second method, with the original potential for comparison.

6.5 Comparison of the effective analogue of the gaussian potential with the original, (as used in 6.4).

Acknowledgements:

My thanks to Professor Konrad Singer for suggesting this work, and for his advice and encouragement during its execution. All of my colleagues have offered much encouragement, and many suggestions, throughout the work, and I should like to thank especially David Fincham, Nicole Grant, and C.S.Murthy.

I wish to thank the S.E.R.C. for a studentship, and the University of London Computer Centre for a generous allocation of computer time. I acknowledge the use of the CERN, DIMFILM, and NAG subroutine libraries at ULCC.

1. Introduction

Real liquids are very complex many body systems indeed, with no obvious simple approximation that enables even a simple model of their properties to be derived. The interparticle interactions cannot be neglected, or taken to involve only infrequent collisions between widely separated atoms, as they can be in simple models of gases and other similarly dilute systems. Liquids also lack the symmetry of crystals, and so are not amenable to lattice dynamical calculations, normal mode analysis, and such solid state techniques.

Liquids are, however, extremely important physical systems, with virtually every process on earth dependent on their properties. Liquid water is the medium in which all of biochemistry takes place, for instance. Water also happens to be one of the more complicated of all liquids, and certainly not the simple system with which any study of liquids must start.

The study of simple liquids has increased very much in recent years, with ideas developing from hard sphere models in the 1950's , through atomic fluids modelled by simple potentials such as that of Lennard-Jones, to the present day models of molecular fluids using potentials that have been fitted to accurate ab initio calculations, or accurate experimental data, or even both. Theoretical approaches have one crucial drawback, however. It is not possible to separate the effects of the potential used from those of the approximations inherent in the theory.

For example, an attempt to model argon by assuming a Lennard-Jones potential and using some integral equation might disagree with experiment either because the potential was not representative of argon, or because the integral equation was not exact.

With the advent of fast electronic computers, it has become possible to make direct computer simulations of a liquid, assuming only the potential acting in the system, These simulations are essentially exact, and so can be used to check the validity of more theoretical approaches. The validity of the model potential used can be checked by comparing the simulation results with experiment, and the accuracy of any integral equation, etc. can be checked by comparison with the simulation for the same model.

The first simulations were of the hard sphere system, but the systems studied have become more complicated as the computers used have increased in power. Recent work includes molecular fluids such as water, aqueous solutions, ionic melts, and much more.

All of this work, however, assumes a framework of classical mechanics, Indeed, most non-simulation work also uses this framework. The use of classical mechanics is an approximation that may be seriously in error for systems composed of light atoms at low temperature. The most obvious possible example is liquid Helium, which quite certainly cannot be described by classical mechanics. Quantum mechanical effects are dominant in its behaviour. Other fluids would show lesser effects, examples being Hydrogen and Neon. Very little work has been done on the inclusion of quantum effects in computer simulations of

simple liquids such as these. It is the aim of this work to study various ways of including these effects in simulations, and to draw some conclusions about their importance. The systems studied will for the most part be atomic fluids, but some will be diatomic.

The quantum effects can be grouped into two classes, those due to interference effects, and those due to the exchange of identical particles. The first relates to the Heisenberg uncertainty principle, the second to the Pauli exclusion principle. These last are very small in the systems to be studied in this work,,and will be neglected. They are important in liquid helium only at very low temperatures, and for systems involving very light particles such as electrons. The importance of the interference effects may be assessed by comparing the De Broglie wavelength with the interparticle separation. If the De Broglie wavelength is not negligible compared with the separation, then interference effects may be of significance. The dimensionless ratio of the two is often quoted as a measure of the importance of these effects, and is often called the De Boer parameter, Λ. There is no particular definition of this quantity; the values tabulated below were obtained from the formula

$$\Lambda^2 = \hbar^2/m\epsilon\sigma^2$$

where m, ϵ, and σ are the mass and Lennard-Jones potential parameters appropriate to the system. Generally the characteristic mass,energy and length associated with the system may be used.

Before considering the inclusion of quantum effects in computer simulations, the two basic classical simulation techniques must be understood. A brief discussion of the two methods is given in chapter 2. These methods are very different in their approach. The Monte Carlo method is, most generally, a way of estimating the value of a multiple integral, such as those arising in statistical mechanics. It uses essentially statistical averaging techniques. The molecular dynamics method, on the other hand, estimates expectation values by averaging over a sufficient part of the history of the system, obtained by numerically solving the equations of motion that govern the system, along one trajectory in phase space. This means that time dependent properties are available for study, which is a definite advantage of the molecular dynamics method.

In passing, it may be noted that the methods described for Monte Carlo simulation of liquids at finite (non-zero) temperature can also be used for ground state calculations for liquid helium, for instance. Since this technique is restricted to the ground state, it will not be discussed further. There is a more sophisticated Monte Carlo method, Green's Function Monte Carlo, that does not require an initial form for the wavefunction. This method has so far only been applied to ground state properties, but can be extended to non-zero temperature. A recent review of both approaches is contained in (28). Since the aim of this work is to extend classical simulation methods into the regime where quantum effects are small, but not negligible, rather than to carry out totally quantum calculations, this work will not be described further.

The easiest approach to the inclusion of quantum effects is to calculate some form of correction in the course of a classical simulation. That is, seek some A_n such that:

(i) the A_n are classical ensemble averages,

(ii) the true quantum results are given by

$$A = A_o + \sum \hbar^n A_n$$

(iii) this series converges sufficiently rapidly.

Such a series expansion, originally due to Wigner, is the subject of chapter 3.

Another simple approach, suggested by the Wigner method, is based on the replacement of the true potential by some effective, temperature dependent, potential. It transpires that such an effective potential can easily be derived by arguments based on Feynman's path integral formulation of quantum mechanics. This formulation leads to several further ways of including quantum effects in simulations, and these are all described in chapter 4.

Finally, in chapter 5 we describe methods that depend on an approximate solution of the time dependent Schrodinger equation, to give a computation that resembles classical molecular dynamics. There are two approximations to be made in this work. Firstly, some form must be assumed for the wavefunction, and secondly, some approximations are required to derive a set of equations of motion that can be numerically solved. These may or may not resemble their classical counterparts.

1.1 The potentials used.

All of the work to be described below has used one of two potentials. The Lennard-Jones 6-12 potential

$$u(r) = 4\varepsilon\{(\sigma/r)^{12} - (\sigma/r)^{6}\} \qquad (1.1)$$

has long been used as a simple representation of the interaction between inert gas atoms, or similar near-spherical particles. The parameters ε,σ that have been used are given in Table 1. These have generally been obtained by fitting to experimental virial or viscosity data. As an alternative to this potential, a simple sum of two gaussians has been used;

$$u(r) = A_1 \exp(-B_1 r^2) - A_2 \exp(-B_2 r^2) \qquad (1.2)$$

It is possible to choose the parameters such that this form approximates the Lennard-Jones potential. (1). However, this form is used primarily as a convenience, since it has no singularity at r=0. No attempt has been made to fit the four parameters in (1.2) to any experiment, the parameters used have been taken from (1), or scaled by the Lennard-Jones parameters from the values in (1). Any agreement with experiment is thus slightly fortuitious, and could probably be improved if the parameters were to be fitted in the usual way.

Throughout this work the classical hamiltonian has been assumed to have the form

$$H = \sum_i p_i^2/2m + \sum_{i<j}\sum u(r_{ij}) \qquad (1.3)$$

The potential has thus been assumed pairwise additive, neglecting three body interactions.

Table 1. Parameters used in the simulations.

a. Atomic fluids

System:	Helium	Neon	Argon
atomic mass/	.06648	.33504	.66335
L-J $\varepsilon/10^{-22}$J	1.4109	5.0804	16.538
L-J $\sigma/10^{-10}$m	2.556	2.79	3.405
A_1 /10^{-17}J	.2046	.737	2.401
B_1 /10^{21} m ^{2}	.1389	.116	.0783
A_2 /10^{-20}J	.0778	.280	.912
B_2 /10^{20} m ^{2}	.1881	.158	.106
De Boer Λ	1.06	.23	.074

b. Diatomic fluids

System:	Fluorine
atomic mass/10^{-25} kg	.31551
L-J $\varepsilon/10^{-22}$ J	7.28
L-J $\sigma/10^{-10}$ m	2.825
A_1 /10^{-17} J	1.057
B_1/ 10^{21} m^{-2}	.113
A_2 /10^{-20} J	.402
B_2 /10^{20} m^{-2}	.153
bond length/10^{-10} m	1.426

This data has been taken from refs. 2,15.

2. Classical simulation techniques.

The techniques used for the classical simulation of fluids have largely been developed in parallel with the large computers which they require. There are many good reviews of these techniques, (3), and so only briefdetails will be given here. The two approaches differ very much, and will thus be described separately.

2.1 Monte Carlo methods.

These methods are so called because they depend on the statistical properties of random numbers, in exactly the manner of games of chance. The name is generally applied to any method that estimates some quantity by using large quantities of random numbers having specified properties. The method was developed for calculations connected with the behaviour of neutrons in reactors, but has since been widely used in other fields.(4). It provides the only means, generally, for estimating the value of multiple integrals, especially when the number of dimensions is large. Such integrals arise in the statistical mechanics of liquids.

Consider a system with Hamiltonian given by (1.3). Here the $\underline{p}_i$ are the momenta of N atoms, labelled 1,...,N, and r_{ij} is the distance between atoms i and j, $|\underline{r}_i - \underline{r}_j|^2$, at positions $\underline{r}_i$ and $\underline{r}_j$. For a system of N atoms there are 6N coordinates. The expectation value of any property $A(\underline{r})$ (we write $\underline{r}$ as shorthand for the 3N dimensional vector of coordinates) can be written as an integral over these 6N variables:-

$$\bar{A} = \frac{\int A(\underline{r}) \exp(-\beta H(\underline{r},\underline{p}))\, d\underline{r}\, d\underline{p}}{\int \exp(-\beta H(\underline{r},\underline{p}))\, d\underline{r}\, d\underline{p}} \qquad (2.1)$$

If we wish to deal with a bulk system, then N will be of the order of 10^{23}, which is clearly quite impossible. For N of the order of 100-1000, however, this is quite feasible if the method of Metropolis et.al. (5) is used. In fact the problem can be simplified, because the form of the Hamiltonian allows the momentum integrals to be performed analytically. Provided that A is a configurational property, independent of the momenta, this leads to the result

$$\langle A \rangle = \bar{A} = \frac{\int A(\underline{r}) \exp(-\beta U(\underline{r}))\, d\underline{r}}{\int \exp(-\beta U(\underline{r}))\, d\underline{r}} \qquad (2.2)$$

where $U(\underline{r})$ is the potential. This simplification is not always available. The expression in the denominator of (2.2) is just the configurational partition function, Q. The configurational properties of most interest are the internal energy, and pressure. These are defined in terms of the partition function by the usual relations of statistical mechanics.

$$U = kT^2 \left(\frac{\partial \ln Q}{\partial T}\right)_V$$

$$P = kT \left(\frac{\partial Q}{\partial V}\right)_T \frac{1}{Q}$$

The configurational internal energy is thus easily shown to be given by (2.2), with $A \equiv U$. The pressure is not so easily obtained, but a volume scaling device gives the result

$$PV = RT - 1/3 \left\langle \sum_{i<j} \sum r_{ij} \frac{du(r_{ij})}{dr_{ij}} \right\rangle$$

for a pairwise additive potential. The quantity in the angular brackets is the virial, which will be denoted by

Φ. These integrals are just expectation values over a probability distribution function $P(\underline{r})$, given by

$$P(\underline{r}) = \exp(-\beta U(\underline{r})) / Q$$

which is a function of 3N coordinates, or 6N, should the momenta not separate out. It is possible, and usually convenient, to define one-body, two-body, etc, functions by integrating out most of the variables. Integrating over all coordinates gives simply that the probability distribution is normalised. Integration over the 3N-3 coordinates of all but one atom leads to the probability of finding an atom in a given place, which is clearly the density. The second such distribution function is the radial distribution function, g(r), defined by

$$g(r) = \frac{V^2 \int \exp(-\beta U(\underline{r}))\, d\underline{r}_3 \ldots d\underline{r}_N}{\int \exp(-\beta U(\underline{r}))\, d\underline{r}_1 \ldots d\underline{r}_N}$$

It is essentially the probability of finding two atoms separated by a distance r. Higher functions can be defined similarly, but are not usually needed. If the potential is pairwise additive, then all of the configurational properties of the system can be expressed in terms of g(r). For instance,

$$U = 2\pi N_o^2/V \int u(r)\, g(r)\, r^2\, dr \qquad (2.3)$$

$$\Phi = 2\pi N_o^2/V \int u'(r)\, g(r)\, r^3\, dr \qquad (2.4)$$

where the prime denotes the derivative.

All of the above refers to atomic systems only, since the orientation of molecules must also be taken into account, which considerably complicates matters. The radial distribution function can be generalised in a number of ways. It could be represented as a function of both centre-of-mass separation and relative orientation,

and since this is not a simple representation, expanded in spherical harmonics. Alternatively, the orientational dependence could be averaged out, giving essentially the probability of finding two molecules with a given centre-of-mass separation, and no information about their orientation.

Instead of using the centre-of-mass separation, the separations between interaction sites can also be used. There may be several site-site correlation functions if the molecules are heteronuclear.

Corresponding to the choice of site-site or c-o-m separations and pair correlation functions, there is a choice of cutoff scheme, since interactions can be cut off if either the site-site distance is above a certain limit, or if the c-o-m distance exceeds this limit. The two are clearly different, and lead to different long range corrections. In this work, a site-site cutoff has been used, with the expressions for virial, long range correction, etc given by (15).

The Metropolis algorithm is quite simple to implement, with due care. A system of N atoms is considered, within a cubic box of side L. Since the inert gases have face centred cubic crystal structures, this box is constructed as some multiple of the unit cell, and so N conveniently takes values of the form $4m^3$, for some integer m. In this work N=32 or 108. These values of N are hardly large enough to qualify as 'bulk', and so a system of periodic boundary conditions is used, with all space filled with replicas of the fundamental box. Thus if an atom has

position $\underline{r}$, then there are images of it at $\underline{r} + \underline{m}L$, where $\underline{m}$ is a vector having integer components. This device also keeps all N atoms within the box, in the sense that an atom leaving one face of the box is replaced by the image entering through the opposite face.

When evaluating the interactions between the atoms, we clearly do not wish to consider an infinity of pairs, and so adopt the minimum image convention , whereby each atom interacts only with the nearest image of the other N-1. This neglects interactions between atoms separated by a distance greater than L/2. In this work, all such terms have been neglected, that is, no interactions over larger distances than L/2 have been included.

The simulation starts by setting the coordinates of all atoms to form a face-centred cubic lattice, and summing all pair interactions to obtain the total potential energy. Any other quantities may also be calculated, of course. One of the atoms is then chosen, either randomly or by some rule, and given a small random displacement, such that its final position is uniformly distributed in a small cube centred on its initial position. The size of this cube is a parameter of the method. The change in energy resulting from this move is calculated, and used* to decide whether or not the move should be allowed. If the move is not allowed the atom is returned to its initial position. The total potential energy is then updated to reflect the current positions of all atoms, along with any other quantities being calculated. Another atom is then chosen, and the procedure repeated many times. Usually

*See appendix II.

the size of the small cube is chosen such that about 50% of the moves are allowed, and the number of moves attempted is large enough for all atoms to move several times each. The desired expectation values are estimated by the averages over all moves made. The procedure is exact in the limit of a large number of moves.

It might be expected that computational efficiency could be improved if all of the atoms were displaced at each move, rather than one. This is not the case, as may easily be shown. If the algorithm for moving one atom is set such that about 50% of moves are allowed, and the same algorithm is used to displace all of the N atoms in each move, then the probability of accepting the move will be of the order of 0.5^N, which is very small. In fact the small cube within which the new position of an atom lies becomes very small, if the probability of accepting a move is kept near 50%, and the method is very inefficient.

In the last few years, a variety of different methods of biasing Monte Carlo calculations have been proposed, (29). These generally bias the moving of each particle by using the forces (and torques) acting on it. These are not normally calculated in the usual algorithm described above, and so there is some additional computation involved.*

In order to compare these biased methods with the usual form, some quantitative measure of the efficiency of the methods must be defined. The simplest such measure is the rms distance moved per particle, per move. The larger this is, the better. The computer time used will suffice as a measure of the computational effort involved.

*See appendix II

Using this measure, it has been found that the "Smart" method leads to a larger rms displacement than the usual method, for a given acceptance ratio. Under optimum conditions for each method, the biased algorithm is about 30% more efficient. However, it also requires about 30% more computer time, and so offers no great advantage. These tests, however, were carried out only for atomic liquids, and this conclusion may not hold in molecular fluids.

The progress of these calculations is monitored by calculating subaverages over blocks of moves. Care must be taken with these, since the results of each move are highly correlated with those that preceeded it. The subaverages must be taken over sufficient moves that successive subaverages are uncorrelated. Since the initial lattice may have a distorting effect on the averaging, the first moves made are discarded, until all traces of the lattice have disappeared. This equilibriation, which may take many moves, is continued until the subaverages show no steady trend; in this work at least the first 50000 moves were discarded. Of course, the calculation need not start from a lattice, any configuration can be used provided that a sufficient number of moves are used to equilibriate the system.

The accuracy of the final average can be estimated in several ways, none of which is particularly reliable. The spread in the subaverages gives some information, but the most reliable method is to repeat the entire calculation using different random numbers. This is computationally expensive, and so not applied to many of the simulations.

It is possible to correct the estimated potential energy, etc. for the effects of the cutoff by assuming that the fluid may be replaced by a continuum beyond the cutoff distance. This is not likely to be correct either for solids, or for very small systems, but is a very good approximation for larger systems. Such corrections will be included in all results quoted, even when they are not likely to be correct. The precise form of the corrections to the potential and virial are given by (2.3,2.4), with the lower limit of the integration at the cutoff distance, and g(r) = 1, that is

$$U_L = 2\pi N_o^2/V \int_{r_c}^{\infty} u(r)\ r^2\ dr$$

$$\Phi_L = 2\pi N_o^2/V \int_{r_c}^{\infty} u'(r)\ r^3\ dr$$

The method has been applied to the Lennard-Jones fluid, with parameters appropriate to either helium or neon, for systems of 32 or 108 atoms. The potential energy and virial obtained are tabulated below. The pressure can be obtained by using the virial with the result given above. It should be noted that this result is a special case of a more general result, (10),

$$PV = 2/3\ \overline{K} - 1/3\ \overline{\Phi}$$

where $\overline{K}$ is the average kinetic energy; since this is known classically to be 3RT/2, the result given above is clear. Quantum mechanically, $\overline{K}$ is bounded below by 3RT/2.

During these simulations the radial distribution function has also been calculated. This function is the probability distribution for the atomic separation, and so can be calculated by accumulating a histogram of the interatomic distances. In this work the interval (0,L/2)

has been divided into 150 equal parts, and a count kept of the number of interatomic distances within each part. Examples of g(r) for both 32 and 108 atom simulations are given in Fig.1, for the same state point.

The same method has been applied to the Gaussian fluid, giving the results in Table 2.2 below. All of these results were obtained using a 108 atom system. Fig.2 shows one of the radial distribution functions obtained, along with one of the corresponding Lennard-Jones results.

The method can be applied to molecular systems with no great difficulty. At each step the orientation of the chosen molecule must be changed, as well as its position. In this work, this change of orientation was carried out by choosing one of the coordinate axes, randomly, and rotating the molecule about this axis, through an angle chosen at random within a small interval. The size of this interval is a second parameter of the method. In the simulations of fluorine that have been carried out using this method, the atom-atom pair correlation function has been calculated in exactly the same fashion as given above for the atomic fluid. The potential energy, virial and pressure obtained for the 2-centre model of fluorine using the gaussian potential are given in Table 2.3, for a number of state points.

The results for the solid state points in Table 2.1 show clearly the discrepancy between the 32 and 108 atom simulations, especially in the virial. In the liquid state, however, there is good agreement, confirmed by the similarity between the radial distribution functions in Fig.1.The estimated error in the potential energy is about

Table 2.1 Results obtained by classical Monte Carlo for the Lennard-Jones fluid.

a. 32 atoms, Neon

$V/(cm^3 mol^{-1})$	T/K	$PE/Jmol^{-1}$	$\Phi/Jmol^{-1}$	P/MPa
16.5	25	-1774	1700	-22
	30	-1739	1067	-6.4
	35	-1687	113	15
17.0	25	-1709	1616	-19
	30	-1686	1271	-10
	35	-1642	419	9
17.5	25	-1669	1924	-25
	30	-1636	1420	-13
	35	-1598	682	4
18.0	25	-1620	2133	-28
	30	-1587	1586	-15
	35	-1563	1227	-6
	"	-1556	977	-2
18.5	25	-1584	2392	-32
	30	-1547	1804	-19
	35	-1511	1111	-4
15.0	15	-2149	4360	-89 *
	20	-2104	3543	-68 *
15.5	15	-2071	4569	-90 *

* These are solid state points.

b. 108 atoms, Neon

V	T	PE	Φ	P
16.5	25	-1775	1587	-19
	30	-1732	826	-2
	35	-1694	181	14
	40	-1664	-341	27
17.0	25	-1721	1767	-22
	30	-1684	1098	-7
	35	-1651	524	7
	40	-1617	-81	21
	45	-1587	-605	34
	50	-1552	-1192	48
17.5	25	-1672	1990	-26
	30	-1640	1314	-11
	35	-1605	738	2
	40	-1573	181	15
18.0	25	-1624	2067	-27
	30	-1594	1517	-14
	35	-1564	933	1
	40	-1534	475	10
18.5	25	-1584	2089	-26
	30	-1551	1544	-14
	35	-1520	1073	-4
	40	-1492	635	7
19.0	45	-1432	390	13
	50	-1408	9	22

b,continued

V	T	PE	Φ	P
21.0	45	-1301	742	6
	50	-1277	590	10
23.0	45	-1182	976	2
	50	-1167	713	8
15.0	15	-2129	4086	-82 *
	20	-2080	3154	-59 *
15.5	15	-2054	4315	-84 *

* These are solid state points.

c. 108 atoms, helium

V	T	PE	Φ	P
22	12.5	-268	322	0
	15.0	-263	199	3
23	12.5	-255	315	0
	15.0	-249	212	2
24	12.5	-247	271	1
	15.0	-236	230	2
25	12.5	-242	283	0
	15.0	-232	214	2
26	12.5	-232	277	0
	15.0	-218	233	2

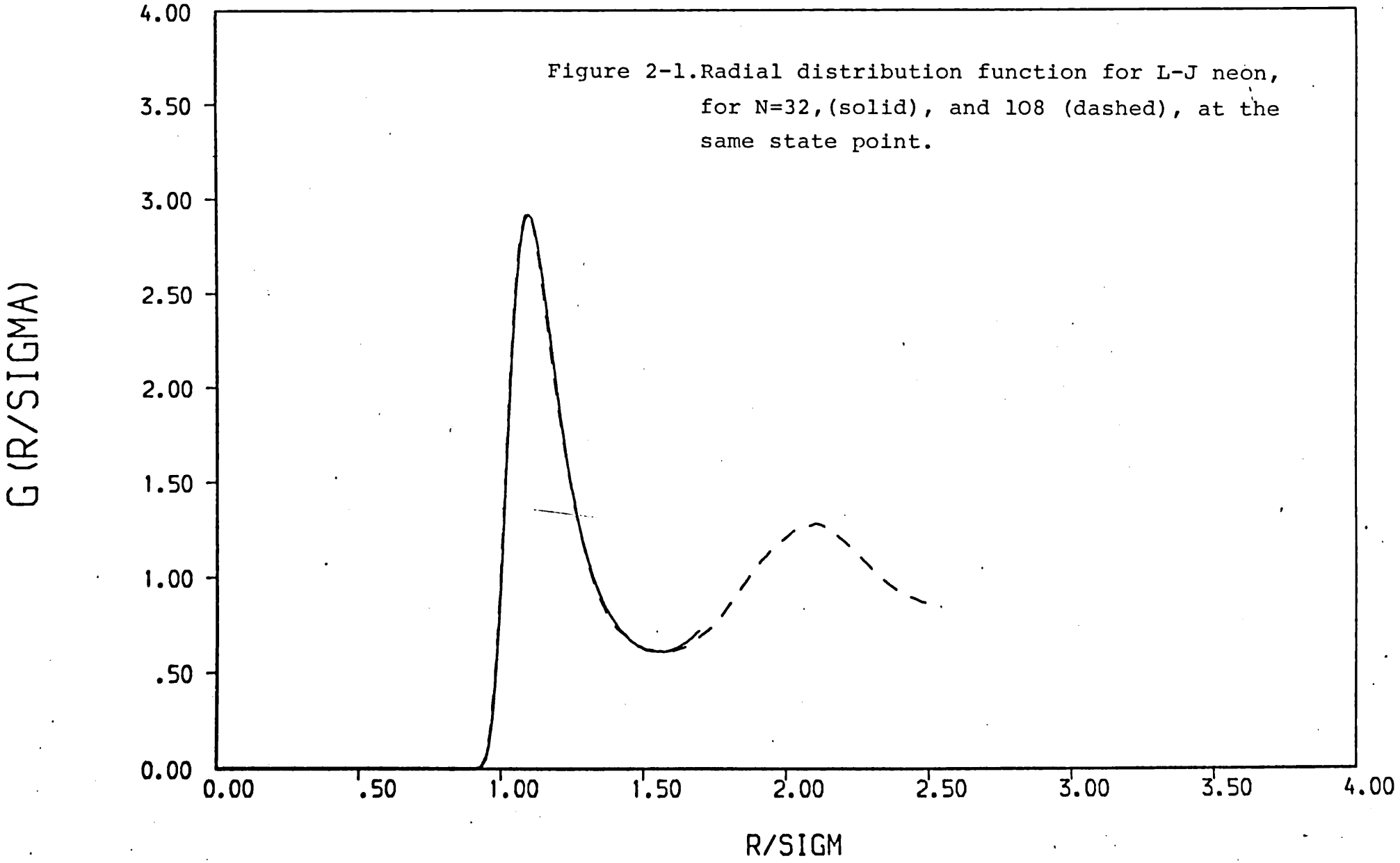

Figure 2-1. Radial distribution function for L-J neon, for N=32, (solid), and 108 (dashed), at the same state point.

Table 2.2 Results obtained by classical Monte Carlo using the Gaussian potential.

V/cm^3mol^{-1}	T/K	$PE/Jmol^{-1}$	$\Phi/Jmol^{-1}$	P/MPa
16.5	25	-1589	805	-4
	30	-1551	52	14
	35	-1527	-369	25
	40	-1485	-1139	43
17.0	25	-1554	1241	-12
	30	-1513	440	6
	35	-1478	-173	21
	40	-1450	-681	33
	45	-1426	-1095	44
	50	-1396	-1680	57
17.5	25	-1510	1448	-16
	30	-1468	601	3
	35	-1441	152	13
	40	-1414	-345	26
18.0	25	-1463	1440	-15
	30	-1434	953	-4
	35	-1403	281	11
	40	-1376	-175	22
18.5	25	-1431	1711	-20
	30	-1397	1212	-8
	35	-1365	440	8
	40	-1341	41	17
19.0	45	-1278	-319	25
	50	-1262	-566	32

b. 108 atoms,Helium

V	T	PE	Φ	P
22	12.5	-237	227	1
	15.0	-234	127	4
23	12.5	-244	160	2
	15.0	-240	138	3
24	12.5	-224	222	1
	15.0	-214	154	3
25	12.5	-214	222	1
	15.0	-211	141	3
26	12.5	-205	242	1
	15.0	-198	183	2

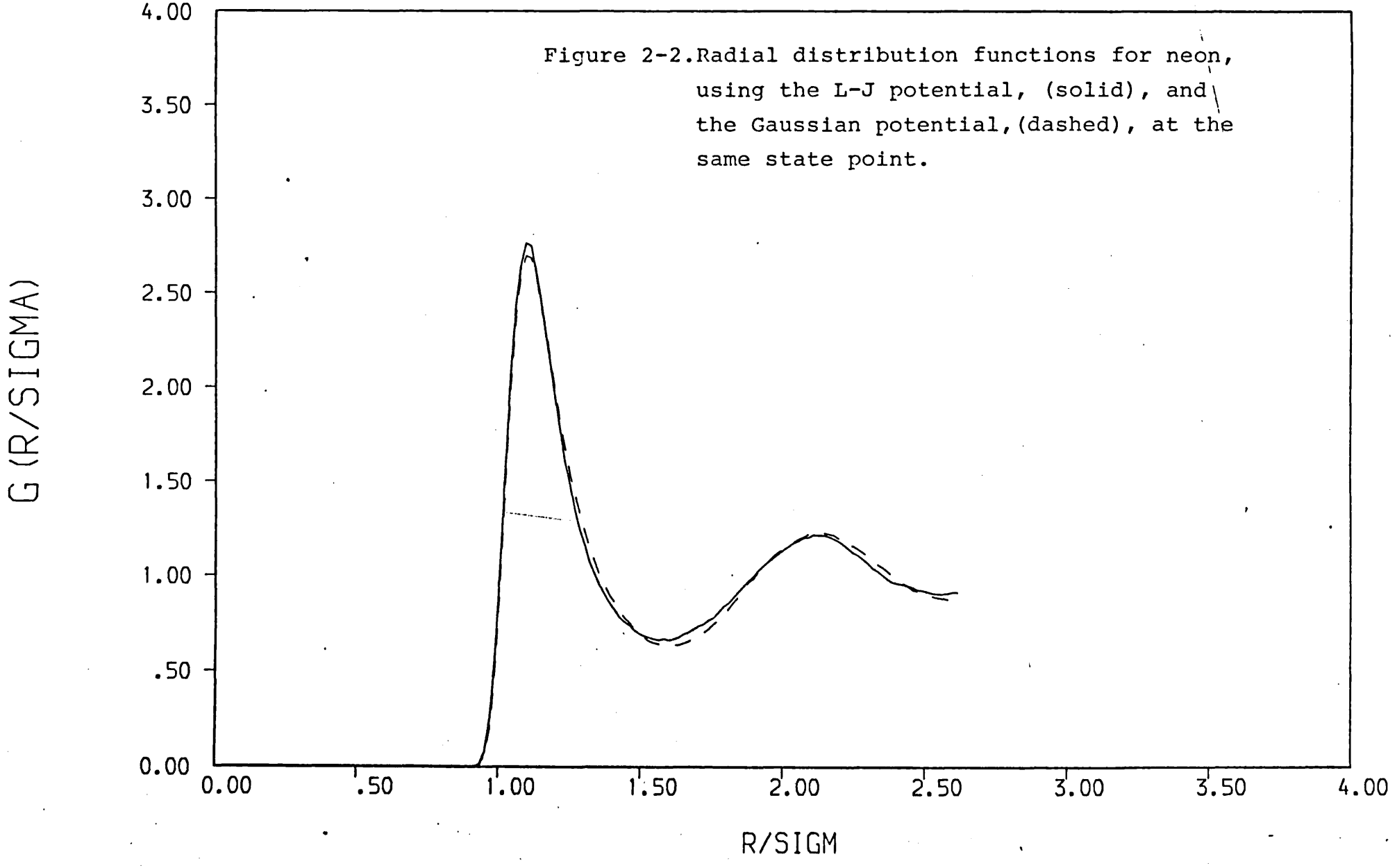

Figure 2-2. Radial distribution functions for neon, using the L-J potential, (solid), and the Gaussian potential, (dashed), at the same state point.

Table 2.3 Results obtained by Monte Carlo simulation of Fluorine using a 2-centre Gaussian potential.

V/cm^3mol^{-1}	T/K	$PE/Jmol^{-1}$	$\Phi/Jmol^{-1}$	P/MPa
22	50	-6469	3921	-40
	60	-6365	1165	5
	70	-6309	142	24
	"	-6280	-72	27
24	50	-6028	8573	-101
	60	-5919	6729	-72
	70	-5823	5486	-52
26	50	-5528	9576	-106
	60	-5475	8422	-88
	70	-5345	6639	-62
28	50	-5316	8562	-87
	60	-5072	7822	-75
	70	-4940	7366	-66
	80	-4893	6388	-52

1% in the worst case, and usually less than this. The error in the virial is considerably larger. This estimate is based on the behaviour of subaverages over blocks of 10000 moves, and on the agreement between 300000 move simulations that used different starting configurations, random numbers, and displacement parameters. Note that the standard deviation of the potential energy, as found from the square mean and the mean square, is not useful as a measure of accuracy.

2.2 Molecular dynamics methods.

These methods follow the time evolution of a system, rather than using statistical techniques to generate an ensemble average. The approach has the advantage that dynamical properties, such as diffusion, can be studied at little extra computational cost. The system is defined by specifying the coordinates and momenta of each atom or molecule initially, and then solving equations of motion to determine the positions and momenta at future times. These equations of motion are usually taken as Hamilton's equations,

$$\dot{\underline{r}} = (1/m)\ \underline{p}$$

$$\dot{\underline{p}} = -\ \underline{\nabla} U$$

where $\underline{r},\underline{p}$ are the 3N dimensional vectors of coordinates and momenta, respectively. The dots indicate time derivatives, U is the potential, here assumed pairwise additive, and m is the atomic mass. This is a system of 6N first order differential equations, which can be numerically solved by a variety of well-known methods, (6).

The same boundary conditions and potential cutoff are used as in the Monte Carlo method already described. In this method, however, the momenta of the particles, as well as their positions, must be set initially. This has been done by choosing the momenta from the normal distribution appropriate to the desired temperature, with the constraint that the total momentum be zero. Initial positions are set on a face-centred cubic lattice, as before. The energy required to melt this lattice is fed into the system by scaling the momenta at intervals in the course of the first steps. When the system is sufficiently equilibriated, as judged by subaverages, this scaling is discontinued, and averages are accumulated over several thousand steps.

The solution of the equations of motion is carried out using a timestep of between 1 and 10 fs, depending on the system being studied. The accuracy of the solution can be monitored by looking at the total energy, which ideally should be conserved exactly. Any change in total energy should be less than about 1 part in 10^4, and may well be less than this in some cases.

The differences between this method and the Monte Carlo method described above are thus quite considerable. The Monte Carlo method generates canonical ensemble averages, while the molecular dynamics method leads to averages in the microcanonical ensemble. There are variants of both methods which provide other ensemble averages, these are described in the reviews (3), and have not been used in this work.

The molecular dynamics method has been applied to atomic systems only as a check on the Monte Carlo calculations, which required the writing of totally new programs. Those results that were checked agreed well. In the case of diatomic systems, the method has been applied to the 2-centre Lennard-Jones model of fluorine. The method has to be extended to deal with the rotation of the molecules, which requires some care. Details are given in (15). The method used has also to deal with the constraint imposed by rigidity of the molecule. The results obtained are given in the table below. They were obtained from 3000 steps of 10 fs, after the system had been equilibriated. The system consisted of 108 molecules, 256 being used as a check at one state point only. The site-site pair correlation function was calculated during the course of these simulations, and one of the results is shown in fig. 3, along with one obtained by Monte Carlo for the 2-centre Gaussian potential.

The results obtained have been checked against those in (15), as far as possible. In all cases good agreement has been obtained.

Table 2.4 Results obtained by Molecular dynamics simulation of F_2 using a 2-centre Lennard-Jones potential.

V/cm^3mol^{-1}	T/K	$PE/Jmol^{-1}$	$\Phi/Jmol^{-1}$	P/MPa
24	58.1	-6592	5057	-50
	70.5	-6444	2109	-5
	76.6	-6378	813	15
	91.1	-6227	-2238	63
25	63.6	-6271	5548	-53
	76.7	-6136	2799	-12
	92.1	-5987	-186	33
	92.8	-5986	-136	32
26	48.1	-6181	9719	-109
	62.5	-6038	7065	-71
	90.5	-5788	2157	1
27	58.8	-5843	8063	-81
	69.7	-5741	6783	-62
	78.5	-5662	5142	-39
	92.9	-5556	3040	-9

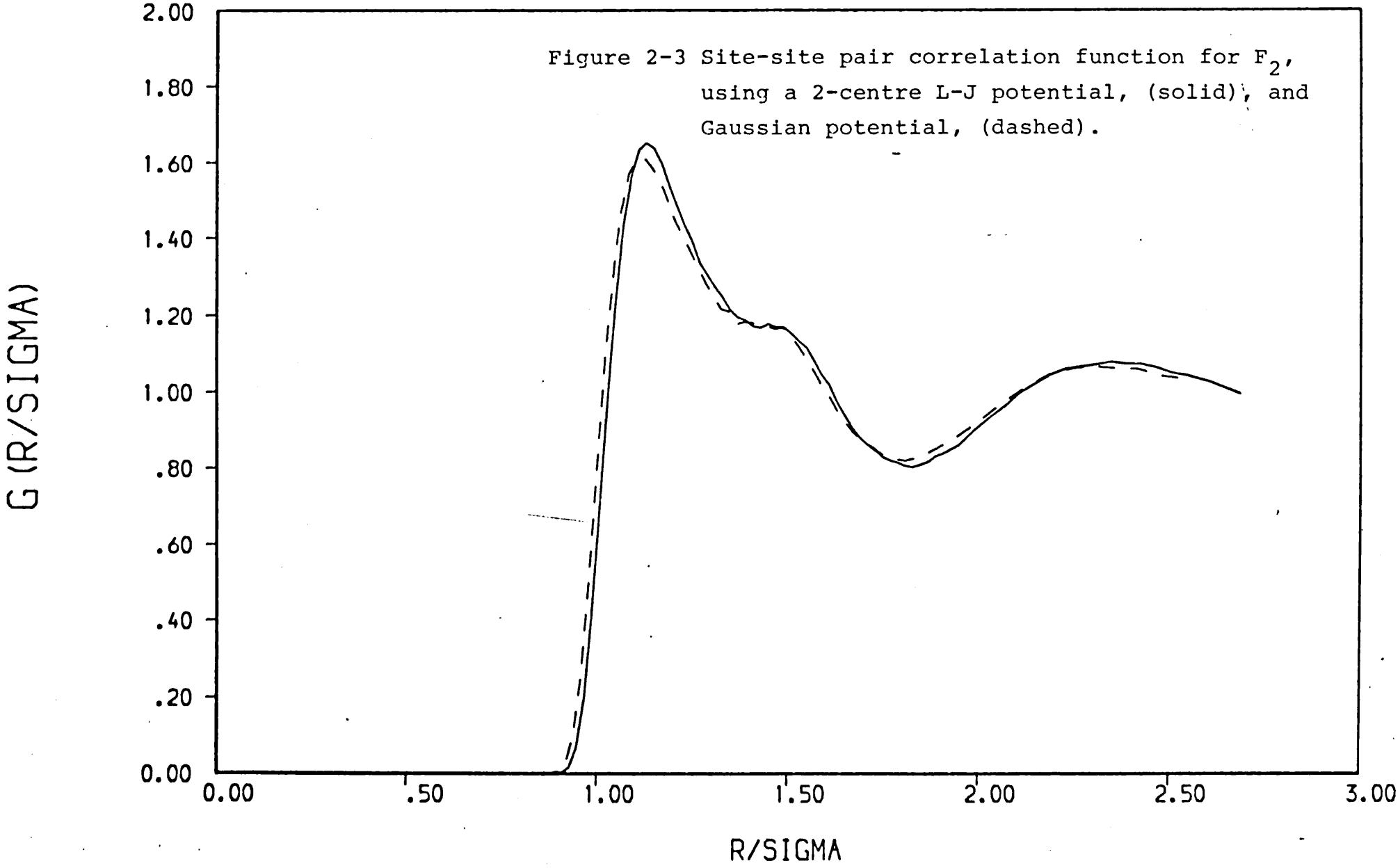

Figure 2-3 Site-site pair correlation function for F_2, using a 2-centre L-J potential, (solid), and Gaussian potential, (dashed).

3. The Wigner expansion.

The classical form of the expectation value (2.2) given in the previous chapter does not carry over into quantum mechanics, unfortunately. The uncertainty principle does not allow simultaneous knowledge of the position and the momentum, so we cannot ask for some function $P(\underline{r},\underline{p})$ such that $P(\underline{r},\underline{p})d\underline{r}\ d\underline{p}$ is the probability of finding the system in a volume element $d\underline{r}\ d\underline{p}$ centred at $(\underline{r},\underline{p})$ in phase space.

Wigner (7) has defined a function $P_w(\underline{r},\underline{p})$ that gives the correct probability distribution for the $\underline{r}$ when the $\underline{p}$ are integrated out, and vice versa. If the system has eigenfunctions $\phi_i(\underline{r})$ with associated eigenvalues E_i, then the density matrix can be written, in the coordinate representation

$$\rho(\underline{r},\underline{r}') = \sum \exp(-\beta E_i)\ \phi_i(\underline{r})\ \phi_i^*(\underline{r}')$$

and in the momentum representation

$$\rho(\underline{p},\underline{p}') = \sum \exp(-\beta E_i)\ \phi_i(\underline{p})\ \phi_i^*(\underline{p}')$$

$$= \int \rho(\underline{r},\underline{r}')\ \exp(-i/\hbar\{\underline{p}.\underline{r} - \underline{p}'.\underline{r}'\})\,d\underline{r}d\underline{r}'$$

The diagonal elements of the density matrix give the probability of finding the system at a particular point in coordinate or momentum space, according to the form used. It is easy to verify that

$$P_w = P_w(\underline{r},\underline{p})$$

$$= \int \rho(\underline{r} + \tfrac{1}{2}\underline{\eta},\underline{r} - \tfrac{1}{2}\underline{\eta})\ \exp(-i/\hbar\underline{p}.\underline{\eta})\,d\underline{\eta}$$

has the property described above. This is not a unique definition of such a function, however.

This function is not itself a probability distribution, since it is not everywhere positive. The expectation of any operator A can be found, provided that A is a linear combination of $\underline{r}$ and $\underline{p}$, or a linear combination of functions of $\underline{r}$ only and $\underline{p}$ only. We have then

$$\bar{A} = \frac{\int A(\underline{r},\underline{p})\ P_w(\underline{r},\underline{p})\, d\underline{r}d\underline{p}}{\int P_w(\underline{r},\underline{p})\ d\underline{r}d\underline{p}}$$

This result is not particularly useful, since P_w is known in terms of the density matrix or the eigenfunctions, and given these the expectation value could be found anyway. In the systems being considered in this work, the eigenfunctions are not known, nor are they likely to be found.

The expansion of P_w in powers of Planck's constant gives rise to a considerable number of useful expressions for dealing with the case of systems with only small quantum effects. Such systems are the principal interest of this work. The first term in these expansions tends to be simple, and successively higher terms become more complicated, being completely intractable after the first few. Each term involves the derivatives of the potential, and their powers. This means that the method cannot be used without modification for systems such as hard spheres, or systems with hard core potentials. The easiest calculations that can be carried out using the method lead to quantum corrections to the second virial coefficient, or directly to free energy corrections.

An expression for the quantum second virial coefficient

is given in (30), along with tables giving the relative magnitudes of different contributions. It is generally the case that corrections due to interference effects involve only even powers of $\hbar$, while those due to exchange effects (here neglected) involve odd powers. Table 3.1 gives this data for helium and neon, as taken from (30). We have

$$B = B_{cl} + (\hbar^2/m)B_1 + (\hbar^2/m)^2 B_2 \pm B_o$$

Here B_o is the contribution from spin effects, its sign depending on whether the system obeys Bose (+), or Fermi (-), statistics. As is clear from the table, this is a negligible effect except at the lowest temperatures. The convergence of the expansion in powers of $\hbar$ is also rapid except at the lowest temperatures, where all terms become equal in magnitude. It is worth noting that the successive terms alternate in sign. For neon at about 35 K, the first correction is of the order of 8% of the classical value, and the second an order of magnitude smaller still.

Table 3.2 contains values for the second virial coefficient, calculated for neon using the equations below,

$$B_{cl} = -2\pi N_o \int (\exp(-\beta u(r)) - 1)\, r^2\, dr$$

$$B_1 = 2\pi N_o \xi \int (\exp(-\beta u(r)) (u'(r)/kT)^2\, r^2 dr$$

where $\xi = \hbar^2/12mkT$, and $B = B_{cl} + B_1$, for both the Lennard-Jones and Gaussian potentials. It can be seen from these results that the corrections for neon are of the order of 10%, and that those for the Gaussian potential are slightly larger than those for the Lennard-Jones.

Table 3.1 Contributions to the second virial coefficient, for the Lennard-Jones system.

	T/K	B^*_{cl}	B^*_o	B^*_1	B^*_2
He^4	27.3	-4.87	0.5	9.16	-4.05
	83.5	8.87	0.093	1.82	-0.19
	256	11.13	0.017	0.48	-0.01
Ne	35.6	-66.2	0.03	3.80	-0.47
	95.0	-6.23	0.007	0.55	-0.01
	392	12.1	0.0008	0.07	0.0

*arbitrary units

Table 3.2 Virial coefficients for neon.

	L-J		Gaussian	
T/K	B^*_{cl}	B^*_1	B^*_{cl}	B^*_1
27.6	-11.37	0.781	-10.19	0.819
46.0	-4.65	0.227	-3.84	0.236
55.2	-3.27	0.156	-2.59	0.162
64.4	-2.36	0.115	-1.76	0.119
73.6	-1.70	0.090	-1.17	0.093

*units of 10^{-5} $m^3 mol^{-1}$

The free energy of a quantum system can be written as a power series in $\hbar$:-

$$A = A_o + \hbar^2 A_1 + \hbar^4 A_2 + \ldots, \qquad (3.1)$$

a result originally due to Wigner (7). It is also an expansion in the derivatives of the potential, and so cannot, for instance, be applied to systems of hard spheres without modification. The method is well described in the literature, (8-12), and so only those results used will be quoted.

The correction of order $\hbar^2$ can be related to the mean square force and torque acting on a rigid molecule (12), and these quantities can be evaluated easily in the normal course of a molecular dynamics simulation. For an atomic fluid the result is:-

$$A_1 = \frac{N_o \overline{F^2}}{24\, m\, k^2 T^2} \qquad (3.2)$$

where $\overline{F^2}$ is the classical mean square force on one atom due to all others. In the case of rigid linear molecules the result also involves the moment of inertia, I, and the mean square torque, $\overline{\Gamma^2}$, with the molecular mass M replacing the atomic mass m.

$$A_1 = \frac{N_o}{24\, k^2 T^2} \left\{ \frac{\overline{F^2}}{M} + \frac{\overline{\Gamma^2}}{I} \right\} - \frac{1}{6I} \qquad (3.3)$$

Once the corrections to the free energy are known, for a range of temperature and molar volume, the corrections to other thermodynamic quantities can be found using the usual thermodynamic relations:-

$$P = -\left(\frac{\partial A}{\partial V}\right)_T \qquad (3.4)$$

$$U = -T^2 \frac{\partial (A/T)}{\partial T} = A - T \frac{\partial A}{\partial T} \qquad (3.5)$$

It is also possible to formulate these results, for atomic fluids, as integrals involving the radial distribution function, g(r). This method has been used by Hansen & Weis (13) for liquid neon near the triple point, and by some others, eg (14). The particular result used is, (9),

$$A_1 = \frac{N_o^2}{24mkTV} \int_0^\infty 4\pi r^2 \nabla^2 u(r)\ g(r)\ dr \qquad (3.6)$$

where g(r) is the radial distribution function, and u(r) is the interatomic potential.

The mean square force (and torque) have been calculated for the atomic systems neon and helium, both using the Lennard-Jones potential, and for the diatomic fluorine, using a 2-centre Lennard-Jones potential. The results obtained are shown in Tables 3.3,3.4, along with the free energy correction obtained via equation 3.2 or 3.3. Some results obtained via (3.6) are also shown, as a check. Table 3.5 contains results obtained via (3.6) for the Gaussian model of helium and neon. These results give free energy corrections that decrease with increasing temperature or molar volume, which is in accord with the expectation that the correction should vanish in the classical limit. Figure 3.1 shows the free energy correction as a function of volume, for several temperatures.

In order to estimate the corrections to the internal

Table 3.3 Mean square force, and free energy corrections for the Lennard-Jones fluid.

$V/ccmol^{-1}$		T/K	$\overline{F^2}/10^{-20}N^2$	$\Delta A/Jmol^{-1}$ (eqn 3.2)	$\Delta A/Jmol^{-1}$ (eqn 3.6)
±6.5	25	25	.148	103	
		30	.192	93	
		35	.250	89	
		40	.303	83	
17.0		25	.138	96	
		30	.184	89	91
		35	.231	82	
		40	.282	77	
		45	.339	73	
		50	.405	71	
17.5		25	.128	89	91
		30	.171	83	83
		35	.217	77	
		40	.266	72	
18.0		25	.121	84	86
		30	.159	77	
		35	.203	72	
		40	.246	67	
18.5		25	.116	81	
		30	.153	74	
		35	.192	68	
		40	.234	64	

Table 3.3, continued

V	T	$\overline{F^2}$	ΔA (eqn 3.2)	ΔA (eqn 3.6)
19.0	45	.263	57	
	50	.311	54	
21.0	45	.221	48	
	50	.255	44	
23.0	45	.190	41	
	50	.223	39	

b. Helium.

V	T	$\overline{F^2}$	ΔA (eqn 3.2)
22.0	12.5	.128	180
	15.0	.172	168
23.0	12.5	.120	169
	15.0	.161	157
24.0	12.5	.121	170
	15.0	.148	144
25.0	12.5	.115	162
	15.0	.141	142
26.0	12.5	.111	156
	15.0	.132	129

Table 3.4 Mean square force and torque, and free energy correction, for F_2, 2-centre L-J potential.

$V/ccmol^{-1}$	T/K*	$\overline{F^2}/10^{-20}N^2$	$\overline{\Gamma^2}/10^{-40}J^2$	$\Delta A/Jmol^{-1}$
24	58.1	1.218	.478	144.51
	70.6	1.623	.634	130.14
	76.6	1.857	.721	125.9
	91.1	2.408	.941	115.5
25	63.6	1.217	.477	120.0
	76.2	1.578	.616	106.4
	92.1	2.037	.796	94.9
	92.8	2.087	.815	95.7
26	48.1	0.736	.289	127.1
	49.1	0.793	.311	131.4
	62.5	1.068	.418	108.8
	90.5	1.756	.682	84.2
27	58.8	0.923	.362	106.1
	69.7	1.145	.450	93.3
	78.5	1.407	.550	90.0
	92.9	1.773	.693	80.8

* The temperature quoted is an average over the molecular dynamics simulation, rather than a fixed parameter as in a Monte Carlo simulation.

Table 3.5 Results obtained for free energy corrections in the Gaussian model of Neon, via eqn. (3.6).

$V/ccmol^{-1}$:	16.5	17.0	17.5	18.0	18.5	19.0	21.0	23.0
T/K								
25	115	104	97	93				
30	106	97	92	86				
35		90	84	80	75			
40	91	84	78	74	70			
45		78				63.5	50	43
50		75				59	49	41

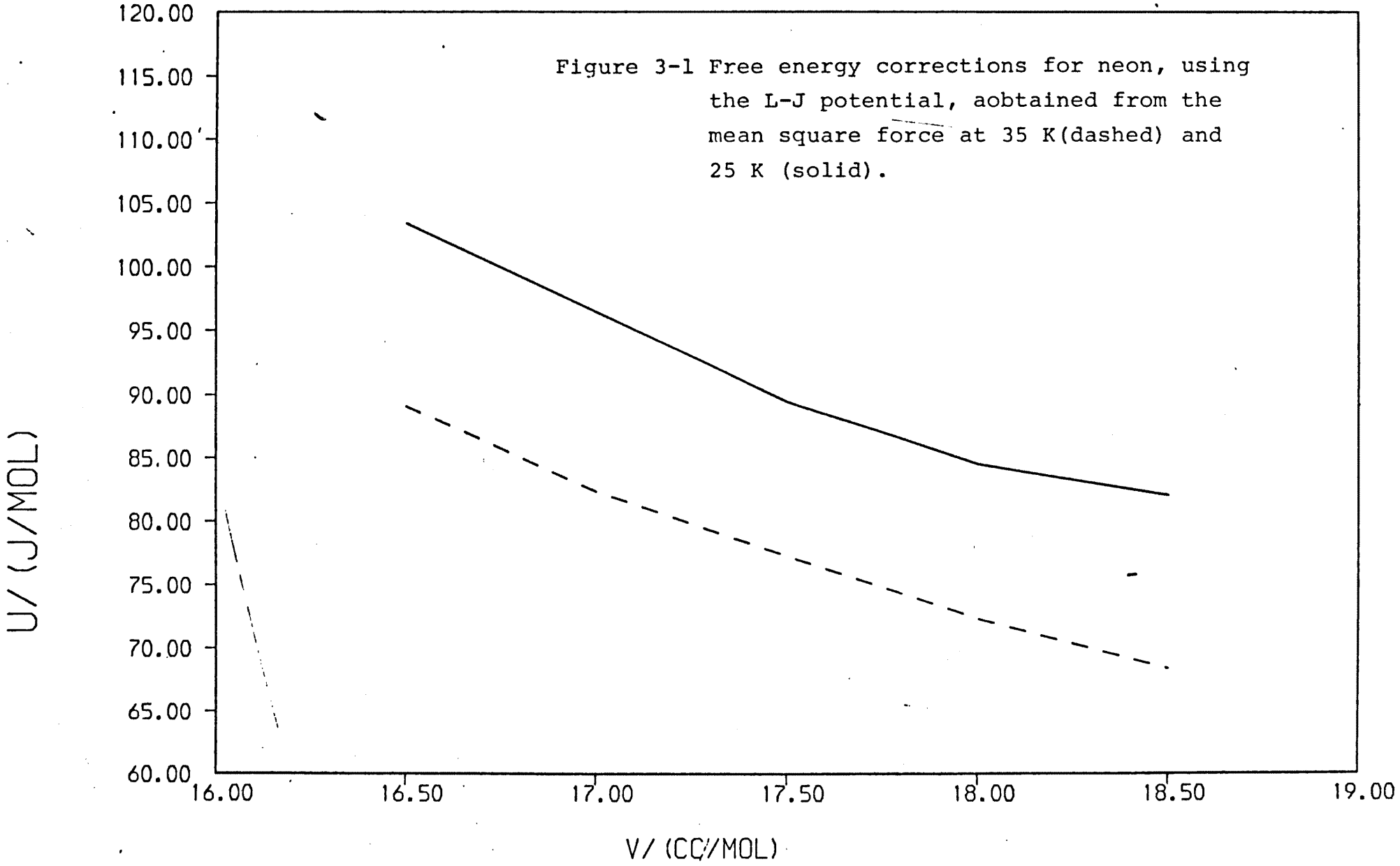

Figure 3-1 Free energy corrections for neon, using the L-J potential, aobtained from the mean square force at 35 K(dashed) and 25 K (solid).

energy and pressure, a series of least-squares fits of the correction ΔA in terms of the volume and temperature were carried out. The resulting cubic splines were then used to interpolate the data, and thus to estimate the derivatives required by (3.3,3.4). For neon, in the range covered by Table 3.1, the internal energy term in $T\,\partial A/\partial T$ is between 25 J/mol at the highest (V,T) point and 50 J/mol at the lowest point. These are very rough figures, in view of the fitting procedure used. The pressure correction varies between 15 and 5 MPa over the same range. The Lennard-Jones data can be scaled to correspond to any other set of parameters (ε',σ'), with care, by using the relations below.

$$T' = T\ (\varepsilon'/\varepsilon)$$

$$V' = V\ (\sigma'/\sigma)^3$$

$$\Delta A' = \Delta A\ (m\sigma^2/m'\sigma'^2)$$

Note the presence of the atomic mass m in these results, which distinguishes this scaling from that applicable to classical Lennard-Jones systems, in which all energies scale as ε. This difference means that the relative importance of the quantum corrections varies as the mass changes.

In the case of the results for fluorine, the three terms in equation (3.3) are all substantial, and approximately in the ratio 2:2:1.

4. Path Integral methods.

The complete dynamical description of any system is contained within the evolution operator $\hat{G}(t)$ for that system. This operator is the solution of the operator equation

$$i\hbar \frac{\partial \hat{G}}{\partial t} = \hat{H}\,\hat{G}, \qquad \hat{G}(0) = \hat{I} \tag{4.1}$$

or, formally,

$$\hat{G}(t) = \exp(-i\hat{H}t/\hbar) \tag{4.2}$$

The operator $\hat{G}$ has two fundamental properties:-

$$\hat{G}(t_1 + t_2) = \hat{G}(t_2)\hat{G}(t_1) \tag{4.3}$$

$$\hat{G}(t)\hat{G}^*(t) = \hat{I} \text{ if } \hat{H} = \hat{H}^* \tag{4.4}$$

The Hamiltonian $\hat{H}$ usually has a complete orthonormal set of eigenfunctions $\{\phi_n\}$, satisfying

$$\hat{H}\,|\phi_n\rangle = E_n\,|\phi_n\rangle$$

The kernel of the operator $\hat{G}$, the Green's function, is given, in the coordinate representation, by

$$G(q_f,q_i;t) = \sum_n \phi_n(q_f)\,\phi_n^*(q_i)\,\exp(-iE_n t/\hbar) \tag{4.5}$$

where q_f, q_i are the final and initial coordinates of the system, separated by time t. $G(q_f,q_i;t)$ may be viewed as a conditional probability for finding the system at q_f, given that it was at q_i at time t before. Equation (4.3) can now be written as an integral:-

$$G(q_f,q_i;t_1+t_2) = \int G(q_f,q;t_2)G(q,q_i;t_1)\,dq \tag{4.6}$$

The trace of the evolution operator, the spectral function,

$$Y(t) = \int G(q,q;t)\,dq \equiv \mathrm{Tr}\ G$$

can easily be related to the partition function, in fact $Y(-i\hbar\beta)$ is the partition function $Z(\beta)$. This analogy is quite general, in that most results for time-dependent problems can easily be transformed to give temperature dependent solutions, since the Schrodinger and Bloch equations are very similar in form. In either case, if we have a short-time (high temperature) approximation, we can use (4.6) recursively to extend the result to longer times, (lower temperatures). Ultimately, we could take the recursion to some limit, and integrate an expression like (4.6) over all points on a path linking initial and final positions. This corresponds to a functional integral, over the path linking the positions, and to that quantum mechanical formulation due to Feynman known as the Path integral. The method is described in (16-18).

Specifically, we have for the density matrix

$$\rho(q_f,q_i;u) = \sum \phi_n(q_f)\phi_n^*(q_i)\ \exp(-uE_n/\hbar) \qquad (4.7)$$

where $u = \hbar\beta$. Differentiating this with respect to β, we find

$$\frac{\partial \rho}{\partial \beta} = -H\rho$$

which is the Bloch equation. Note the resmblance between this and (4.1), and between (4.7) and (4.5). Clearly this is related to the partion function Z,

$$Z(\beta) = \rho(q,q;\hbar\beta)\ dq = \mathrm{Tr}\ \rho = \sum \exp(-\beta E_n)$$

The problem with using this directly is that the ϕ_n and E_n are not known for any but the simplest systems, and certainly not for liquids.

For small η, this can be approximated:-

$$\rho(q_f,q_i;\eta) = \left\{\frac{m}{2\pi\eta\hbar}\right\}^{\frac{1}{2}} \exp -\left\{\frac{m}{2\eta\hbar}(q_f-q_i)^2 + \frac{\eta}{\hbar} V((q_f+q_i)/2)\right\}$$

Using (4.6), we can then write, for any u,

$$\rho(q_f,q_i;u) = \int \exp -\sum_{j=1}^{N} \left\{\frac{m}{2\hbar\eta}(q_{j+1} - q_j)^2 + \frac{\eta}{\hbar} V(q_j)\right\} Dq \tag{4.8}$$

where Dq is shorthand for $dq_1 \ldots dq_{N-1}$, together with the constant factor, and the integral is over all paths q(u) s.t. $q_o=q_i$, $q_j=q(j\eta)$, $q_N=q_f$, $u=N\eta$, and we take the limit $N\to\infty$. The partition function is then obtained by taking $q_i=q_f$, and integrating again:-

$$Z(\beta) = \int \exp\{-(1/\hbar)\int \tfrac{1}{2}m\dot{q}(u) + V(q(u))\ du\}Dq(u) \tag{4.9}$$

where the integral is over all closed paths, the inner integral is over $(0,\hbar\beta)$, and $\dot{q}$ is dq/du. The requirement that the paths be closed is essentially taking the trace.

If V(q) is essentially indepenent of u, that is, if the potential V changes only on a scale large compared with the De Broglie wavelength, then the expression above can be simplified by use of $V(q(u)) \simeq V(q(0))$, to obtain the classical result.

Taking this approximation one stage further, V(q) can be expanded about some value, not necessarily u=0, and the expansion truncated at some point. A number of useful results can be derived in this way, including the Wigner expansion of the free energy as used in the previous chapter.

4.1 Effective potentials.

If a mean position is defined for any one path, the result (4.9) can be transformed into an integral over all paths having a given mean position, and then an integral over this position, rather than the integration over all starting positions involved in (4.9). If the potential is replaced by a Taylor expansion about this mean position, defined by

$$\bar{q} = \int q(u)\, du$$

then a whole series of approximations can be obtained, as higher terms in the Taylor expansion are retained. The classical partition function results if $V(q(u))$ is taken as $V(\bar{q})$. The next term, in $V'(\bar{q})(q(u) - \bar{q})$, clearly vanishes given the definition of $\bar{q}$, as will all terms in odd derivatives of V. Retaining the second derivative, we find

$$Z(\beta) = \left(\frac{mkT}{2\pi\hbar^2}\right)^{\frac{1}{2}} \int \exp -\beta\left(V(\bar{q}) + \frac{\beta\hbar^2}{24m} V''(q)\right) d\bar{q} \qquad (4.10)$$

Since we have neglected terms in the exponent in $\hbar^4$, we can expand the exponential, and again neglect terms in $\hbar^4$:-

$$Z(\beta) = \left(\frac{mkT}{2\pi\hbar^2}\right)^{\frac{1}{2}} \int \{\exp -\beta V(\bar{q})\}\left(1 - \frac{\beta^2\hbar^2}{24m} V''(\bar{q})\right) d\bar{q} \qquad (4.11)$$

The corresponding free energy may easily be derived, using $\ln(1+x) \simeq x$, and shown to be precisely the result given by the Wigner expansion, equation (3.2). This was derived in (12) by a completely different argument. If higher terms were retained, higher derivatives would be entering through the expansion in (4.10), while powers of lower

derivatives enter into the expansion of the exponential.

An alternative approach would be to carry out classical simulations, but with a potential that contained the necessary modifications to lead to approximate quantum results. For instance, one might use

$$V_{eff} = V(q) + (\hbar^2/24mk^2T^2)\ V''(q)$$

or even include higher terms. However, Feynman has given a variational theorem (16,17) that allows the choice of an optimum effective potential, with the result

$$V_{eff}(q) = \left(\frac{6mkT}{\hbar^2\pi}\right) \int V(s)\ \exp -6mkT(q-s)^2/\hbar^2\ ds \tag{4.12}$$

in one dimension. A very similar result is in fact to be found in (9). When generalised to three dimensions, the result is

$$V_{eff}(\underline{q}) = \left(\frac{\nu}{4\pi}\right)^{3/2} \int V(\underline{r} + \underline{q})\ \exp -\nu\underline{r}^2/4\ d\underline{r} \tag{4.13}$$

where $\nu=12mkT/\hbar^2$. This integral can easily be evaluated for the Gaussian potential (1.2), when the effective potential is also Gaussian, but with modified parameters, given by

$$\begin{aligned} A^* &= (\nu/(4B + \nu))^{3/2}\ A \\ B^* &= (\nu/(4B + \nu))\ B \end{aligned} \tag{4.14}$$

The effect of these changes is to make the potential well shallower, and to make the potential more repulsive. This is in accord with the fact that the quantum effects are essentially repulsive. Note also that the parameters tend to their classical values in the high temperature, high mass limit, as they should. Taylor expansion of $V(\underline{r}+\underline{q})$ about $\underline{r}=0$ shows that the first term agrees with the result obtained via the Wigner expansion, but that higher terms do not.

The approach is clearly very simple to implement, since all that is required is that V_{eff} replace V. Some care is required with the integral in (4.13), since it may not exist for some potentials with a singularity. In these cases, such as the Lennard-Jones potential, the result may be approximated by expansion of the potential about its minimum. In the case of the Lennard-Jones potential, this procedure again leads to effective ε,σ, to be used in classical calculations. Expressions for these have been given by Young (19):-

$$\varepsilon^* = (1 - 14.3x^{-1} + 104.9x^{-2})\ \varepsilon$$
$$\sigma^* = (1 + 3.77x^{-1})\ \sigma \qquad (4.15)$$

where $x=\nu\sigma^2/4$. The scaling properties of the Lennard-Jones potential make simulations using these parameters unecessary, but the Gaussian potential does not have this property.Table 4.1 thus contains results similar to those presented in Table 2.2, but using the effective parameters given by (4.14). The Monte Carlo method was used in precisely the same fashion as described above in chapter 2. The results of Table 2.1 have been scaled with the effective parameters (4.15), to obtain the results shown in Table 4.2. The method has one disadvantage, in that the kinetic energy is not calculable. This is not a serious problem, but makes the calculation of pressure and internal energy difficult. The pressures in the two tables have been calculated by assuming the value 3RT/2, which is the classical result. Figures 4.1,4.2 show typical radial distribution functions obtained for the gaussian potential by this method, and also the classical results for comparison. The change in the position and height of the first maximum should be noted, this will be discussed in more detail in chapter 6.

The effective parameters for the gaussian potential have also been used on simulations of the diatomic fluid previously simulated to give the results in Table 2.3. The results are shown in Table 4.3, and one of the radial distribution functions obtained is compared with its classical counterpart in figure 4.3. This system, which roughly models fluorine, will be discussed further in chapter 6.

Table 4.1 Results obtained by Monte Carlo simulation using the effective Gaussian potential, for 108 atoms.

a.Neon

$V/ccmol^{-1}$	T/K	$PE/Jmol^{-1}$	$\Phi/Jmol^{-1}$	P*
16.5	25	-1542	-9	12.2
	30	-1508	-716	29.6
	35	-1467	-1363	45.1
	40	-1440	-1908	58.7
17.0	25	-1500	362	5.1
	30	-1465	-398	22.5
	35	-1437	-867	34.1
	40	-1405	-1470	45.9
	45	-1385	-1800	57.3
	50	-1351	-2410	71.7
17.5	25	-1453	486	2.6
	30	-1435	117	12.0
	35	-1404	-470	25.6
	40	-1370	-1088	39.7
18.0	25	-1413	704	-1.5
	30	-1390	262	9.0
	35	-1373	-55	17.2
	40	-1340	-690	31.2
18.5	25	-1387	1089	-8.3
	30	-1363	639	1.9
	35	-1334	96	14.0
	40	-1311	-318	23.7

a,cont.

V	T	PE	Φ	P*
19.0	45	-1256	-555	29.4
	50	-1226	-1130	41.7
21.0	45	-1141	117	16.0
	50	-1122	-183	22.7
23.0	45	-1044	371	10.9
	50	-1030	216	14.9

* Pressures assume classical KE of 3RT/2.

b. Helium

V	T	PE	Φ	P*
22	12.5	-132	-1039	20.4
	15.0	-146	-832	18.3
23	12.5	-129	-827	17.2
	15.0	-138	-785	16.7
24	12.5	-127	-731	14.4
	15.0	-133	-703	14.9
25	12.5	-124	-609	12.3
	15.0	-127	-621	13.3
26	12.5	-118	-599	11.6
	15.0	-127	-492	11.1

* Pressures assume classical KE of 3RT/2

Table 4.2 Results obtained by scaling the results of Table 2.1 with effective L-J parameters.

a.Neon

V/ccmol^{-1}	T/K	PE/Jmol^{-1}	/Jmol^{-1}	P/Mpa *
17.27	23.6	-1671	1496	-17.5
17.14	28.56	-1649	785	-1.4
17.05	33.56	-1624	172	13.0
16.98	38.55	-1603	-328	25.3
17.80	23.6	-1622	1665	-20.1
17.67	28.56	-1603	1045	-6.3
17.57	33.56	-1583	502	6.4
17.49	38.55	-1558	-72	19.8
18.33	23.57	-1576	1875	-23.4
18.18	28.56	-1560	1251	-9.8
18.08	33.56	-1539	707	2.4
18.01	38.55	-1515	174	14.6
18.85	23.6	-1531	1948	-24.0
18.70	28.56	-1517	1444	-13.0
18.60	33.56	-1499	894	-1.0
18.53	38.55	-1478	457	9.1
19.37	23.6	-1494	1969	-23.7
19.22	28.56	-1476	1469	-13.1
19.12	33.56	-1456	1028	-3.3
19.04	38.55	-1438	612	6.1

* Pressures assume classical KE of 3RT/2.

Table 4.3 Results obtained for the 2-centre gaussian model of fluorine, using an effective potential.

$V/ccmol^{-1}$	T/K	$PE/Jmol^{-1}$	$\Phi/Jmol^{-1}$	P/MPa *
22	50	-6287	525	11
	60	-6262	-722	33
	70	-6143	-2278	61
24	50	-5889	5079	-53
	60	-5789	4201	-37
	70	-5737	3715	-27
26	50	-5416	8568	-93
	60	-5359	6900	-69
	70	-5302	6455	-60
28	50	-5115	7592	-75
	60	-4977	6452	-58
	70	-4836	5989	-50
	80	-4817	4991	-35

*Pressures assume classical KE 3RT/2.

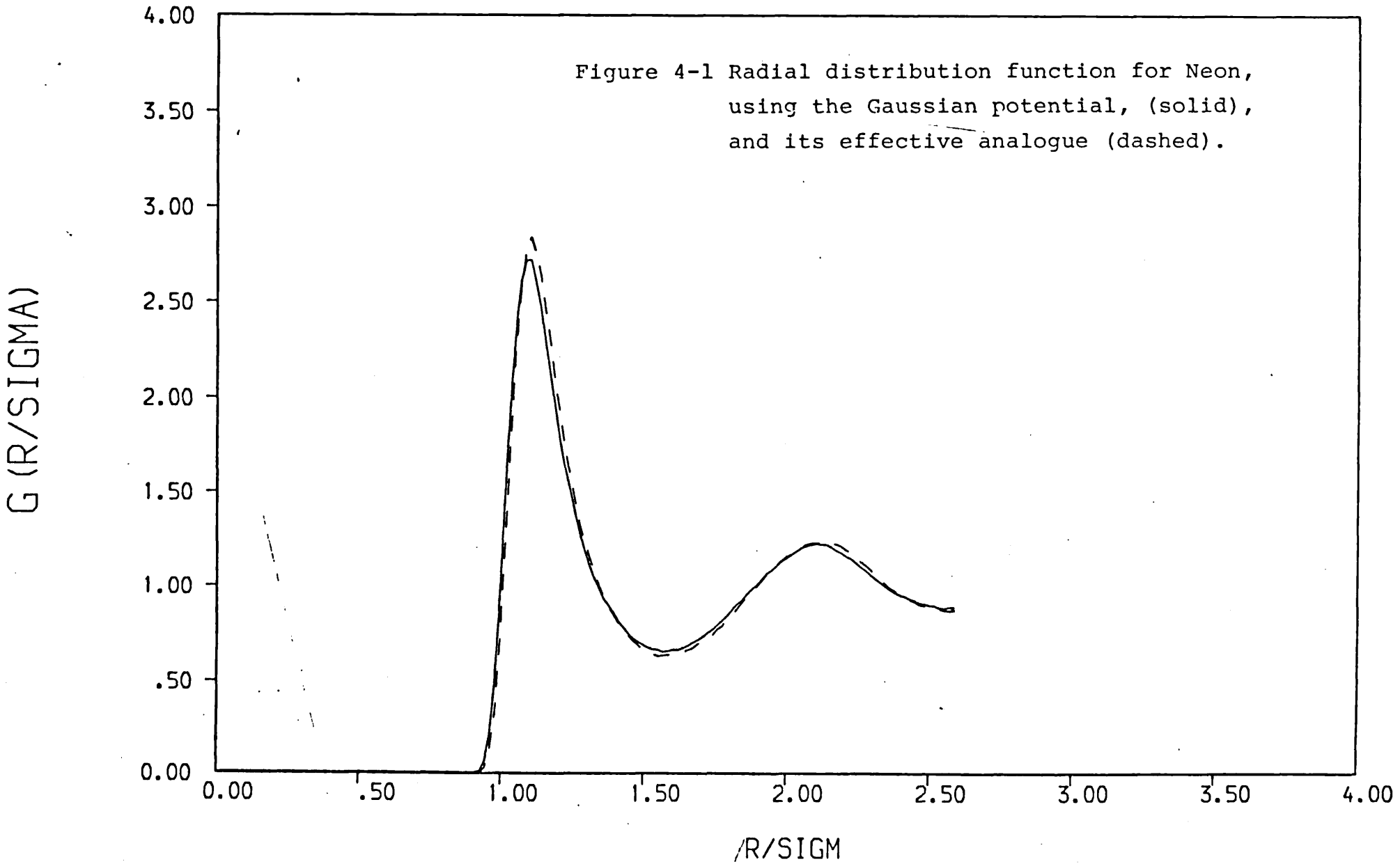

Figure 4-1 Radial distribution function for Neon, using the Gaussian potential, (solid), and its effective analogue (dashed).

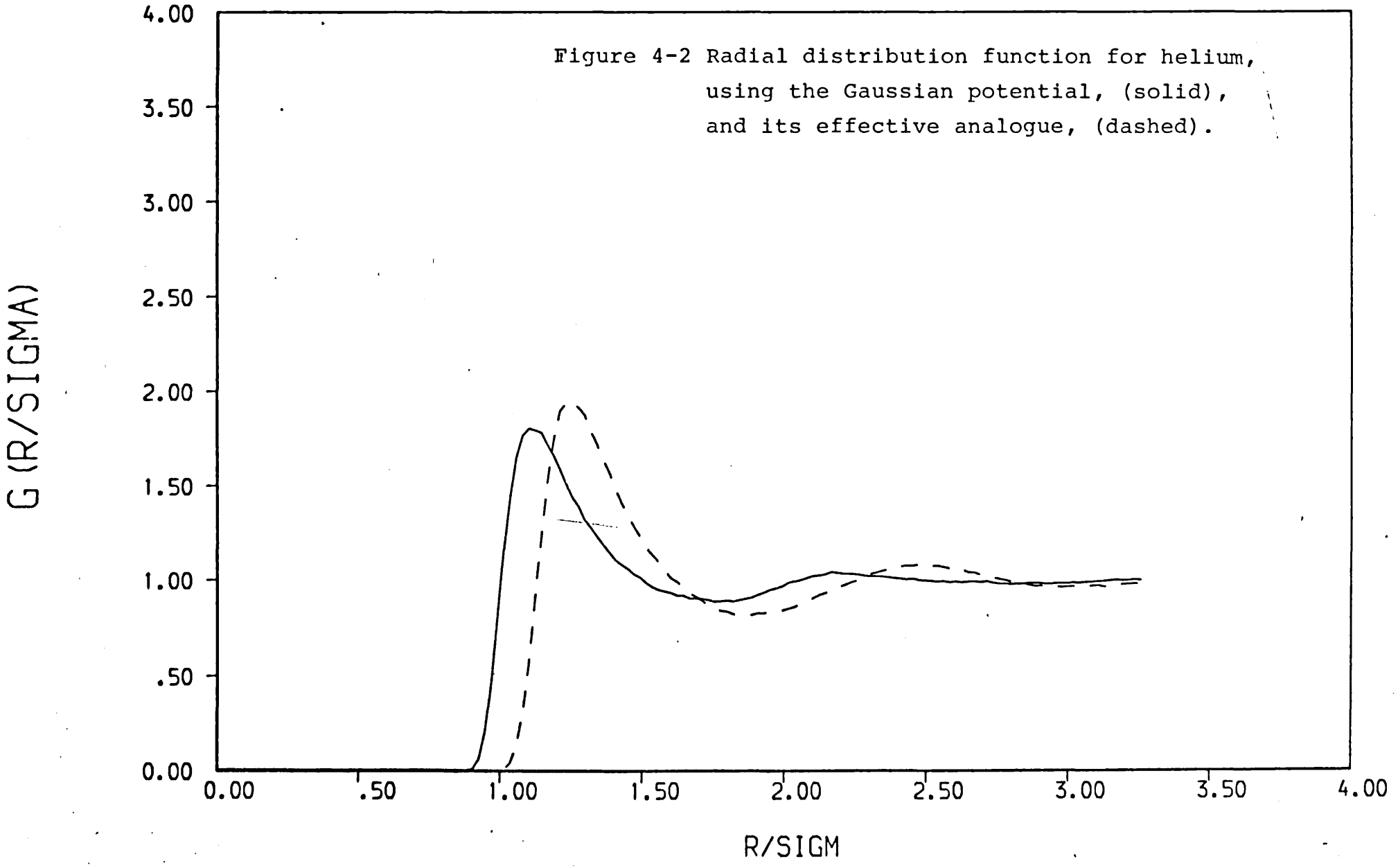

Figure 4-2 Radial distribution function for helium, using the Gaussian potential, (solid), and its effective analogue, (dashed).

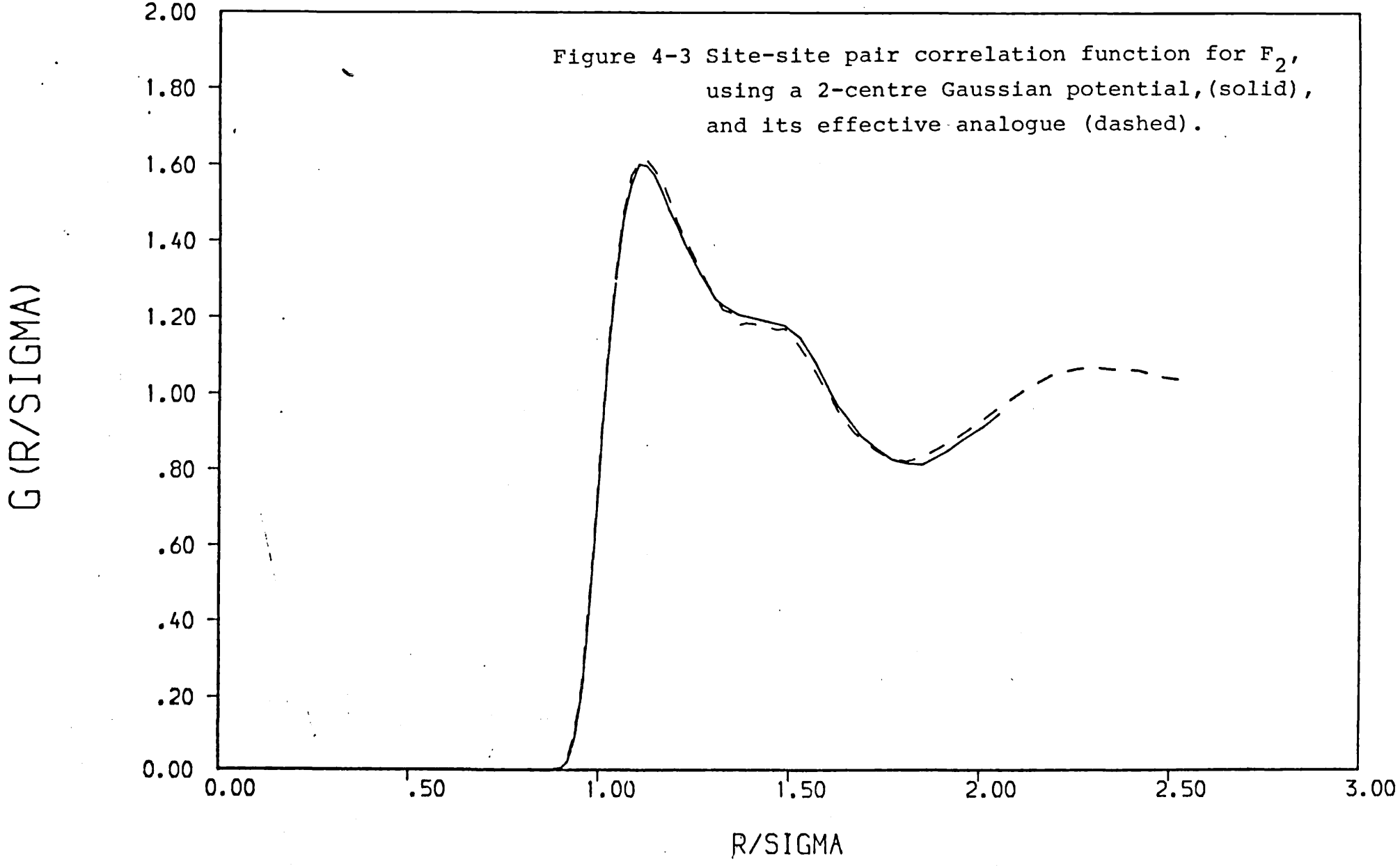

Figure 4-3 Site-site pair correlation function for F_2, using a 2-centre Gaussian potential, (solid), and its effective analogue (dashed).

4.2 The method of Stratt and Miller.

The result (4.9) can be used to derive less severe approximations in which the kinetic energy can be found directly. However, the classical framework of the previous approaches will be lost. The possibilities are many and varied, but those that retain some similarity to classical methods would seem preferable.

Equation (4.9) is an integral over all closed paths in configuration space. As an approximation to this, we might restrict the set of paths in some way. This can be done if, for each initial point q_i, we consider only the one path making the largest contribution to the integral. That is, we require that path q(u) for which

$$\int_0^{\hbar\beta} \tfrac{1}{2}m\,\dot{q}^2(u) + V(q(u))\,du$$

is a minimum. If we write $p = m\dot{q}(u)$, and use the Euler-Lagrange equation, we find at once that

$$\frac{\partial V}{\partial q} = \dot{p} \tag{4.16}$$

This defines one path for each starting point. Since we require the path to be closed, we consider the path from u=0 to $u=\frac{1}{2}\hbar\beta$, and then return to the starting point by the same path. The final result for the partition function is

$$Z(\beta) = \int \exp\{-\frac{2}{\hbar}\int_0^{\frac{1}{2}\hbar\beta} \frac{p^2(u)}{2m} + V(q(u))du\}\,Dq(u) \tag{4.17}$$

where the integral is over all points q(0), $p=q\dot{m}$, and $\dot{p}=\partial V/\partial q$. This approach has been used by Feynman (17),

and described fully, with simple applications, by Stratt and Miller (20). The method is exact for the harmonic oscillator, but underestimated quantum effects when applied to simple systems such as two helium atoms with a Lennard-Jones potential. This is to be expected in any such approximation.

The calculation proceeds exactly as in a classical Monte Carlo calculation, but calculates the integral in the exponent of (4.17) at each move. This requires the approximate solution of the equations of motion that define the path, which in turn requires methods similar to those used for molecular dynamics. The only notable differences are the sign of $\partial V/\partial q$ in (4.16), and the requirement that the solution be found only over the interval $(0,\hbar\beta)$. The Monte Carlo method used differs from the normal version in that every atom is given a random displacement in both position and momentum at each move. The momenta are of course involved in the integration, since they cannot be separated as they can classically. The number of steps of "molecular dynamics" required to cover the interval $(0,\hbar\beta)$ clearly increases as the temperature is reduced. In this work 8-12 steps were found to be adequate, and the results show no significant if this figure is increased. The potential and kinetic energy averages are easily obtained by taking the average over all moves of the values obtained at $u=\hbar\beta/2$.

The method has been applied to both the Lennard-Jones and Gaussian models of both neon and helium, using a system of 32 atoms with the boundary and cutoff exactly

as in classical simulations. 12000 Monte Carlo moves, each of 8 steps, were used, starting from an equilibriated configuration. Note that a configuration produced by a classical simulation cannot be used to start a simulation using this method. The results obtained are presented in Tables 4.4,4.5 for the Lennard-Jones and Gaussian potentials, respectively. Figures 4.4-4.7 show some of the radial distribution functions obtained, compared with their classical counterparts. The accuracy of this method is not as high as might be desired, and certainly worse than the classical simulation results already reported, as is clear from the data in the tables. The results will be discussed alongside those obtained by other methods in chapter 6.

4.3 Use of Fourier series.

The integrals used so far have been over closed paths, or, more precisely, over the one most important path for each starting point. If the whole set of paths is to be included, then the expression (4.8), for finite N, is a clear place to start. It has been shown (31) that this result for the partition function can be related to the classical partition function of a hypothetical system with N times as many atoms. This approach has been used by Chandler (21), Barker (22), and others. This can easily be seen if the integral in the exponent of (4.9) is replaced by a finite quadrature, and $\dot{x}$ is replaced by some difference scheme.

Table 4.4 Results obtained for the Lennard-Jones fluid using the method of Stratt and Miller.

a.32 Neon atoms

V ($ccmol^{-1}$)	T (K)	PE ($Jmol^{-1}$)	Φ ($Jmol^{-1}$)	KE ($Jmol^{-1}$)	P (MPa)
16.5	25	-1730	1236	420	-7.9
	30	-1667	74	422	15.5
	"	-1666	-107	428	19.4
	35	-1635	-400	468	27
	40	-1578	-1393	512	49
17.0	25	-1709	1865	376	-22
	30	-1658	1204	347	-10
	35	-1562	-337	503	26
	40	-1601	70	482	17
17.5	25	-1615	1485	337	-15.4
	30	-1610	1189	379	-8
	35	-1553	415	514	12
	40	-1523	-661	529	32
18.0	25	-1539	1430	371	-13
	30	-1486	559	445	6
	35	-1485	318	481	12
	40	-1486	-155	517	22
18.5	25	-1471	733	469	3.6
	30	-1500	1214	453	-5
	35	-1480	1096	490	-2
	40	-1503	1138	551	-0.4

Table 4.5 Results obtained for the Gaussian fluid, using the method of Stratt and Miller.

a. 32 Neon atoms

V ($ccmol^{-1}$)	T (K)	PE ($Jmol^{-1}$)	Φ ($Jmol^{-1}$)	KE ($Jmol^{-1}$)	P (MPa)
16.5	25	-1554	468	428	7.8
	30	-1526	180	449	14.5
	35	-1488	-582	458	30.3
	40	-1419	-2065	489	61.5
17.0	25	-1476	505	415	6.4
	30	-1429	-377	418	23.7
	35	-1387	-1069	479	39.7
17.5	25	-1460	395	372	6.6
	30	-1442	741	406	1.3
	35	-1385	-611	464	29.3
	40	-1367	-926	558	38.9
18.0	25	-1406	984	389	-3.8
	30	-1372	668	426	3.4
	35	-1390	361	452	10.0
	40	-1313	-1103	570	41.0
18,5	25	-1385	1388	447	-8,9
	30	-1356	996	446	-1.8
	35	-1323	221	483	13.4
	4Φ	-1329	-5	484	17.5
b. 108 atoms					
18.0	30	-1373	-264	425	20.6

c 32 Helium atoms

V	T	PE	Φ	KE	P
22	12.5	-208	474	134	-3.1
	15.0	-208	5ΦΦ	172	-2.3
23	12.5	-194	439	143	-2.2
	15.0	-197	555	169	-3.1
24	12.5	-185	511	132	-3.4
	15.0	-185	539	175	-2.6
25	12.5	-178	594	125	-4.5
	15.0	-178	635	161	-4.2
	"	-178	618	164	-4.2
26	12.5	-165	532	138	-3.2
	15.0	-168	637	161	-4.0

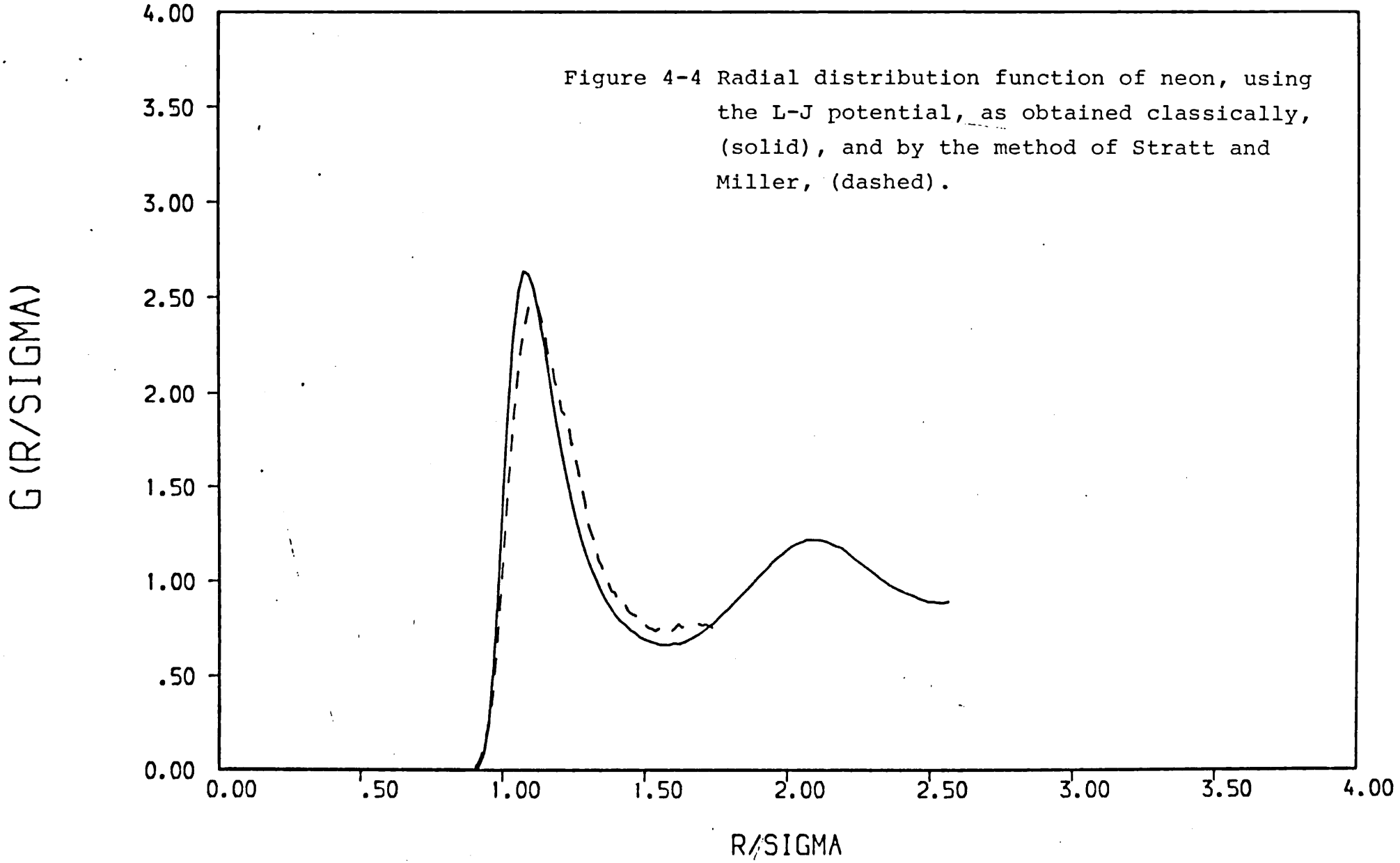

Figure 4-4 Radial distribution function of neon, using the L-J potential, as obtained classically, (solid), and by the method of Stratt and Miller, (dashed).

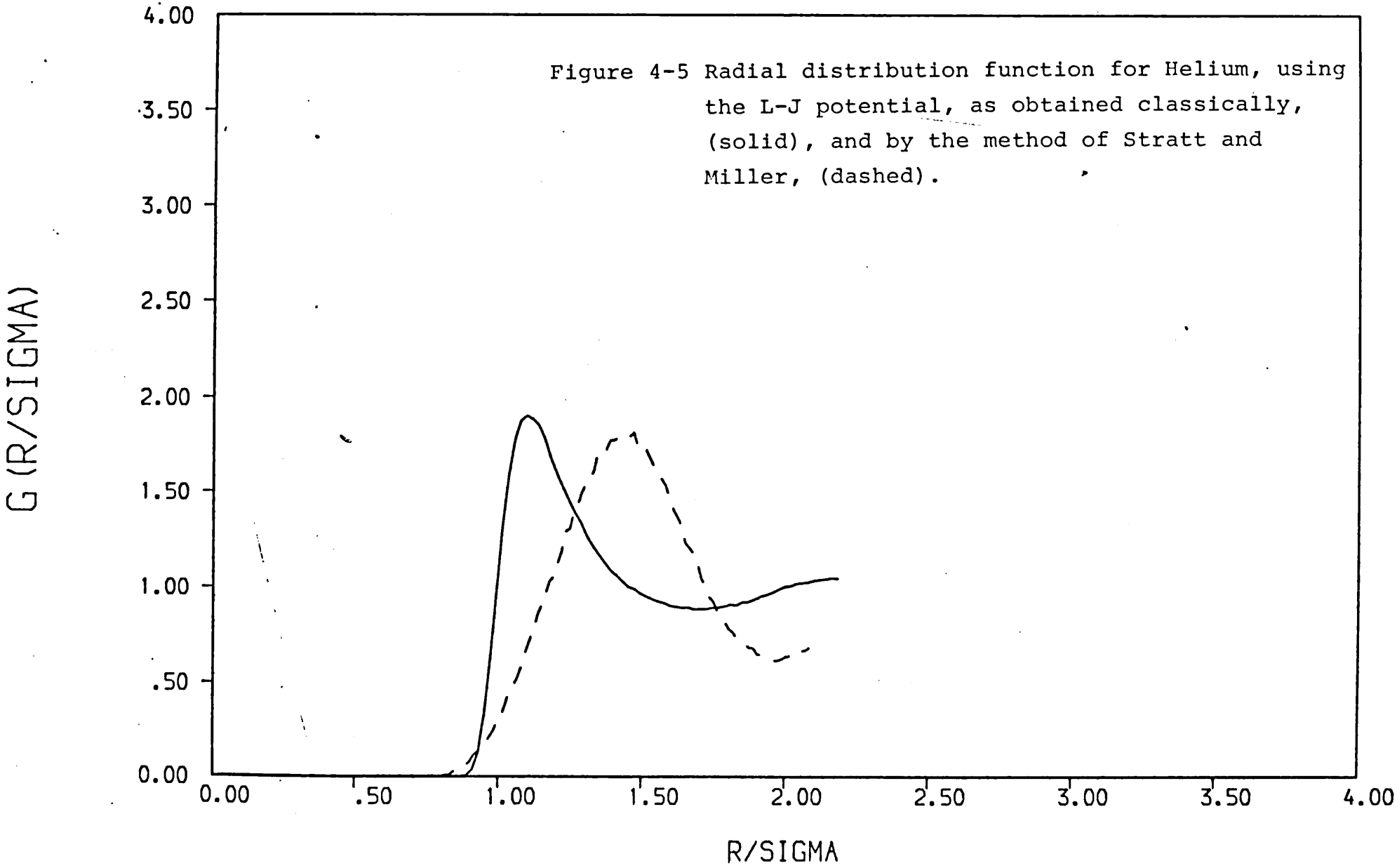

Figure 4-5 Radial distribution function for Helium, using the L-J potential, as obtained classically, (solid), and by the method of Stratt and Miller, (dashed).

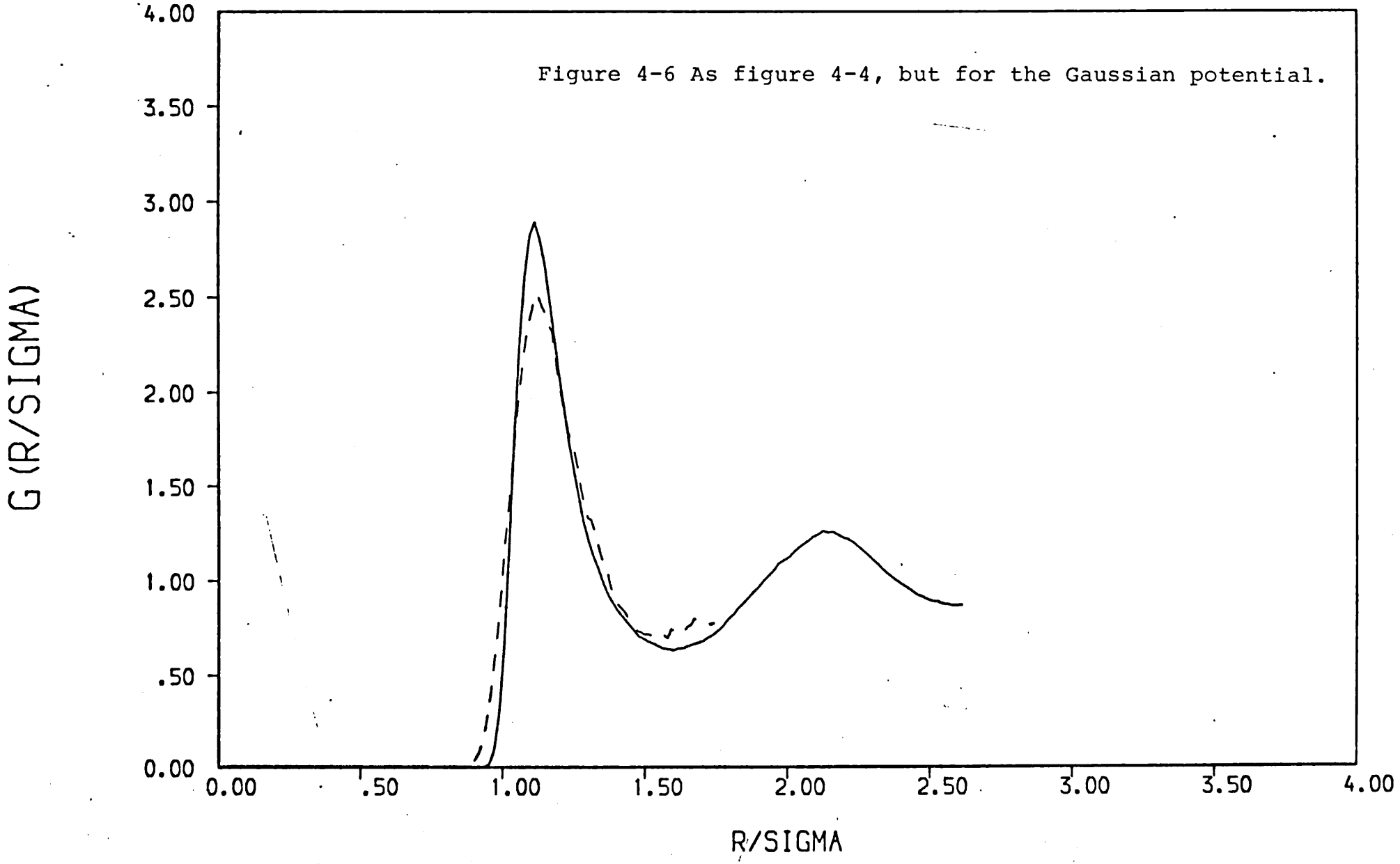

Figure 4-6 As figure 4-4, but for the Gaussian potential.

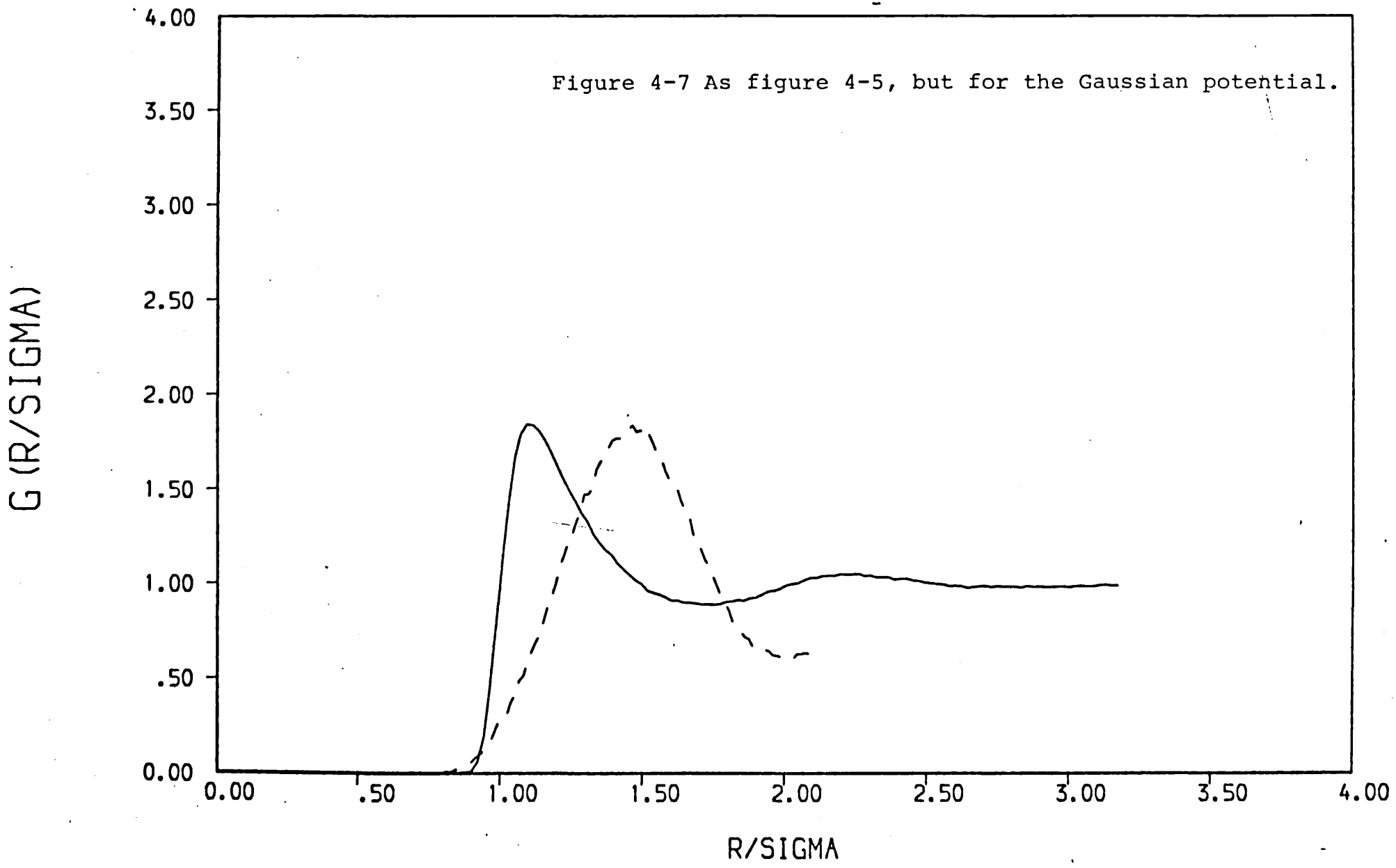

Figure 4-7 As figure 4-5, but for the Gaussian potential.

$$\int \exp -\frac{1}{\hbar} \int \tfrac{1}{2}m\sum_{i=1}^{N} \dot{x}_i(u) + V(x_1 \ldots x_N)\, du \quad Dx(u)$$

$$\simeq \int \exp -\frac{\beta}{P} \sum_{j=1}^{P} \{ \frac{P^2 m}{2(\hbar\beta)^2} \sum_{i=1}^{N} (x_i^{j+1} - x_i^j)^2 + V(x_1^j, \ldots x_N^j) \}$$

This is the classical partition function for a system of N molecules, each being cyclic, and having P atoms. These molecules interact, but note that each site only interacts with the corresponding sites in the other molecules.

An alternative method involves a change of variables. Since the path is closed, $q(0) = q(\hbar\beta)$, it is possible to write the path as a fourier series:-

$$q(u) = q_i + \sum_j a_j \sin \frac{j\pi u}{\hbar\beta} \tag{4.18}$$

$$\dot{q}(u) = \sum_j a_j \frac{j\pi}{\hbar\beta} \cos \frac{j\pi u}{\hbar\beta} \tag{4.19}$$

The kinetic energy is then given by $\frac{1}{2}m\dot{q}^2$, and the kinetic energy term in the exponent in (4.17) can be integrated analytically. This leaves the potential term to be estimated numerically. Essentially, the N points used to define the path in (4.8) are replaced by N fourier coefficients, where we would like in principle to take N infinite. The integrations over the intermediate points are replaced by integrations over the fourier coefficients, which require similar Monte Carlo techniques. The method lacks the similarity with a classical polymer system, but it is to be hoped that the convergence with N is different, and hopefully better.

The method has been tested by carrying out several runs for helium using the Gaussian potential, and truncating the fourier series at between 4 and 32 terms.

The results obtained are shown in Table 4.6. The radial distribution functions obtained for N=4 and N=32 are plotted in figure 4.8. There is little N dependence in these results, which suggest that the method may be more useful than the method of Chandler et.al., although it lacks the analogy with classical polymer systems.

Table 4.6 Results obtained for the Gaussian model of helium using the fourier series method with N coefficients , V=24 cc/mol,T=15K, 32 atoms.

N	PE (J/mol)	Φ (J/mol)	KE (J/mol)
4	-201.5	-22.5	130.2
10	-200.2	124.8	136.9
24	-206.0	33.2	138.6
32	-199.8	193.4	134.0

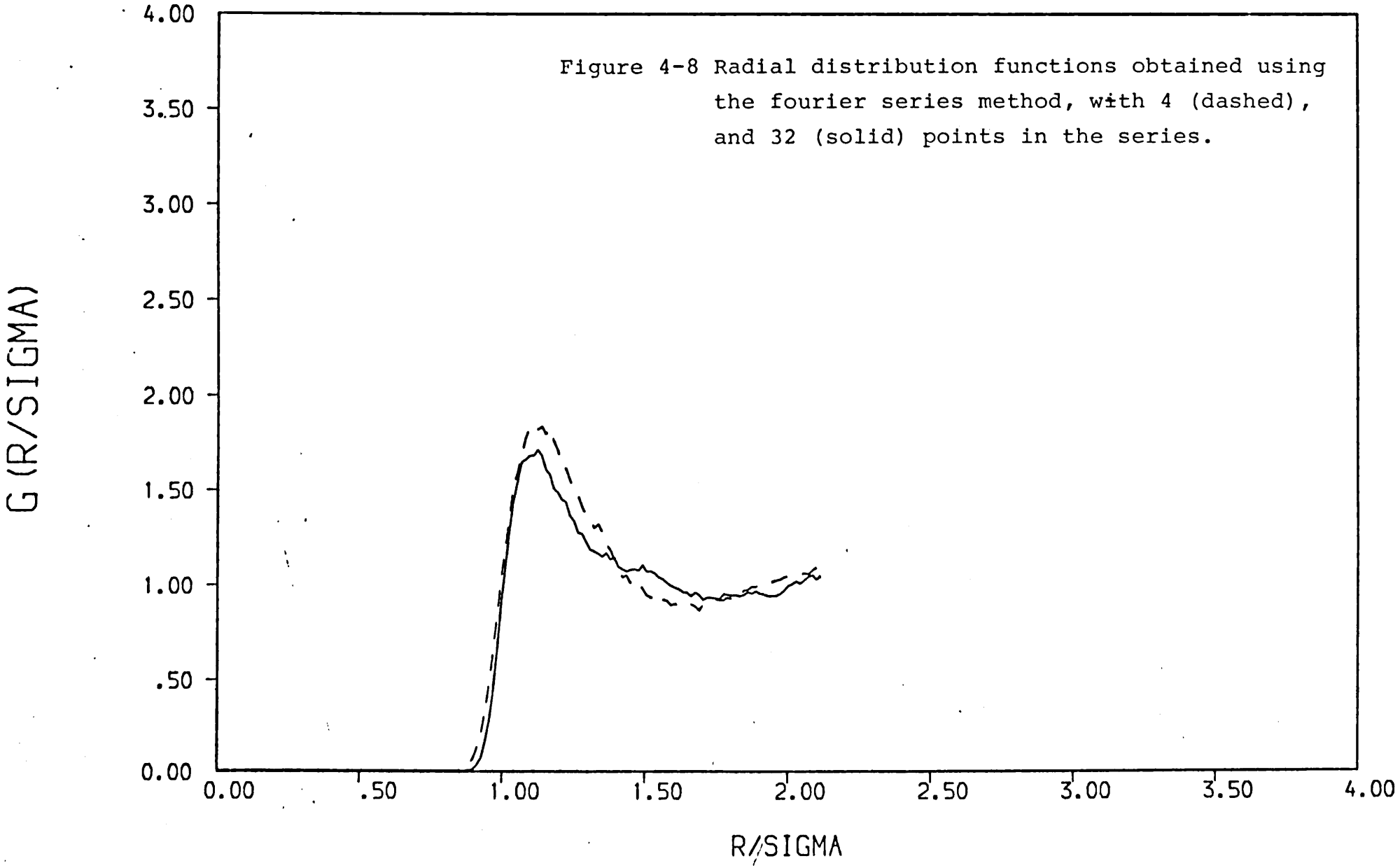

Figure 4-8 Radial distribution functions obtained using the fourier series method, with 4 (dashed), and 32 (solid) points in the series.

5. Wavepacket methods.

The methods described in the preceding chapter were all Monte Carlo methods, and thus could give no answers to dynamical questions. This section will introduce a semiclassical analogue of the molecular dynamics method, by which dynamical information could in principle be obtained. The objective of the work is to derive a set of equations of motion for an assumed time-dependent wavefunction, and then to numerically solve these, in precisely the manner of a molecular dynamics simulation.

The form of the wavefunction is important, since it is central to the whole approach. The form used here is a product of atomic functions

$$\Psi = \prod_j \phi_j \tag{5.1}$$

where the atomic functions ϕ_j, j=1,...,N, are gaussian wavepackets with time dependent parameters specifying the position, momentum, and shape. This form combines several useful properties, apart from being physically realistic (i.e. continuous, etc.) The precise form used is, in two dimensions,

$$\begin{aligned}\phi_j = \exp \tfrac{i}{\hbar}\{ & A_{jx}(x-X_j)^2 + A_{jy}(y-Y_j)^2 + \\ & B_{jxy}(x-X_j)(y-Y_j) + P_{jx}(x-X_j) + \\ & P_{jy}(y-Y_j) + D_j \}\end{aligned} \tag{5.2}$$

Here the upper case letters denote functions of time, that is, $A_{jx} \equiv A_{jx}(t)$. The A,B,D parameters are complex, while X,P are real. The generalisation to 3 dimensions is obvious. The subscript j will be omitted where this

does not affect clarity. The complex parameters specify the shape of the wavepacket, and its extent. With this form, we have

$$\langle\phi|\hat{x}|\phi\rangle = X(t) \tag{5.3}$$

$$\langle\phi|\hat{p}_x|\phi\rangle = P_x(t) \tag{5.4}$$

and require D to be such that the wavepacket is correctly normalised to unity:-

$$\langle\phi|\phi\rangle = 1 \tag{5.5}$$

In fact, this requirement leads to a relation between Im D and the A,B parameters, and also to the constraint that the Im A must be positive. Various integrals that have been used in the manipulation of these wavepackets are summarised in appendix I.

The next stage of the work involves deriving a set of equations of motion for all of the parameters. Two methods for doing this have been suggested by Heller, (23,24), in connection with applications in scattering theory. The first of these methods relies upon Taylor expansion of the potential about the instantaneous centre X,Y,Z of the wavepackets, while the second relies on a variational principle (25). This second method is considerably more complicated to implement.

5.1 Expansion of the potential.

The Schrodinger equation is

$$i\hbar\frac{\partial\Psi(\underline{r},t)}{\partial t} = \hat{H}\Psi(\underline{r},t) \tag{5.6}$$

with Hamiltonian $\hat{H}$ given by

$$\hat{H} = -\frac{\hbar^2}{2m}\nabla^2 + V(\underline{r}) \tag{5.7}$$

Here N atoms of mass m are located at positions given by the 3N dimensional vector $\underline{r}$, and $V(\underline{r})$ is the potential. If we assume a wavefunction of the form (5.1,5.2), we can write

$$\frac{\partial \Psi}{\partial t} = \sum \frac{\partial \phi_j}{\partial f_k} \frac{\partial f_k}{\partial t} \frac{\partial \Psi}{\partial \phi_j} \qquad (5.8)$$

where the sum is over atoms j, and parameters f_k, the parameters f_k being the various X,P,A,B,D. With the form (5.2) it is easy to see that the r.h.s of (5.8) is a quadratic function of the coordinates, multiplying the wavefunction. The same is true of the kinetic energy operator in (5.7). The potential $V(\underline{r})$ does not generally have this property, but we can replace it if we Taylor expand about the centre of the wavepackets, and discard cubic and higher terms. This will of course be exact for harmonic potentials.

The expression (5.8) can be substituted into the Schrodinger equation, with the approximate potential, and powers of the coordinates equated to obtain a set of equations of motion, since the time derivatives will be involved only on the l.h.s. of (5.6). These will be valid provided that the neglected part of the potential is small. This is not true for systems with Lennard-Jones or similar potentials except at very low temperatures.

At this point it is convenient to recall Ehrenfest's theorem, which states that the expectation values of the position and momentum obey the classical equations of motion, that is,

$$\frac{d}{dt} \langle x \rangle = \langle p \rangle / m \qquad \frac{d}{dt} \langle p \rangle = - \langle \frac{dV}{dx} \rangle$$

a. 1-dimensional harmonic oscillator.

We have

$$H = -\frac{\hbar^2}{2m}\frac{\partial^2}{\partial x^2} + \tfrac{1}{2}m\omega^2 x^2 \qquad (5.9)$$

$$\Psi = \exp\frac{i}{\hbar}\left(A(x-X)^2 + P(x-X) + D\right) \qquad (5.10)$$

Taylor expand the potential about X:-

$$\tfrac{1}{2}m\omega^2 x^2 = \tfrac{1}{2}m\omega^2\{X^2 + 2(x-X)X + (x-X)^2\} \qquad (5.11)$$

Substituting into (5.9), and collecting terms in powers of (x-X), we find three equations:-

$$\dot{D} = \dot{X}P - \tfrac{1}{2}m\omega^2 X^2 - \frac{P^2}{2m} + \frac{i\hbar}{m}A \qquad (5.12a)$$

$$-\dot{P} + 2A\dot{X} = m\omega^2 X + 2AP/m \qquad (5.12b)$$

$$\dot{A} = -\tfrac{1}{2}m\omega^2 - 2A^2/m \qquad (5.12c)$$

Equation (b) of this set is nothing more than the classical equations of motion, as expected by Ehrenfest's theorem. Using the same equation in (a), we find

$$D = \frac{P^2}{2m} - \tfrac{1}{2}m\omega^2 X^2 + \frac{i\hbar}{m}A$$

Further, if we set $A(0)=\frac{1}{2}im\omega$, then $A(t)=A(0)$ for all t, and the wavepacket does not spread. D(0) is set by the requirement that the wavepacket be normalised, and we choose the time origin such that $X(0)=0$. These initial conditions lead easily to a solution of these equations of motion:-

$$\dot{X}(t) = \frac{P(0)}{m\omega}\sin\omega t \qquad (5.13a)$$

$$P(t) = P(0)\cos\omega t \qquad (5.13b)$$

$$A(t) = A(0) = \tfrac{1}{2}im\omega \qquad (5.13c)$$

$$D(t) = \frac{P^2(0)}{m}\left\{\frac{t}{2} + \frac{\sin 2\omega t}{4\omega}\right\} + \frac{i\hbar}{4}\ln\left\{\frac{m\omega}{\hbar\pi}\right\} \qquad (5.13d)$$

We thus have the wavefunction, (and hence density matrix) as a function of time. The diagonal elements of the density matrix are given by

$$\rho(x,x;t) = \left(\frac{m\omega}{\hbar\pi}\right) \exp\left\{-\frac{m\omega}{\hbar}\left(x - \frac{P(0)\sin\omega t}{m\omega}\right)^2\right\} \tag{5.14}$$

This is clearly a gaussian whose centre oscillates in time between the classical turning points at $x=P(0)/m\omega$. Note that if $P(0)=0$, this reduces to the correct ground state wavefunction result, which is well known, and that (5.13d) is such as to preserve normalisation. The kinetic and potential energy expectation values are

$$\langle \tfrac{1}{2}m\omega^2x^2 \rangle = \tfrac{1}{4}\hbar\omega + (P(0)\sin\omega t)^2/2m \tag{5.15}$$

$$\langle -\frac{\hbar}{2m}\frac{d^2}{dx^2} \rangle = \tfrac{1}{4}\hbar\omega + (P(0)\cos\omega t)^2/2m \tag{5.16}$$

We thus obtain the correct zero point energy, and have energy conservation. Note that the zero point energy is shared equally between the potential and kinetic terms.

In summary, the method is exact for this problem, as it should be. The essential point to note are that the correct zero point energy emerges, shared equally between the two halves of the Hamiltonian, that the wavepacket can be chosen to retain normalisation, and that energy is conserved. These points may be obvious here, but in a more complicated system they might not be. Such more complicated systems might not be analytically soluble.

b. N body problem.

The N atoms will each be represented by a wavepacket of the form (5.2). The Taylor expansion of the potential is more complicated now, but not unduly so. Let $\underline{r}_j$ be the space coordinate of particle j, and let $\underline{R}_j$ be its time-dependent centre. The Schrodinger equation is now

$$i\hbar\frac{\partial\Psi}{\partial t} = -\frac{\hbar^2}{2m}\nabla^2\Psi + V(\underline{r}_1,\ldots,\underline{r}_N)\Psi \qquad (5.16)$$

In this work the potential has been assumed to be pairwise additive. The condition of normalisation gives a relation between the imaginary parts of the A,B and D parameters.

$$\langle\phi_j|\phi_j\rangle = (\hbar\pi)^{3/2} \exp(-2D'_j/\hbar) (\Delta_j)^{-\frac{1}{2}}$$

where Δ_j is the determinant

$$\begin{vmatrix} 2A'_{jx} & B'_{jxy} & B'_{jxz} \\ B'_{jxy} & 2A'_{jy} & B'_{jyz} \\ B'_{jxz} & B'_{jyx} & 2A'_{jz} \end{vmatrix} \qquad (5.17)$$

and Ω' is used as shorthand for Im Ω. This condition is used to set the initial vlue of D_j, but is not used at any other point in the calculation. It therefore gives a check on the stability of the numerical solution of the eqautions of motion. It would be possible to use the condition to eliminate some of the equations, but the ability to use it as a check is more important. Energy conservation provides another such check.

The expansion of the potential about the point $\underline{R}$ leads to a rather lengthy expression:-

$$V(r_1,\ldots,r_N) = V(R_1,\ldots,R_N) + \sum_{j,\alpha}(r_{j\alpha}-R_{j\alpha})\left(\frac{\partial V}{\partial r_{j\alpha}}\right) + \tfrac{1}{2}\sum_{j,\alpha}(r_{j\alpha}-R_{j\alpha})^2\left(\frac{\partial V}{\partial r_{j\alpha}}\right) + \sum_{j,\alpha\neq\beta}(r_{j\alpha}-R_{j\alpha})(r_{j\beta}-R_{j\beta})\left(\frac{\partial V}{\partial r_{j\alpha}\partial r_{j\beta}}\right) + \sum_{\substack{j\neq k\\ \alpha,\beta}}(r_{j\alpha}-R_{j\alpha})(r_{k\beta}-R_{k\beta})\left(\frac{\partial V}{\partial r_{j\alpha}\partial r_{k\beta}}\right) \qquad (5.18)$$

Here α,β represent the cartesian components of $\underline{r},\underline{R}$, etc, j,k run over atoms 1...N, and the derivatives are to be evaluated at $\underline{r}=\underline{R}$. Higher derivatives are neglected. The last term on the r.h.s contains cross term involving two atoms, which cannot be accomodated unless the wavefunction contains similar cross terms, that is, unless the product (5.1) is abandoned. This would be prohibitively awkward to do. We therefore use an approximation in the spirit of Hartree, and replace

$$V_j = \tfrac{1}{2}\sum_{j\neq k} v_{jk}(r_{jk})$$

where v_{jk} is a pair interaction, and $r_{jk} = |\underline{r}_k - \underline{r}_j|$, by

$$\bar{V}_j = \tfrac{1}{2}\sum_{j\neq k} \langle\phi_k|v_{jk}|\phi_k\rangle \qquad (5.19)$$

When applied to (5.18) this has the effect of eliminating the cross terms, since the expectation value of $\underline{r}_k-\underline{R}_k$ vanishes by symmetry. The terms in the potential first derivative also vanish, by the same argument. Using these results, (5.16) becomes

$$i\hbar\frac{\partial\phi_j}{\partial t} = -\frac{\hbar^2}{2m}\nabla_j^2\phi_j + \tfrac{1}{2}\bar{V}_j\,\phi_j \qquad (5.20)$$

This immediately can be written as a set of N equations each involving only one atom. These equations involve

the other atoms only through the potential derivatives.

$$i\hbar\frac{\partial\phi_j}{\partial t} = -\frac{\hbar^2}{2m}\nabla^2\phi_j + \{\tfrac{1}{2}\sum_{k\neq j} v_{jk}(R_{jk}) + \sum (r_{j\alpha}-R_{j\alpha})\frac{\partial V}{\partial r_{j\alpha}} + \sum (r_{j\alpha}-R_{j\alpha})^2\frac{\partial^2 V}{\partial r_{j\alpha}^2} + \sum (r_{j\alpha}-R_{j\alpha})(r_{j\beta}-R_{j\beta})\frac{\partial^2 V}{\partial r_{j\alpha}\partial r_{j\beta}} \tag{5.21}$$

The time derivatives can be substituted from (5.8), with the results shown below:-

$$\frac{\partial\phi}{\partial A_{jx}} = \frac{i}{\hbar}(x_j - X_j)^2\,\phi_j$$

$$\frac{\partial\phi}{\partial B_{jxy}} = \frac{i}{\hbar}(x_j - X_j)(y_j - Y_j)\,\phi_j$$

$$\frac{\partial\phi}{\partial P_{jx}} = \frac{i}{\hbar}(x_j - X_j)\,\phi_j$$

$$\frac{\partial\phi}{\partial D_j} = \frac{i}{\hbar}\,\phi_j$$

$$\frac{\partial\phi}{\partial X_j} = -\frac{i}{\hbar}\{2A_{jx}(x_j - X_j) + B_{jxy}(y_j - Y_j) + B_{jxz}(z_j - Z_j) + P_{jx}\}\,\phi_j \tag{5.22}$$

All of these results can then be substituted into (5.21), and coefficients of powers of the coordinates collected. This will result in a set of equations which will, with a little rearrangement, give a useful set of equations of motion. We find:-

Constant terms--

$$D = \frac{i\hbar}{m}(A_x + A_y + A_z) - \tfrac{1}{2}\sum_k v_{jk} + \underline{R}.\underline{P} - \frac{1}{2m}(\underline{P}.\underline{P}) \tag{5.23}$$

Since the equations now involve only atom j, the subscript j will be omitted for clarity.

Linear terms--

These give a set of equations which are again satisfied by the classical equations of motion;-

$$\dot{X}_j = P_{jx}/m$$

$$\dot{P}_{jx} = -(\partial V/\partial r_{jx}) \qquad (5.24)$$

Quadratic terms--

These give two sets of equations, for the A and B parameters respectively:-

$$\dot{A}_x = -\frac{1}{2m}\{4A_x^2 + B_{xy}^2 + B_{xz}^2\} - \tfrac{1}{2}\left(\frac{\partial^2 V}{\partial r_x^2}\right)$$

$$\dot{B}_{xy} = -\frac{1}{2m}\{4B_{xy}(A_x + A_y) + 2B_{xz}B_{yz}\} - \left(\frac{\partial^2 V}{\partial r_x \partial r_y}\right) \qquad (5.25)$$

These results could be written more elegantly using matrix and vector notation, but since FORTRAN does not allow such things the full notation used above will be used to remain as close as possible to the expressions actually written in FORTRAN.

The potential derivatives used in the equations of motion are, in the case of the Lennard-Jones potential,

$$\left\{\frac{\partial V}{\partial r_x}\right\} = -24\varepsilon \sum_{k\neq j} (d_x/R_{jk}^2)(S - 2T) \qquad (5.26)$$

$$\left\{\frac{\partial^2 V}{\partial r_x^2}\right\} = 24\varepsilon \sum_{k\neq j} \{(S - 2T)/R_{jk}^2 + (d_x^2/R_{jk}^4)(28T - 8S)\} \qquad (5.27)$$

$$\left\{\frac{\partial V}{\partial r_x \partial r_y}\right\} = 24\varepsilon \sum_{k\neq j} (d_x d_y/R_{jk}^4)(28T - 8S) \qquad (5.28)$$

Here we have written $d_x \equiv R_{kx} - R_{jx}$; $S = (\sigma/R_{jk})^6$, and $T = S^2$. We thus have a complete set of equations of motion, and can set up a molecular dynamics style simulation. Since the potential has been Taylor expanded, the method will be applicable only at low temperatures for solids, that

is, only within the region where the harmonic approx. is valid.

The potential expectation value can be calculated from (5.26-5.28), and the expectation values of $(x - X)^2$, etc, which are given by

$$\langle x^2 \rangle = \langle \phi | (x - X)^2 | \phi \rangle = \frac{\hbar}{2} \left(4A'_y A'_z - B'^2_{yz} \right) / \Delta \qquad (5.29)$$

Here (5.17) has been used to eliminate a factor of unity. The kinetic energy expectation is given by a sum of terms like $(\partial^2\phi/\partial x^2)$, and each of these is given by

$$-\frac{\hbar}{2m} \frac{\partial^2 \phi}{\partial x^2} = -\frac{i\hbar}{m} A_x + \frac{1}{2m} \{ P_x^2 + 4A_x^2 \langle x^2 \rangle + B_{xy}^2 \langle xy \rangle + B_{xz}^2 \langle xz \rangle + 2B_{xy} B_{xz} \langle yz \rangle + 4A_x (B_{xy} \langle xy \rangle + B_{xz} \langle xz \rangle) \} \qquad (5.30)$$

Note the presence of the classical kinetic energy. We now have a complete prescription for carrying out a molecular dynamics calculation , in that the equations of motion can be numerically solved using standard methods, and the expectation values of both potential and kinetic energies can be calculated. However, before this can be attempted, initial values must be supplied for all of the parameters. The positions can be set on a face-centred cubic lattice, precisely as in a classical simulation, and the momenta can be chosen from the appropriate normal distribution. There remain only the A,B,D parameters, and the D are determined by the requirement of normalisation. The real parts of the D, the phase of the wavefunction, can be ignored, as they nowhere enter into the calculation. In the case of the harmonic oscillator, these parameters were chosen such that the derivatives $\dot{A}$ vanished. Hence these parameters are chosen by requiring that initially their time derivatives vanish.

The method has the advantage that the classical kinetic and potential energies can be calculated alongside the quantum results, which in turn allows checking against a classical molecular dynamics simulation. This also means that a comparison of classical and quantum results is possible without carrying out a separate classical calculation.

The method has been implemented using a standard Runge-Kutta algorithm to integrate the equations of motion of 108 wavepackets. As an initial test, the harmonic oscillator problem was used, since the results are already known. The potential used was

$$V(r_1,\ldots,r_N) = \tfrac{1}{2}k \sum_j (r_j - L_j)^2 \qquad (5.31)$$

where L_j is the jth lattice site. The equations of motion obtained are those for a set of 3N non-interacting oscillators, with force constant k. The wavepacket parameters were set so that their derivatives vanished, and the mass and force constant were chosen . These were appropriate to a frequency $\omega = 4.216 \times 10^{12}$ Hz, and thus to a zero point energy $3N_o\hbar\omega/2 = 4016.31$ J mol^{-1}. This was the value obtained in the simulations. Several points were checked with this program, notably that energy and normalisation were conserved. Some of the results are given in Table 5.1.

The method is exact for harmonic potentials, numerically as well as analytically. The effect of non-harmonic terms in the potential has been investigated by adding such a term to the potential given by (5.31), and varying its

magnitude. This term gives rise to a loss of energy conservation, loss of normalisation, more so if the anharmonic part is larger. This failure is entirely in accord with the derivation of the method.

Table 5.1 Results obtained for 108 harmonic oscillators using Heller's first method.

Steps	Potential (classical)	Kinetic	Potential (quantum)	Kinetic
150	74.839	72.89	2089.9	2080.0
1450	74.365	73.36	2081.5	2080.5
150	748.39	728.9	2755.5	2736.0
150	3741	3644	5749	5651
1450	7436	7336	9443	9343

The method has been applied to the Lennard-Jones solid at low temperatures, 1,2 K for Neon, and 10 K for argon. The results obtained are presented in Table 5.2, where each result was obtained from a run of 1000 steps of .75 fs, starting from an equilibriated 108 atom system. The difference between the classical and quantum total energy will be referred to as the Zero point energy. It is clear that the zero point energy of Argon is larger than that of Neon, at the minimum in the quantum total energy. This is in accord with the prediction of the Debye model, and the known Debye temperatures of the two substances. The results for the quantum total energy are shown in Figure 5.1, along with ground state results obtained by Hansen (26).

Table 5.2 Results obtained for Lennard-Jones solids using Hellers First method.

a. Argon,10K

V	PE_c	PE_q	KE_c	KE_q	TE_c	TE_q	ZPE	$\langle x^2 \rangle$
cc/mol	←	-	-	J/mol	-	-	→	$10^{-22} m^2$
18	-6597	-5851	127	873	-6470	-4978	1492	0.51
19	-7609	-6964	113	758	-7496	-6206	1290	0.59
20	-8162	-7601	116	677	-8046	-6924	1122	0.68
21	-8408	-7918	119	610	-8289	-7308	981	0.79
22	-8450	-8019	133	564	-8317	-7455	862	0.91
23	-8366	-7985	121	501	-8245	-7484	761	1.04
25	-7952	-7649	148	452	-7804	-7197	607	1.40

b. Neon, 2K

V	PE_c	PE_q	KE_c	KE_q	TE_c	TE_q	ZPE	$\langle x^2 \rangle$
12.0	-2608	-2193	26	441	-2582	-1752	830	1.80
12.5	-2592	-2224	24	392	-2568	-1832	736	2.06
13.0	-2550	-2223	25	352	-2525	-1871	654	2.30
13.25	-2521	-2212	28	337	-2493	-1875	618	2.50
13.5	-2489	-2196	29	323	-2460	-1873	620	2.66
13.75	-2454	-2176	31	311	-2423	-1865	558	2.80
14.0	-2417	-2153	32	297	-2385	-1856	529	3.00
14.5	-2339	-2099	32	270	-2307	-1829	478	3.50
15.0	-2258	-2040	31	247	-2227	-1793	434	4.00

c Neon, 1K

V	PE_c	PE_q	KE_c	KE_q	TE_c	TE_q	ZPE	$\langle x^2 \rangle$
12.0	-2620	-2209	13	423	-2607	-1786	821	1.84
12.5	-2603	-2240	12	374	-2591	-1866	725	2.07
13.0	-2561	-2239	13	334	-2548	-1905	643	2.30
13.25	-2533	-2230	14	317	-2519	-1913	606	2.50
13.5	-2501	-2215	15	301	-2486	-1914	572	2.65
13.75	-2467	-2198	16	286	-2451	-1912	539	2.80
14.0	-2430	-2176	16	271	-2414	-1905	509	3.0

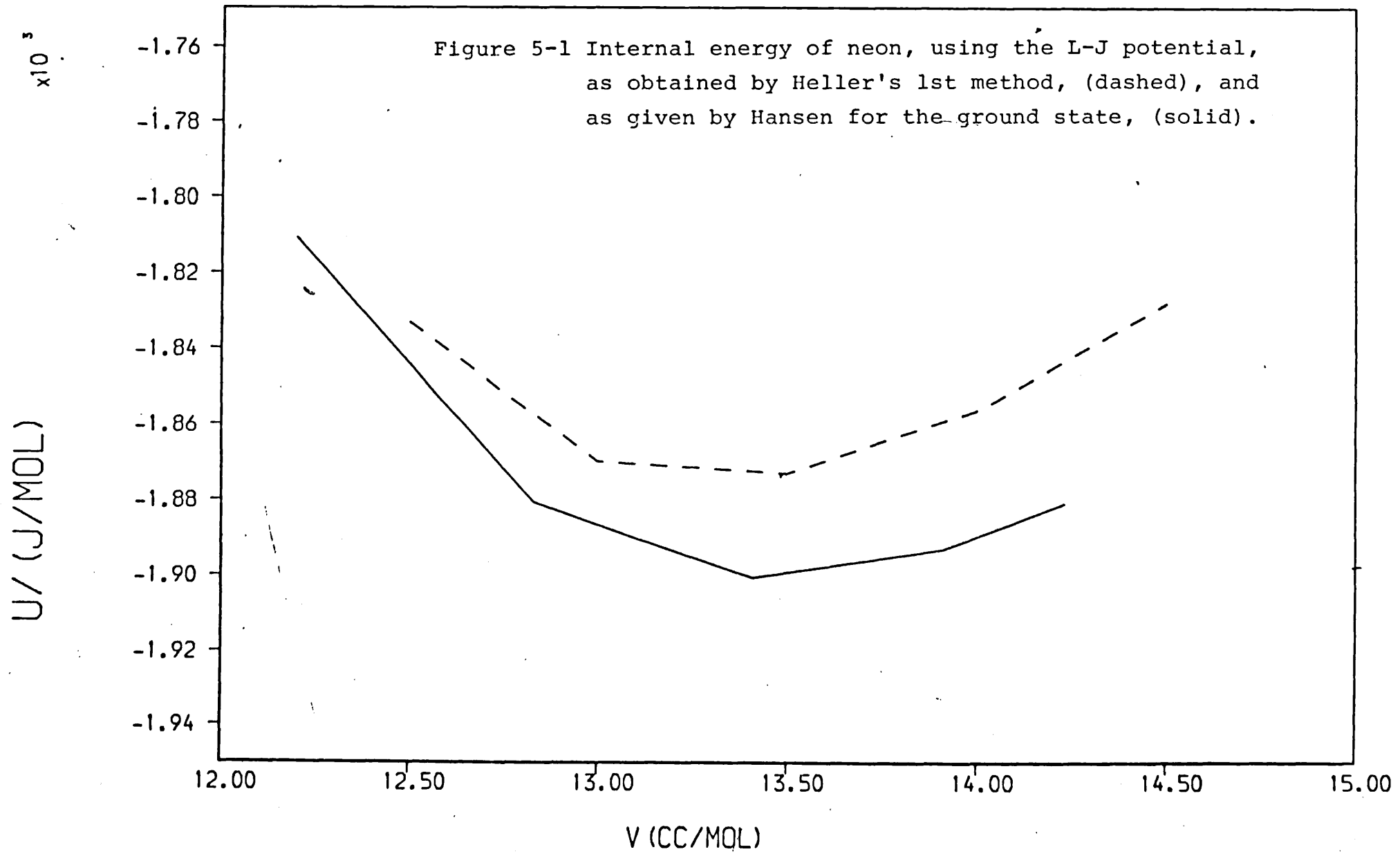

Figure 5-1 Internal energy of neon, using the L-J potential, as obtained by Heller's 1st method, (dashed), and as given by Hansen for the ground state, (solid).

It is possible to formulate this method slightly differently, (27), to obtain an added insight into the structure of the equations. For this application, the matrix notation is most convenient. Equation (5.25) can be written

$$\dot{\underline{\underline{A}}} = (-1/2m)\ \underline{\underline{A}}\ \underline{\underline{A}} - \tfrac{1}{2}\underline{\underline{V}}'' \qquad (5.32)$$

where $\underline{\underline{V}}''$ is the 3x3 matrix of potential second derivatives. Define

$$\dot{\underline{\underline{Z}}} = \mu \underline{\underline{Z}}\ \underline{\underline{A}} \qquad \mu = 1/\sqrt{2m}$$

Then

$$\ddot{\underline{\underline{Z}}} = \mu(\dot{\underline{\underline{Z}}}\ \underline{\underline{A}} + \underline{\underline{Z}}\ \dot{\underline{\underline{A}}})$$

$$\underline{\underline{Z}}\ \dot{\underline{\underline{A}}} = -(1/2m)\ \underline{\underline{Z}}\ \underline{\underline{A}}\ \underline{\underline{A}} - \tfrac{1}{2}\underline{\underline{Z}}\ \underline{\underline{V}}''$$

and

$$\ddot{\underline{\underline{Z}}} = -\tfrac{1}{2}\underline{\underline{Z}}\ \underline{\underline{V}}'' \qquad (5.33)$$

This equation has just the form of the harmonic oscillator equation, but where $\underline{\underline{V}}''$ varies with time.It is especially obvious from this formulation that problems will arise if ever the second derivatives become negative, since this corresponds to imaginary frequencies.

5.2 Variational approach.

The method described above obtains an approximate solution of the time-dependent Schrodinger equation by expanding the potential about the instantaneous centre of the wavepackets, and discarding cubic and higher terms. This clearly assumes that these terms are negligible, which certainly restricts the method to low temperature solids. An alternative approach is suggested by Heller, (24). This uses a variational principle due to McLachlan, (31), which says that for a system having wavefunction ψ and hamiltonian H, and if Θ is to be an approximation to $d\psi/dt$, then

$$I = \int \{H\psi - \Theta\}^2 \qquad (5.34)$$

should be a minimum for all allowed variations in ψ. The method has many possible applications, wherever the wavefunction can be written in a form containing time dependent parameters, such as (5.2), or a form like

$$\psi = \sum_n a_n(t)\ \phi_n$$

for some basis set $\{\phi_n\}$. The form (5.2) will be used throughout this work, and the time-dependent parameters will be referred to as the s_m, collectively. The variational principle leads easily to a set of equations in the $\dot{s}_m$, (eqn 2.7 in (24)):-

$$\int \left\{\frac{\partial \Psi}{\partial s_m}\right\}^{\bullet} H\Psi \, d\nu = i\hbar \int \left\{\frac{\partial \Psi}{\partial s_m}\right\}^{*} \{\Sigma \dot{s}_n \frac{\partial \Psi}{\partial s_n}\} d\nu \qquad (5.35)$$

This is clearly a set of linear equations, and if written as such we have

$$\underline{\underline{A}}\ \underline{\dot{s}} = \underline{B} \qquad (5.36)$$

For a wavefunction of the form (5.2), with 13 parameters, this gives rise to a set of (complex!) equations in 13N unknowns, where N is the number of atoms represented. Equation (5.19) is thus used to reduce the problem to N sets of 13 x 13 equations, one for each atom. It must be stressed that no expansion of the potential is used.

The elements of $\underline{\underline{A}}$ are related only to the form of the wavefunction used, whereas the elements of $\underline{B}$ depend on the Hamiltonian also. In the results below, the notation $\langle X|Y\rangle$ has been used for the integral $\int(\partial\phi/\partial X)^{*}\partial\phi/\partial Y$, and the expectation values defined by (5.29) have been used. All results not quoted below can be obtained by symmetry. The subscript labelling the atoms has been omitted for clarity, these equations hold for each atom.

$$\begin{aligned}\langle X|X\rangle = \{\ & 4|A_x|^2\langle x^2\rangle + 2(A_xB_{xy}^{*} + A_x^{*}B_{xy})\langle xy\rangle \\ & + |B_{xy}|^2\langle y^2\rangle + 2(A_xB_{xz}^{*} + A_x^{*}B_{xz})\langle xz\rangle \\ & + |B_{xz}|^2\langle z^2\rangle + (B_{xy}B_{xz}^{*} + B_{xy}^{*}B_{xz})\langle yz\rangle \\ & + P_x^2\ \}/\hbar^2 \end{aligned} \tag{5.37}$$

$$\begin{aligned}\langle Y|X\rangle = \langle X|Y\rangle^{*} = \{\ & 2A_x^{*}B_{xy}\langle x^2\rangle + (4A_xA_y^{*} + |B_{xy}|^2)\langle xy\rangle \\ & + 2A_y^{*}B_{xy}\langle y^2\rangle + (2A_xB_{yz}^{*} + B_{xz}B_{xy}^{*})\langle xz\rangle \\ & + B_{xz}B_{yz}^{*}\langle z^2\rangle + (2A_y^{*}B_{xz} + B_{xy}B_{yz}^{*})\langle yz\rangle \\ & + P_xP_y\ \}/\hbar^2 \end{aligned} \tag{5.38}$$

$$\langle P_x|X\rangle = -\{2A_x\langle x^2\rangle + B_{xy}\langle xy\rangle + B_{xz}\langle xz\rangle\}/\hbar^2 \tag{5.39}$$

$$\langle P_y|X\rangle = -\{2A_x\langle xy\rangle + B_{xy}\langle y^2\rangle + B_{xz}\langle yz\rangle\}/\hbar^2 \tag{5.40}$$

$$\langle P_x|P_x\rangle = \langle x^2\rangle/\hbar^2 \tag{5.41}$$

$$\langle P_x|P_y\rangle = \langle xy\rangle/\hbar^2 \tag{5.42}$$

$$\langle A_x|X\rangle = -P_x\langle x^2\rangle/\hbar^2 \tag{5.43}$$

$$\langle A_y|X\rangle = -P_x\langle y^2\rangle/\hbar^2 \tag{5.44}$$

$$\langle B_{xy}|X\rangle = -P_x\langle xy\rangle/\hbar^2 \tag{5.45}$$

$$\langle B_{xy}|Z\rangle = -P_z\langle xy\rangle/\hbar^2 \tag{5.46}$$

$$\langle D|X\rangle = -P_x/\hbar^2 \tag{5.47}$$

$$\langle A_x|A_y\rangle = \langle x^2y^2\rangle/\hbar^2 \tag{5.48}$$

$$\langle B_{xy}|B_{xy}\rangle = \langle x^2y^2\rangle/\hbar^2 \tag{5.49}$$

$$\langle D|A_x\rangle = \langle x^2\rangle/\hbar^2 \tag{5.50}$$

$$\langle D|B_{xy}\rangle = \langle xy\rangle/\hbar^2 \tag{5.51}$$

$$\langle D|D\rangle = 1/\hbar^2 \tag{5.52}$$

$$\langle P_x|A_x\rangle = \langle P_x|B_{xy}\rangle = \langle P_x|D\rangle = 0 \tag{5.53}$$

All others may be obtained from the above by using the symmetry with respect to (x,y,z). The other values required are

$$\langle x^4\rangle = 3\langle x^2\rangle^2$$

$$\langle x^2yz\rangle = 3\langle x^2\rangle\langle yz\rangle + \tfrac{1}{2}\hbar^2 B'_{yz}/\Delta$$

etc, where Δ is given by (5.17), and the ' denotes the imaginary part.

The terms arising from the kinetic energy part of the Hamiltonian are more complicated, and again only some will be quoted. The remainder are either related by symmetry to those given, or simply related to the kinetic energy expression (5.30).

$$\int \left\{\frac{\partial\phi}{\partial X}\right\}^* \frac{\partial^2\phi}{\partial x^2}\, dV = P_x A_x/m + {}^{iP_x}/_{(2m\hbar)} \times \{$$

$$4A_x^2\langle x^2\rangle + B_{xy}^2\langle y^2\rangle + B_{xz}^2\langle z^2\rangle + P_x^2$$

$$+ 4A_x(B_{xy}\langle xy\rangle + B_{xz}\langle xz\rangle) + 2B_{xy}B_{xz}\langle yz\rangle$$

$$+ 4A_x^*(2A_x\langle x^2\rangle + B_{xy}\langle xy\rangle + B_{xz}\langle xz\rangle)$$

$$+ 2B_{xy}^*(2A_x\langle xy\rangle + B_{xy}\langle y^2\rangle + B_{xz}\langle yz\rangle)$$

$$+ 2B_{xz}^*(2A_x\langle xz\rangle + B_{xy}\langle yz\rangle + B_{xz}\langle z^2\rangle)\} \qquad (5.54)$$

$$\int \left\{\frac{\partial\phi}{\partial P_x}\right\}^* \frac{\partial^2\phi}{\partial x^2}\, dV = -i/(2m\hbar) \times \{$$

$$4A_xP_x\langle x^2\rangle + 2B_{xy}P_x\langle xy\rangle + 2B_{xz}P_x\langle xz\rangle$$

$$+ 4A_yP_y\langle xy\rangle + 2B_{yz}P_y\langle xz\rangle + 2B_{xy}P_y\langle x^2\rangle$$

$$+ 4A_zP_z\langle xz\rangle + 2B_{xz}P_z\langle x^2\rangle + 2B_{yz}P_z\langle xy\rangle \} \qquad (5.55)$$

The only remaining elements to be evaluated are the potential energy terms, which depend on the form of the potential, as well as the form of the wavefunction. Initially, the harmonic oscillator potential was used, binding each atom to its initial position. This system can easily be solved exactly. The results obtained were in precise agreement with the exact answer, and the same results as obtained using the first method above.

The addition of an anharmonic term to the potential did not lead to the same problems as the first method, that is, the wavepackets did not spread in the same way. These simple cases do not require the Hartree-like approximation,which makes them much simpler to implement.

The form of the integrals involved is much simplified if the potential is taken as a sum of Gaussians, indeed, the integrals do not exist if the potential has the Lennard-Jones form. This is one of the main reasons for the use of the Gaussian potential. The difficulty could be removed by the use of devices such as the expansion of the potential about its minimum, or truncating it in such a way that the integrals exist, but that the results are not affected.

The Gaussian potential also has the advantage that all of the integrals required can be evaluated analytically, using the results given in the Appendix. Specifically, (A.2) is used twice, once to obtain $\bar{V}_j$, and again to find the expectation value $\langle\phi_j|\bar{V}_j|\phi_j\rangle$. The substitutions

$$\begin{aligned} \underline{r}_k - \underline{r}_j &\rightarrow \underline{r}_k - \underline{R}_k - (\underline{r}_j - \underline{R}_k) \\ \underline{r}_j - \underline{R}_k &\rightarrow \underline{r}_j - \underline{R}_j - (\underline{R}_k - \underline{R}_j) \end{aligned} \qquad (5.56)$$

will be found useful in this context. Specifically,

$$\begin{aligned} \bar{V}_j &= \tfrac{1}{2} \sum_{k\neq j} \langle\phi_k|u_{jk}|\phi_k\rangle \\ &= \tfrac{1}{2} \sum A_n \int \phi_k^* \exp(-B_n r_{jk}^2)\, \phi_k \, d\underline{r}_k \end{aligned}$$

where the summation is over $k\neq j$, and $n=1,2$ from (1.2). Then, using (A.2), we have

$$\bar{V}_j = \tfrac{1}{2} \sum A_n \left(8\pi^3/\det \underline{\underline{\Omega}}_k\right)^{\frac{1}{2}} \exp\left(\tfrac{1}{2}\underline{\eta}_{kj}\cdot\underline{\underline{\Omega}}_k^{-1}\cdot\underline{\eta}_{kj} - \mu_{kj}\right)$$

where

$$\mu_{kj} = B_n (\underline{r}_j - \underline{R}_k)^2 + 2/\hbar D_k'$$

$$\underline{\eta}_{kj} = -2B_n(\underline{r}_j - \underline{R}_k)$$

and

$$\underline{\underline{\Omega}}_k = \begin{pmatrix} 2(B_n + 2/\hbar\, A'_{kx}) & 2/\hbar\, B'_{kxy} & 2/\hbar\, B'_{kxz} \\ 2/\hbar\, B'_{kxy} & 2(B_n + 2/\hbar\, A'_{ky}) & 2/\hbar\, B'_{kyz} \\ 2/\hbar\, B'_{kxz} & 2/\hbar\, B'_{kyz} & 2(B_n + 2/\hbar\, A'_{kz}) \end{pmatrix}$$

Note that the $\underline{\underline{\Omega}}_k$ is a symmetric, positive definite matrix, independent of particle j.This much simplifies the computation, since the matrix inverse need only be calculated once for each atom, rather than for each pair. The same devices can be used again to obtain the final expectation value. The various integrals like

$$\langle\phi_j|(x_j - X_j)\,\bar{V}_j|\phi_j\rangle$$

and

$$\langle\phi_j|(x_j - X_j)^2\bar{V}_j|\phi_j\rangle$$

can readily be obtained by differentiating the final result with respect to parameters, as shown in the appendix.

It is worth noting that the $\bar{V}_j$ are functions of the parameters A_{kx}, etc., which was not the case in the first method, where the equations of motion for particle j were independent of the shape of the wavepackets k, only depending on their centres. This is a very significant difference, and is expected to lead to very considerable differences between the two methods. It also implies a considerable difference in the computational effort needed to implement the two methods.

Given all of these integrals, it is possible to set up, and solve, the set of linear equations (5.36) to obtain the time derivatives of the parameters. These can then be used in a numerical integration algorithm to obtain the wavefunction as a function of time. A check on the accuracy of the algorithm can be obtained if the normalisation of each wavepacket is calculated at each step, since this should be unity always. The algorithm used for the first method, (a fourth order Runge-Kutta scheme) requires the evaluation of the derivatives four times for each step. This is not possible with this method, because of the computer time involved, and so a predictor-corrector algorithm was used. In order to achieve good conservation of normalisation, a fifth order algorithm was required, with a timestep of .75 fs.

The method has been tested, as far as possible, by allowing only one atom to move, with the remainder held fixed. This is of course very much quicker than a full scale simulation. These tests show that normalisation and total energy are both conserved, as they should be. These results apply for the Gaussian potential modelling neon, at temperatures in the liquid region.Similar tests for the first method were unsatisfactory above about 5 K, as a comparison.

The method has been applied to a number of low temperature simulations of neon, comparable with those carried out using the first method. The results are shown in table 5.3, for a system of 108 atoms interacting through the Gaussian potential. Note especially that the zero-point energy obtained is larger, and that the wavepackets are

narrower, than in the corresponding results in Table 5.2. These are more likely due to the difference between the Lennard-Jones and Gaussian potentials, than to the methods used. To test this, the first method was applied to the Gaussian potential, to obtain the results in Table 5.4. Comparing these with equivalent Lennard-Jones data from Table 5.2. we see:-

1. The potential energy is some 300 J/mol more positive for the Gaussian potential than for the L-J.
2. The total energy has a minimum at about 13.5 cc/mol.
3 The wavepacket widths are very similar.

Looking to the results in Table 5.3, using the second method, we see that the method leads to a slightly more negative potential energy, and a considerably more positive kinetic energy, with the total energy being more positive. The wavepackets are noticeably narrower than in the results for the first method. These differences are readily explained in terms of the better handling of the strongly repulsive part of the pair potential in the second method.

The zero point energies are also larger, but these should not be taken seriously, since the classical averages obtained in the second method are not in fact true classical averages, because the trajectory is not the classical one. We have, by Ehrenfest's theorem,

$$\frac{d}{dt} \langle p_x \rangle = - \langle \frac{dV}{dx} \rangle$$

and note that the r.h.s. is not generally equal to the classical force. If, and only if, they are equal, then the centre of the wavepacket follows the classical

trajectory, and classical and quantum results can be obtained simultaneously. Since they are not equal in the second method, the classical averages cannot be found. As a consequence, it has not been possible to define the temperature. In a classical simulation, this would be done by using the known relation between temperature and mean kinetic energy, but no such relation is possible quantum mechanically.

In passing, it should be said that Ehrenfests theorem also leads to some equations of motion for the parameters of the wavepackets. In addition to the result quoted above, we have

$$\frac{d}{dt} \langle x \rangle = \langle p_x \rangle / m$$

These results can be used to eliminate six of the thirteen equations for each atom, leading to a 7x7 matrix problem, which is computationally much easier. This simplification does not in any way alter the results, which provides a very useful check on the programming.

The method has been applied to neon, and to a lesser extent helium and argon, over a wide range of conditions. Each run was started from an fcc lattice, and the wavepackets were initialised by the same condition as was used in the first method, that is, by requiring that the wavepacket width be initially stationary. The dependence of the $\bar{V}_j$ on the wavepacket parameters complicates this procedure, since no equation analogous to (5.32) can be written. 32 atoms were used, in the usual periodic boundary conditions, with a timestep of .75 fs. Each run consisted of 6000 steps, with averages being taken over

the last 4000. Table 5.5 gives the results obtained. A comparison of these results with classical data is not easy, lacking temperature, but the results seem to be generally reasonable. The lower energy states are solids, the higher liquid. Note that the method is totally stable under all of the conditions used here. The wavepackets representing helium are the widest, with those representing the heavier systems being narrower by a factor of about three. This is expected, since the expectation values of kinetic and potential energy tend to the classical values as the A_x etc. tend to infinity, in which limit the width of the wavepackets becomes zero. The extent of the wavepackets can clearly be seen in the single particle density matrix, nl(r), defined by

$$nl(\underline{r}) = \int \Psi^*(\underline{r}_1+\underline{r},\underline{r}_2,\ldots,\underline{r}_N)\ \Psi(\underline{r}_1,\ldots,\underline{r}_N)\ d\underline{r}_1\ldots d\underline{r}_N$$

This function has been calculated as a function of $|\underline{r}|$ by averaging over all atoms, and over each 100th step in the simulations reported above. While the wavepackets are not generally spherically symmetric, at any given time, they are so on average. The results obtained for typical helium and neon runs are shown in Figure 5-3. Note that nl(0) = 1, by normalisation of the wavefunction.

The radial distribution function can be estimated by calculation of the expectation value of a delta-function, and using the definition of the latter,

$$\delta(x) = \int_{-\infty}^{\infty} \exp ikx\ dx.$$

Clearly, this is related to the probability of finding two particles a distance $\underline{r}$ apart,

$$< \Psi \mid \delta(\underline{r}_i - \underline{r}_j - \underline{r}) \mid \Psi > .$$

It is not easy to calculate g(r) from this approach, and the computational effoert involved is considerable. Classically, if two particles are located at $\underline{r},\underline{r}'$, then the distance between them is certainly $|\underline{r} - \underline{r}'|$, but in the case of wavepackets centred at $\underline{R},\underline{R}'$ there is a finite probability of finding the particles separated by a range of distances in the neighbourhood of $|\underline{R} - \underline{R}'|$. The extent of this neighbourhood clearly depends on the extent of the wavepackets. Two examples of the results obtained are shown in Figures 5.4,5.5, the first being for Argon at V_m = 33.5 cc/mol, T≃ 120 K, the second for Neon, V_m = 18.5 cc/mol, T≃ 40 K. These should be regarded with caution, in view of the small size of the system, (32 atoms), and the limited number of time steps used in the simulation, (each tenth step, in a run of 1000).

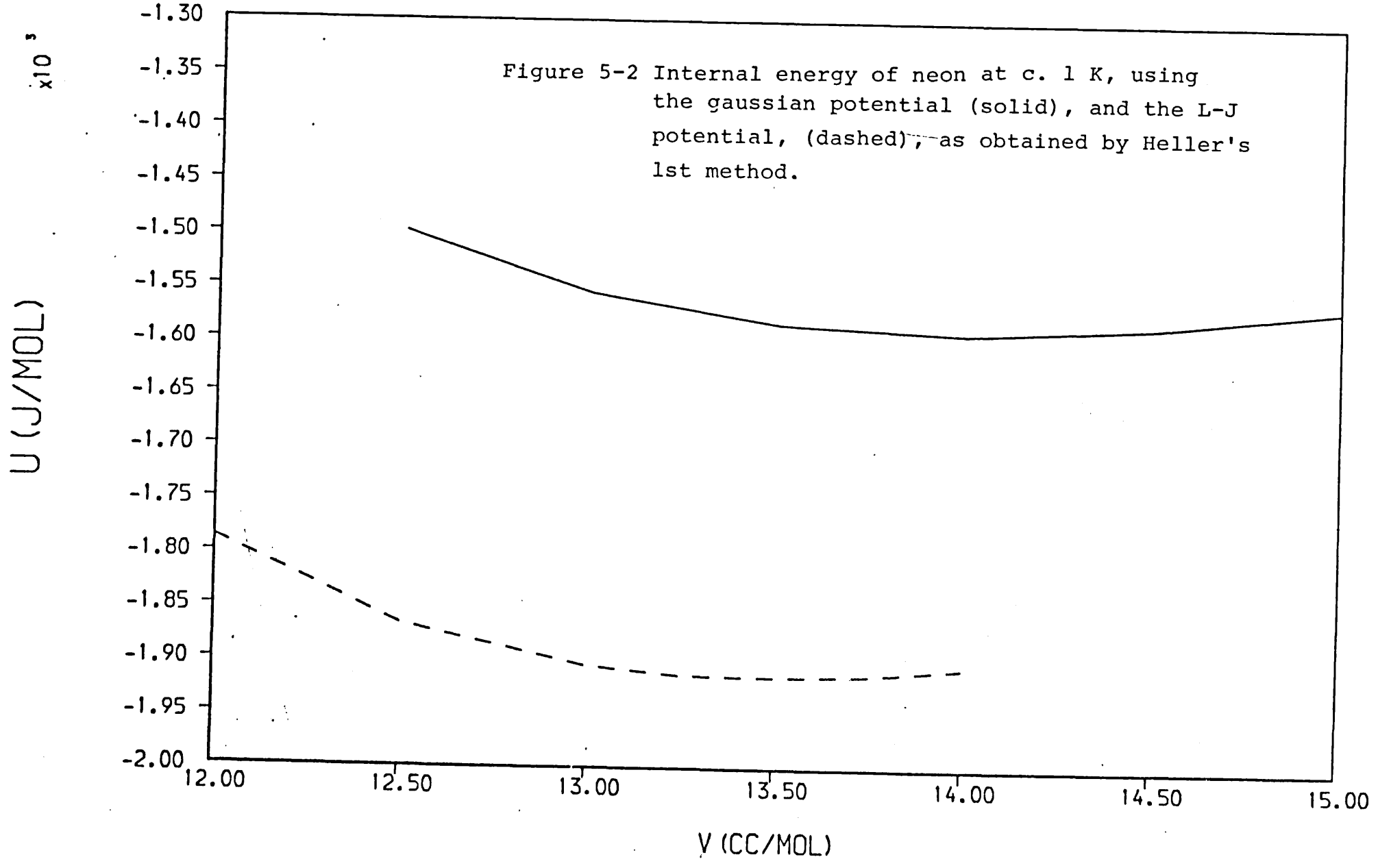

Figure 5-2 Internal energy of neon at c. 1 K, using the gaussian potential (solid), and the L-J potential, (dashed), as obtained by Heller's 1st method.

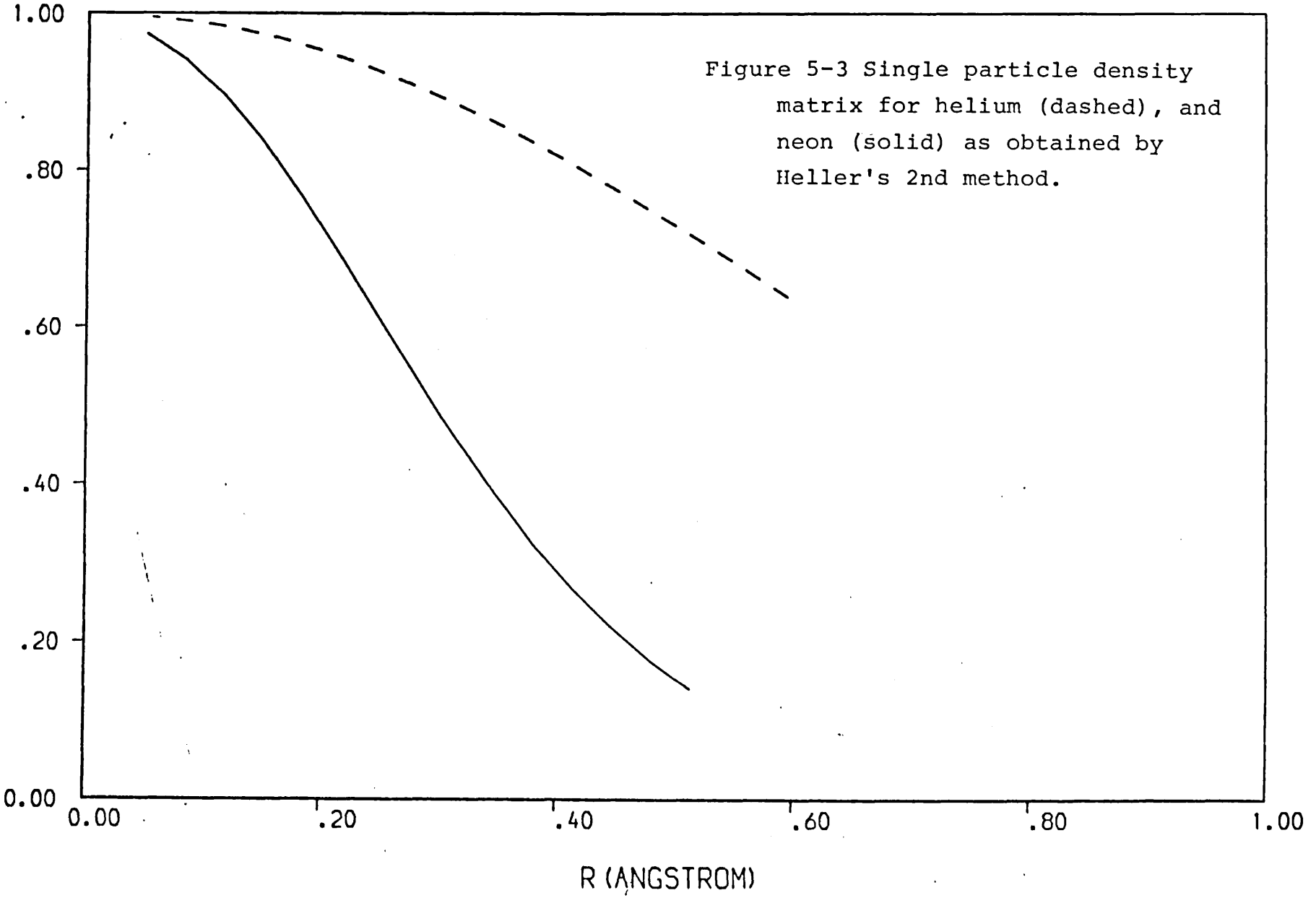

Figure 5-3 Single particle density matrix for helium (dashed), and neon (solid) as obtained by Heller's 2nd method.

Table 5.3 Results obtained for the Gaussian model of Neon, using the second method of Heller.

$V/(ccmol^{-1})$	$PE_q/(Jmol^{-1})$	$KE_q/(Jmol^{-1})$	$TE_q(Jmol^{-1})$	$ZPE/(Jmol^{-1})$	$\langle\hat{x}^2\rangle/(10^{-22}m)$
12.5	-1976	476	-1500	838	.16
13.0	-1988	431	-1557	749	.17
13.5	-1978	393	-1585	671	.19
14.0	-1952	360	-1592	602	.21
14.5	-1915	330	-1585	543	.23
15.0	-1877	305	-1572	491	.24

Table 5.4 Results obtained for the Gaussian model of Neon using the first method of Heller.

$V/(ccmol^{-1})$	$PE_q/Jmol^{-1}$	$KE_q/Jmol^{-1}$	$TE_q/Jmol^{-1}$	$ZPE/Jmol^{-1}$	$\langle x^2 \rangle / 10^{-21} m^2$
12.5	-1947	386	-1561	748	.20
13.0	-1964	330	-1624	655	.23
13.5	-1955	303	-1652	576	.26
14.0	-1928	270	-1657	508	.30
14.5	-1889	240	-1649	450	.35

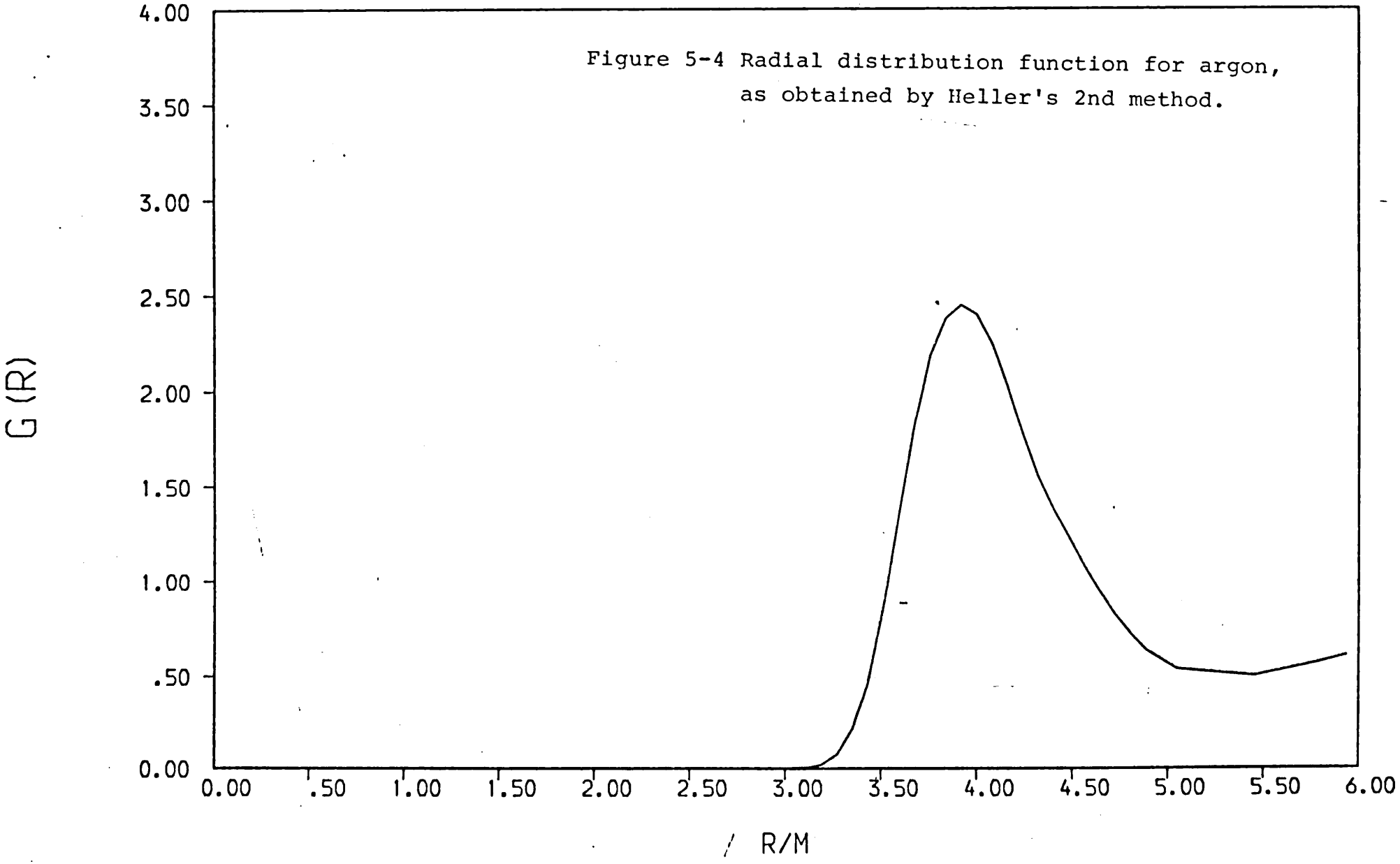

Figure 5-4 Radial distribution function for argon, as obtained by Heller's 2nd method.

Table 5.5 Results obtained for the Gaussian potential using Heller's second method.

$V/(ccmol^{-1})$	$PE/(Jmol^{-1})$	$KE/(Jmol^{-1})$	$TE/(Jmol^{-1})$	$\langle x^2 \rangle/(10^{-21}m^2)$	s/l
16.5	-1623	477	-1146	.33	s
	-1603	525	-1078	.34	s
	-1583	572	-1011	.35	s
	-1562	621	-941	.36	s
	-1542	670	-872	.37	s
	-1394	840	-554		l
	-1329	973	-356		l
	-1290	1117	-173		l
	-1232	1219	- 13		l
	-1162	1305	143		l

Table 5.5,cont.

V	PE	KE	TE	$\langle x^2 \rangle$	s/l
17.0	-1573	465	-1108	.36	s
	-1554	514	-1040	.36	s
	-1535	564	-971	.37	s
	-1512	610	-902	.37	s
	-1485	652	-833	.38	s
	-1352	828	-524		l
	-1304	976	-328		l
	-1233	1083	-150		l
	-1184	1194	10		l
	-1136	1312	176		l

Table 5.5,cont.

V	PE	KE	TE	$\langle x^2 \rangle$	s/l
17.5	-1524	455	-1069	.37	s
	-1504	503	-1001	.38	s
	-1481	549	-932	.39	s
	-1454	591	-863	.39	s
	-1396	607	-789	.39	l
18.0	-1473	444	-1029	.41	s
	-1452	490	-962	.40	s
	-1425	533	-892	.40	s
	-1374	553	-821	.41	s
	-1356	604	-752	.42	l
18.5	-1421	431	-990	.42	s
	-1397	476	-921	.42	s
	-1354	522	-832	.42	s
	-1334	533	-801	.45	l
	-1309	598	-711	.45	l

Table 5.5, cont.

b. Helium.

V	PE	KE	TE	$\langle x^2 \rangle$	s/l	Φ/Jmol^{-1}
22.0	-161	320	159	1.41	s	-68
	-143	371	228	1.40	s	51
	-129	425	296	1.40	l	116
24.0	-141	294	153	1.58	s	-66
	-125	347	222	1.56	l	27
	-111	400	289	1.55	l	113
26.0	-123	272	149	1.73	s	-53
	-110	328	221	1.74	l	30
	-96	381	285	1.70	l	116
28.0	-108	254	146	1.84	s	-40
	-96	311	215	1.86	l	43
	-84	367	283	1.92	l	118
c.Argon						
33.5	-4362	1620	-2742	0.50	l	

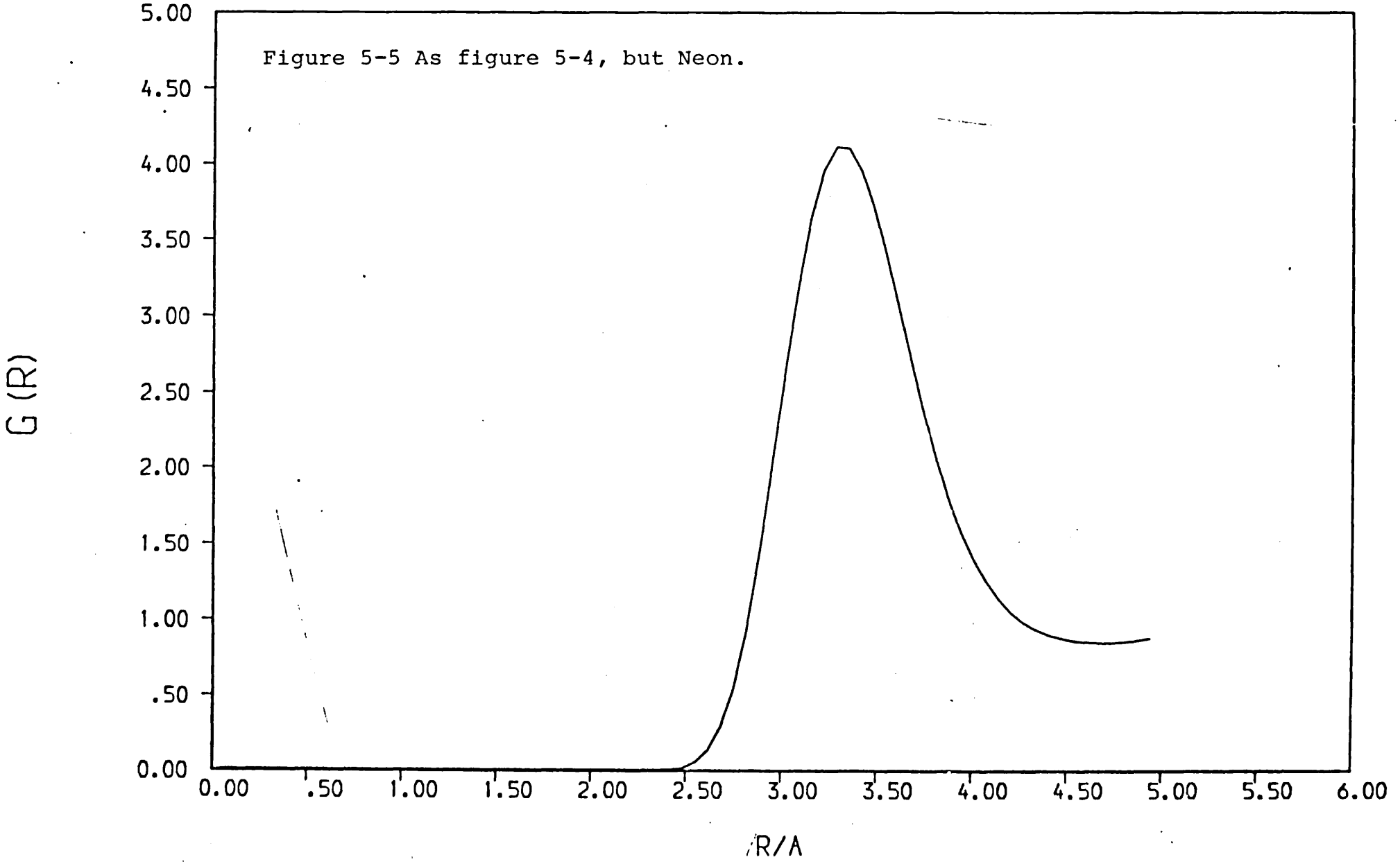

Figure 5-5 As figure 5-4, but Neon.

6. Conclusions and discussion.

In the preceeding chapters a number of different approaches have been used to include quantum effects in the computer simulation of simple systems. This chapter will gather together the results from all of these, and attempt to compare them, both to determine the importance of quantum effects, and the usefulness of the various methods. Several other possibilities will also be briefly discussed, although this dscussion will not be exhaustive.

6.1 The magnitude of quantum corrections.

The quantum corrections for Neon, as shown in chapter 3 using the Wigner expansion, are about 8-10%, with the $O(\hbar^4)$ correction to the second virial coefficient being about an order of magnitude smaller again. The same conclusion has been reached by Hansen & Weis (13), who used (3.6) and the higher order equivalent for a single state point. They used the Lennard-Jones potential, with ε=36.76K, σ=2.786 A, T=23.92K, and molar volume 15.76 cm^3mol^{-1}. The free energy correction obtained was, to second order in $\hbar$, 132 $Jmol^{-1}$, with the next term of the Wigner expansion amounting to 3.3 $Jmol^{-1}$. The classical free energy is given as -1367 $Jmol^{-1}$ at this state point.

This result is entirely comparable with the figures presented in chapter 3 of this work. Note that the second correction has the same sign as the first, which was not the case in the virial coefficients tabulated in table 3.1. The scaling properties of the Lennard-Jones potential enable this result to be scaled to correspond to both helium and argon, as pointed out previously. The results

are:-

	$A/(Jmol^{-1})$	A_1	A_2
Helium	-380	790	119
Neon	-1367	132	3.3
Argon	-4452	44	0.4

(These all correspond to $kT/\varepsilon=.65, \rho\sigma^3=.83$). The figures for helium clearly show that the Wigner expansion, as used in this work, does not converge nicely under the conditions of large quantum corrections. The results presented in chapter 3 are for a much higher temperature and lower density, where the convergence is likely to be better.

The free energy corrections have been fitted with a cubic spline, using a least-squares procedure, and the fitted function has been used to estimate the derivatives of the free energy with respect to both temperature and volume, for Neon. These results are tabulated in Table 6.1, for both Lennard-Jones and Gaussian potentials. The errors in the fitted function are everywhere small compared with the function values, and of the same order of magnitude as the errors in the simulation data.

The variation in ΔU and ΔP with both temperature and volume is marked, and in accord with the expectation that the corrections decrease with increasing temperature and molar volume. Figures 6.1 - 6.3 show these corrections as functions of either temperature or volume.The Gaussian potential leads to slightly larger corrections than the Lennard-Jones potential, for the reasons already stated above.

Table 6.1 Derivatives of free energy correction obtained from least squares spline fit, and related thermodynamic properties.

$V/(ccmol^{-1})$	T/(K)	$-\partial\Delta A/\partial V=\Delta P/(MPa)$	$\partial\Delta A/\partial T$	ΔU
16.5	25			
	30		-1.53	139
	35		-1.12	128
	40		-0.85	117
17.0	25	13.8		
	30	11.5	-1.34	129
	35	10.8	-1.11	121
	40	10.9	-0.88	112
	45	10.9	-0.67	103
	50	10.0		
17.5	25	10.9		
	30	10.3	-1.25	120
	35	9.8	-1.09	115
	40	9.7	-0.84	106
18.0	25	8.4		
	30	9.0	-1.24	121
	35	8.9	-1.06	114
	40	8.6	-0.86	106
18.5	25	6.4		
	30	7.9	-1.29	113
	35	8.1	-1.03	104
	40	7.5	-0.80	96
19.0	45		-0.52	80
21.0	45		-0.44	68
23.0	45		-0.36	57

b. Neon, Gaussian potential

V	T	ΔP	∂ΔA/∂T	ΔU
16.5	25			
	30		-1.69	157
	35		-1.57	
	40		-1.36	145
17.0	25	16.6		
	30	14.7	-1.46	141
	35	12.9	-1.37	138
	40	11.4	-1.19	132
	45	10.1	-0.92	119
	50	9.1		
17.5	25	12.3		
	30	12.1	-1.32	131
	35	11.1	-1.24	127
	40	10.1	-1.04	119
18.0	25	10.5		
	30	9.9	-1.24	121
	35	9.4	-1.17	121
	40	8.9	-1.01	114
18.5	25	8.1		
	30	8.0	-1.21	
	35	8.0	-1.15	115
	40	7.9	-0.97	109
19.0	45	6.9	-0.66	93
21.0	45	4.6	-0.64	78
23.0	45		-0.57	68

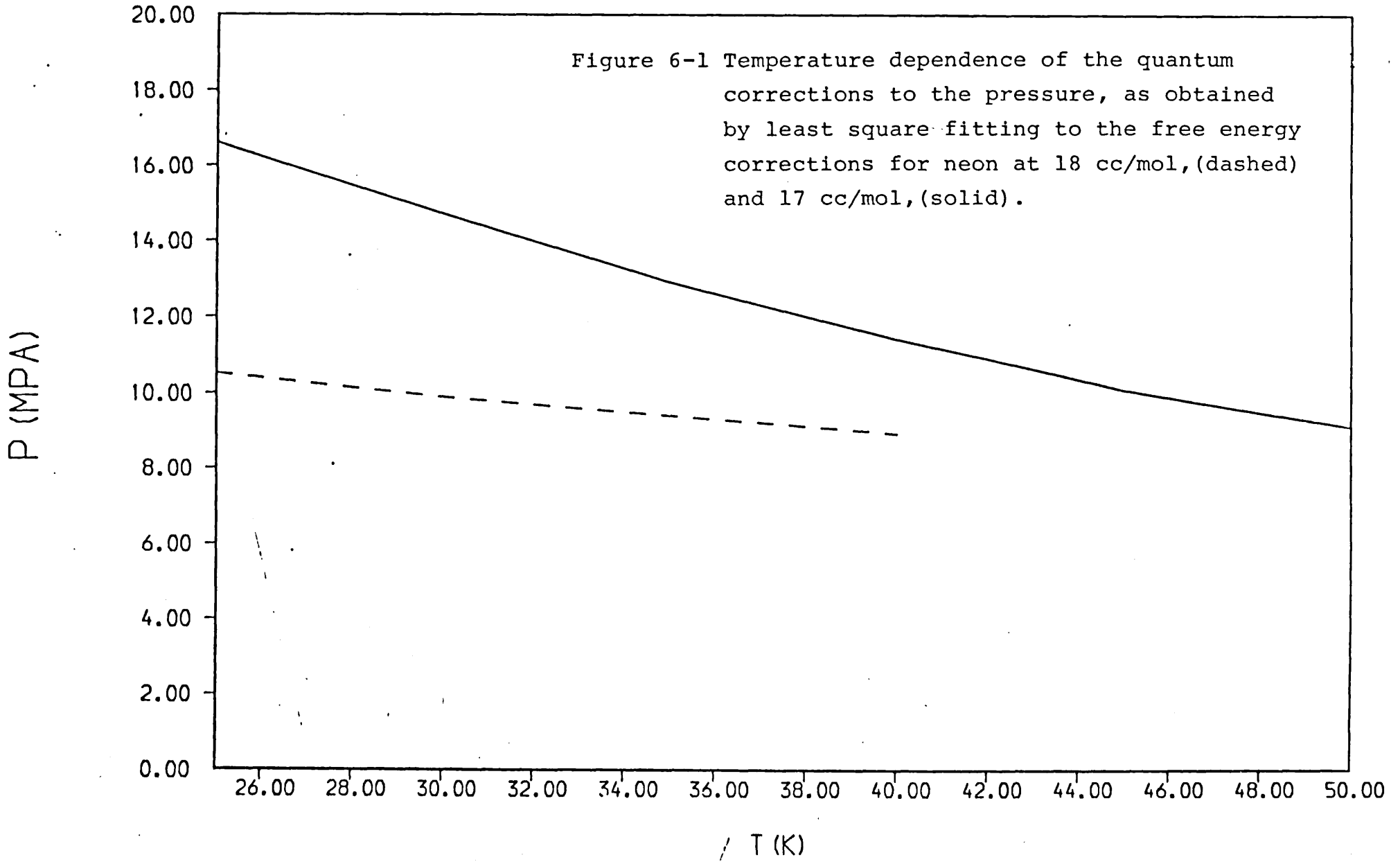

Figure 6-1 Temperature dependence of the quantum corrections to the pressure, as obtained by least square fitting to the free energy corrections for neon at 18 cc/mol,(dashed) and 17 cc/mol,(solid).

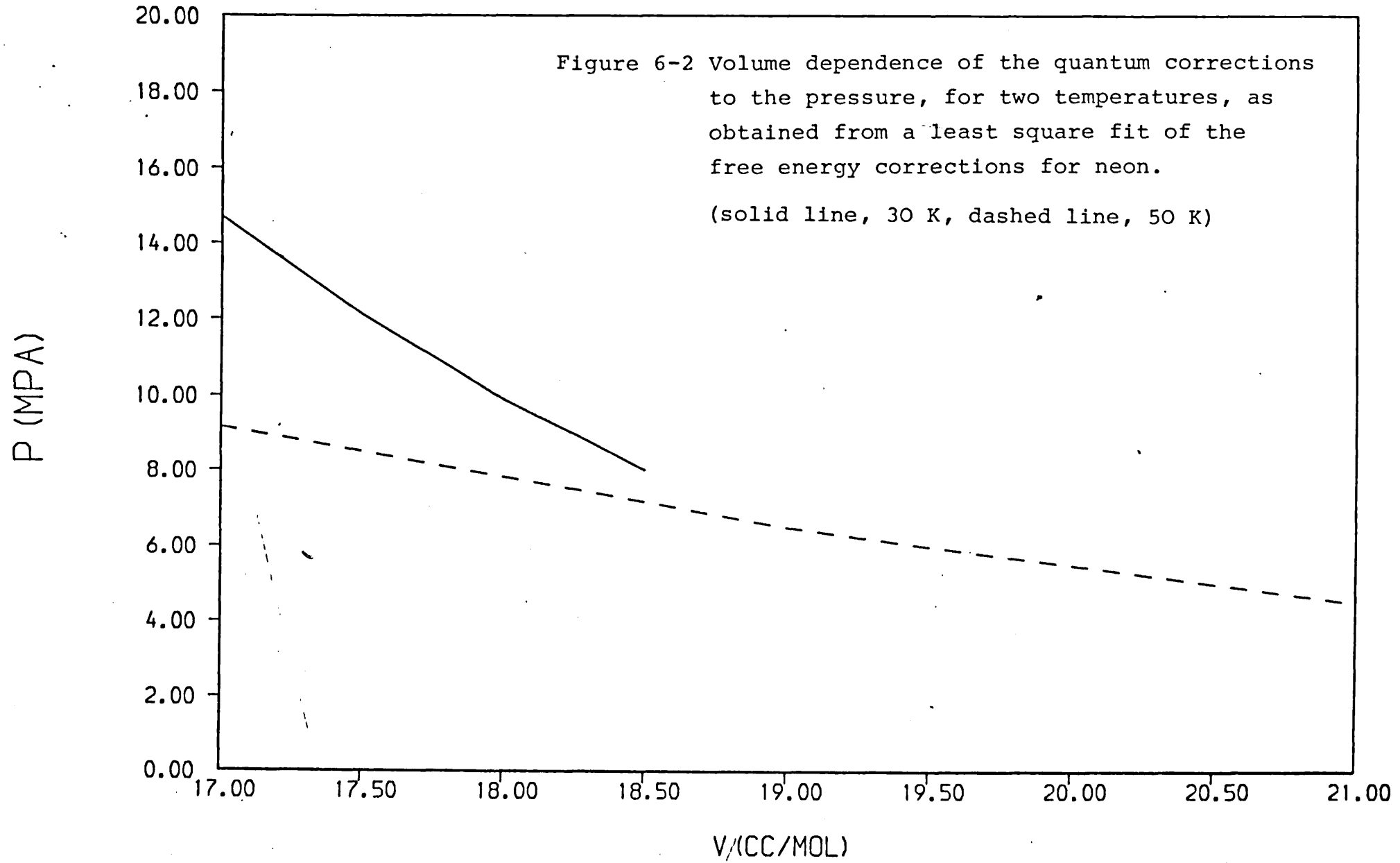

Figure 6-2 Volume dependence of the quantum corrections to the pressure, for two temperatures, as obtained from a least square fit of the free energy corrections for neon.

(solid line, 30 K, dashed line, 50 K)

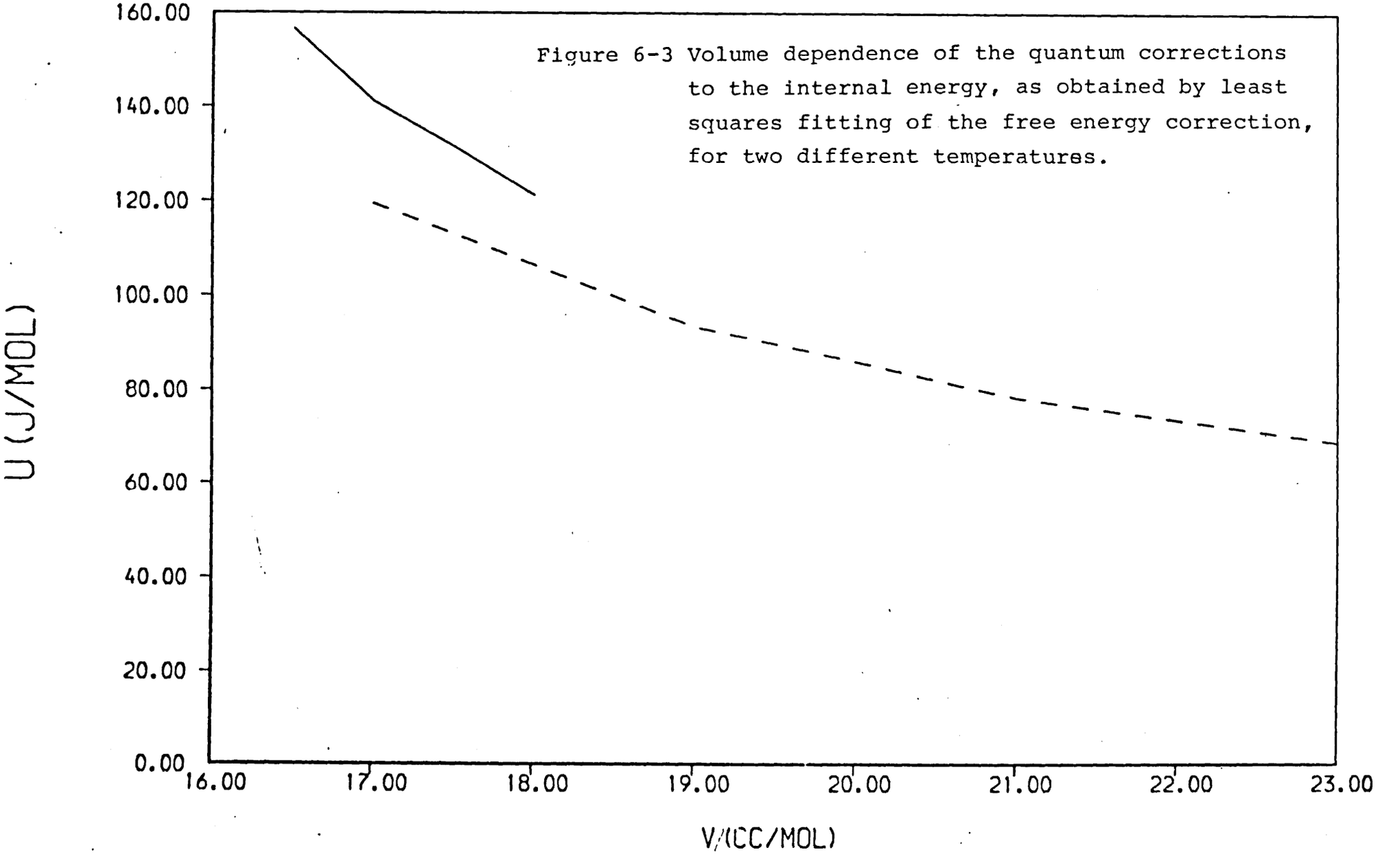

Figure 6-3 Volume dependence of the quantum corrections to the internal energy, as obtained by least squares fitting of the free energy correction, for two different temperatures.

The effective potential approach used in chapter 4 has the advantage that the radial distribution function can be calculated, exactly as in a classical simulation. Unfortunately, a classical simulation must also be carried out if any comparison is to be made. The method gives no details of the kinetic energy average, which has been assumed to be 3RT/2 where necessary, as in the pressure calculation.

The use of the effective potential in place of its classical analogue in an otherwise unmodified simulation is not entirely correct, of course. The partition function is given by the usual expression

$$Q = \int \exp(-\beta V_{eff}(\underline{r})\ d\underline{r}$$

and then the internal energy is given by

$$U = kT^2 \frac{\partial \ln Q}{\partial T}$$

$$= \frac{kT^2}{Q} \frac{\partial Q}{\partial T}$$

$$= \int V_{eff}(\underline{r})\ \exp(-\beta V_{eff}(\underline{r}))d\underline{r}$$

$$- T\int\{\frac{\partial}{\partial T} V_{eff}(\underline{r})\}\exp(- V_{eff}(\underline{r}))\ d\underline{r}$$

The last term here does not vanish, since the effective potential is temperature dependent. There is thus a term in the internal energy that is omitted if the classical formalism is used. A calculation for neon using the Gaussian potential gave 86.2 $Jmol^{-1}$ for this contribution, which is not negligible. Interestingly, the free energy correction for the same state point, as obtained from the mean square force, was 86.1 $Jmol^{-1}$. It is thus possible to calculate the corrections using the effective

potential method, but not by simply replacing the usual potential by its effective analogue.

Table 6.2 shows the differences, (quantum-classical), for the potential energy and pressure, ΔPE, and ΔP, as obtained from Tables 2.2 and 4.1. Also shown is the term in $T(\partial \Delta A/\partial T)$, which can be identified as the correction to the internal energy due to the potential, (9). These are very inaccurate figures, and should not be taken as more than qualitative results. Even so, the agreement between the effective potential method and the Wigner expansion is reasonable. In the case of helium, the effective potential leads to an average potential energy that is considerably more positive than might be expected from the method of Stratt and Miller, but in agreement with the free energy corrections, as far as any numerical comparison can be made.

The radial distribution functions obtained for the effective potentials show, especially for helium, but to a lesser extent also for neon, a shift in the position of the first maximum compared with the classical result. The peak is shifted to larger distance, which is hardly surprising in view of the difference between the classical and effective parameters. As can easily be seen from (4.14), the parameters in the gaussian potential are all reduced to obtain the effective potential, which has the effect of reducing the well depth, and increasing the range of the potential. Both of these changes reflect the known repulsive nature of the quantum effects.

Table 6.2 Quantum-classical differences obtained by Monte Carlo simulation using effective and classical potentials, (Tables 2.2,4.1) compared with $-T\partial\Delta A/\partial T$, from Table 6.1.

V ($ccmol^{-1}$)	T (K)	ΔPE ($Jmol^{-1}$)	ΔP (MPa)	$-T\partial\Delta A/\Delta T$ * ($Jmol^{-1}$)
16.5	25	47	16.0	
	30	43	15.5	50.7
	35	60	20.0	55.0
	40	44	15.6	54.0
17.0	25	54	17.2	
	30	48	16.5	43.8
	35	41	13.6	48.0
	40	45	13.0	47
17.5	25	57	18.3	
	30	33	9.2	39.6
	35	37	12.4	43.4
	40	44	14.1	41.6
18.0	25	50	13.6	
	30	44	12.1	37.2
	35	30	6.3	41.0
	40	36	9.5	40.4
18.5	25	44	11.3	
	30	34	10.2	36.3
	35	31	6.3	40.2
	40	30	6.5	38.0

* See table 6.1b for this data.

The height of the first peak is increased by this method, which is not the result expected in consequence of all previous work on the subject. However, there are two effects involved, which must be separated carefully. Classically, increasing σ at constant volume will increase the height of the peak. Decreasing σ, however, means that atoms can penetrate further into the repulsive region, in distance terms, for a given temperature. This last effect will tend to broaden and shorten the peak. There are thus two opposing effects, and in approximate treatments of this kind it is not clear that both will be correctly included.

The method of Stratt and Miller differs from the other methods described in that the kinetic energy is estimated, (by a Monte Carlo method!!), although the computational effort required is substantial, compared with the other methods. As a consequence of this computational limitation, the results obtained are not as accurate as the classical results, and so no useful numbers can be found by looking at the differences between the classical and quantum data. The quantum corrections are of the order expected from the other methods, but beyond this nothing can be said.

The radial distribution functions again show a shift in the position of the first peak, to larger separations, and now the peak height is reduced, albeit slightly. The results obtained for helium are quite striking, and very different from those obtained using the effective potential method. (Compare figs. 4.2,4.5).

The fourier series method is even more expensive, and the results quoted were obtained from exceedingly short simulations, as can be seen from the level of noise in the radial distribution functions,(Fig. 4.8). They show that the method might be useful, especially if the Monte Carlo algorithm were improved, possibly using some more refined form of importance sampling.

The wavepacket methods described in the previous chapter have produced sufficient results to justify further development. The extension to more realistic potentials, possibly including coulomb interactions, (and, even more remotely, to diatomic systems), might lead to many very interesting results.

The first method, based on an expansion of the potential, is valid only when this expansion is accurate,i.e., when the potential is essentially harmonic. This is true for solids at very low temperatures, with the exception of helium, for which no temperature is sufficiently low! The method may find some application for the study of such low-temperature systems, especially if extended to deal with mixtures, or molecular solids.

The second method, using a variational approach, is very much more powerful, although correspondingly harder to implement. The potential energy expectation here is interesting, as it is not strictly a pairwise additive function, even if the potential itself is, because of the complicated interdependence of the wavepacket width parameters. A small simulation has bee carried out for a system of two atoms, and the potential energy expectation value plotted as a function of their separation, along

with the original potential used, (Fig. 6.4). The same potential is shown in Fig. 6.5, along with its effective analogue, as a comparison. The effective potential is everywhere greater than the original, whereas the result obtained using the wavepacket is less than the original for small separations. This property will clearly solve the problem with the effective potential, as described above.

The method is completely stable and produces results in very good agreement with the Monte Carlo methods. For comparison, Table 6.3 gives results obtained for one neon state point, using the Gaussian potential. This case is not handled at all well by the method of Stratt and Miller. All of the methods lead to a potential correction of the order of 30 J/mol, and a kinetic energy correction of the order of 70-100 J/mol. This agreement is extremely good.

The possibilities for future development of this method are considerable. It can be extended to use other potentials, other forms of wavefunction, etc. One of the most interesting possibilities would be to replace the wavepackets used here, with time dependent parameters, by linear combinations of wavepackets with fixed centres and widths, the coefficients being time dependent. Such a scheme would allow proper handling of tunnelling, in a way not possible in the method used here.

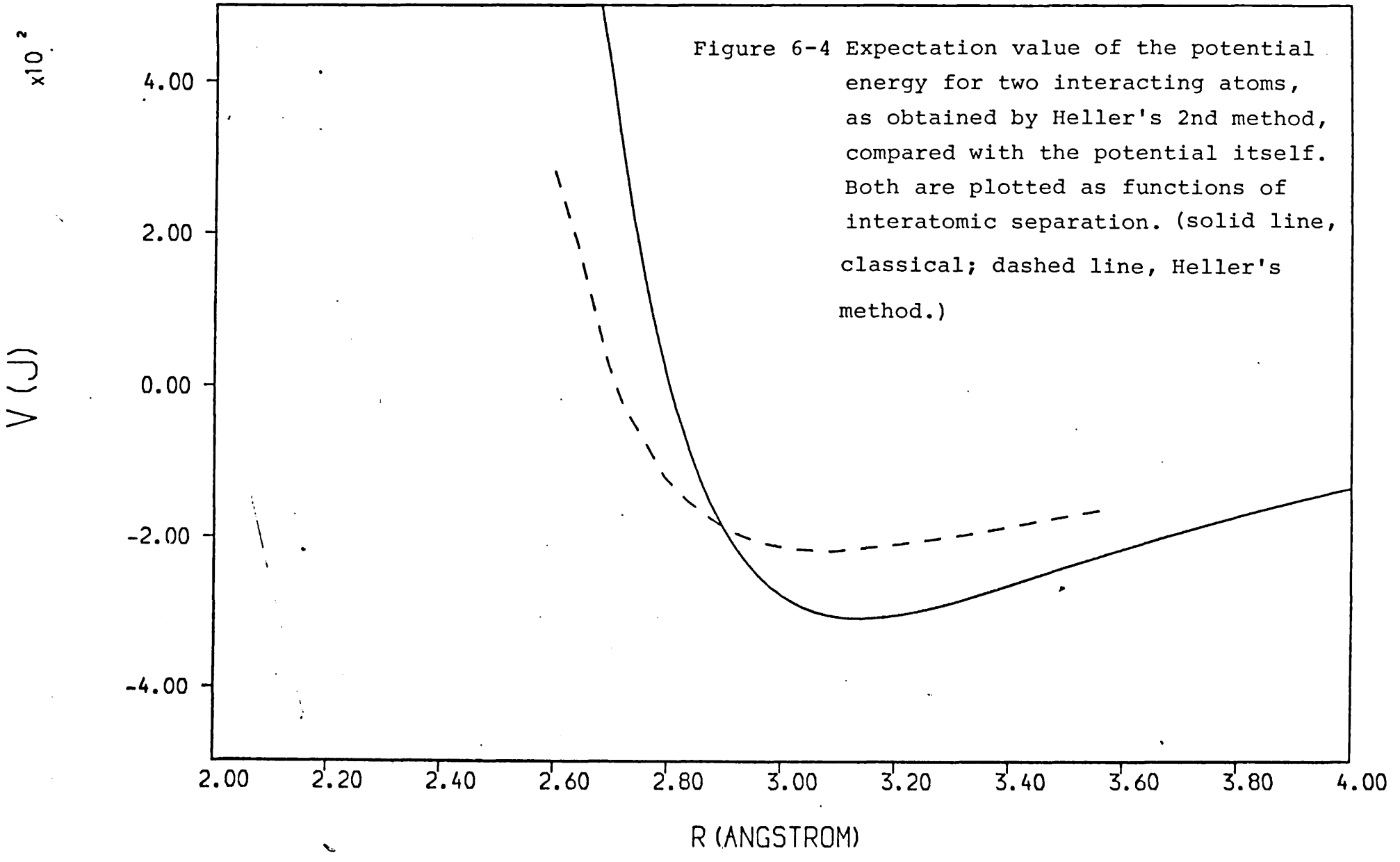

Figure 6-4 Expectation value of the potential energy for two interacting atoms, as obtained by Heller's 2nd method, compared with the potential itself. Both are plotted as functions of interatomic separation. (solid line, classical; dashed line, Heller's method.)

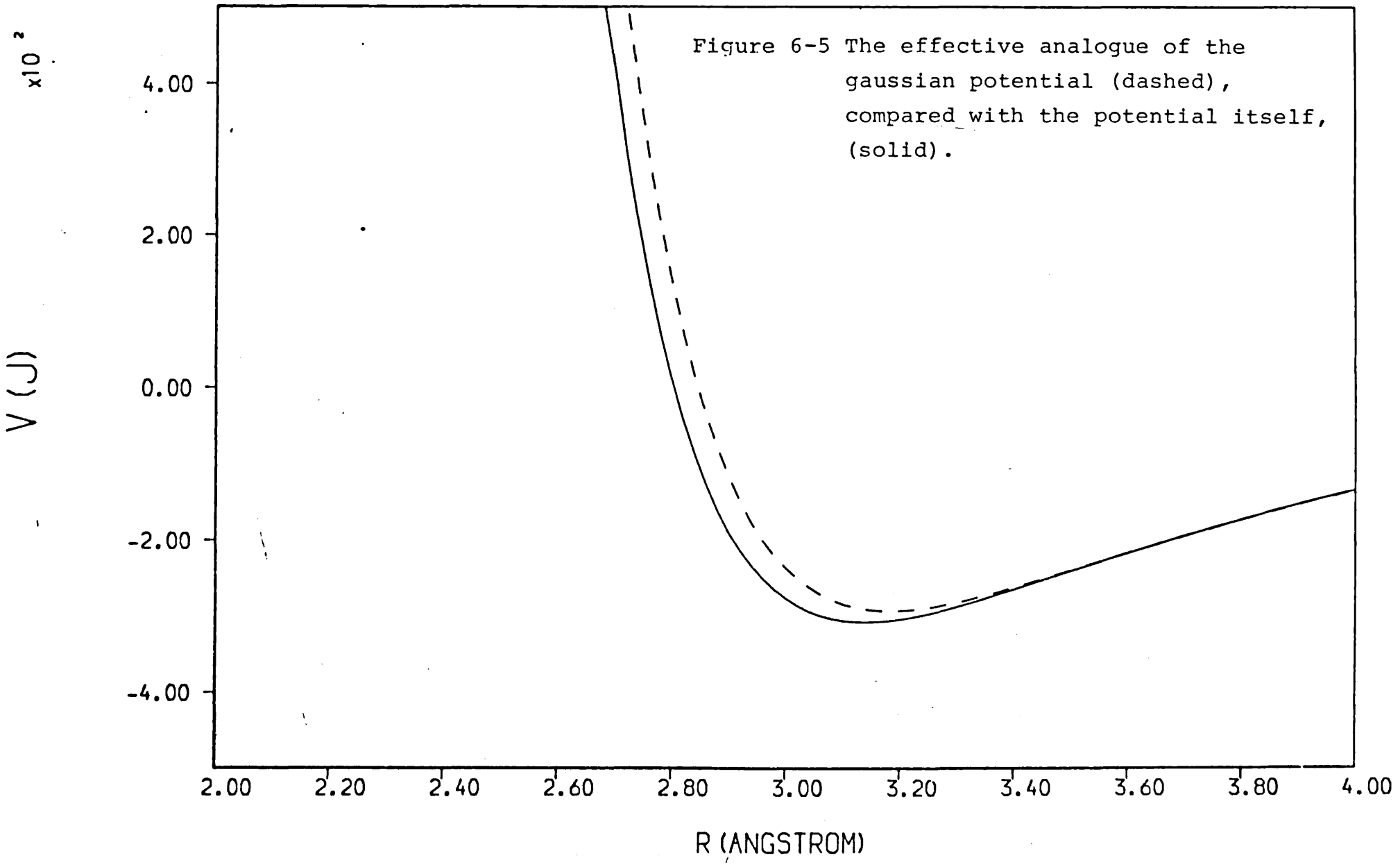

Figure 6-5 The effective analogue of the gaussian potential (dashed), compared with the potential itself, (solid).

Table 6.3 Results obtained for neon, using the gaussian potential, by various methods. (T = 40K, V = 18.5 cc/mol).

Method	N	PE	KE	P	ΔPE	ΔKE	ΔP(MPa)
classical	108	-1341	498	17.2	-	-	-
effective	108	-1311	-	23.7	+30	†	+6.5
Wigner expansion					+39	70	+7.9
Stratt-Miller	32	-1329	484	17.5	+10	-10	+0.3
Heller 2*	32	-1309	598	-	+32	+100	-

† Not calculated at this state point, but expected to agree with Wigner expansion figure.

* Temperature not defined in this method, comparison not exact!

6.2 Other possibilities:-

There are a number of approaches to the inclusion of quantum effects in simple models of liquids that have not been explored in this work, because they are not simulation based methods. Perhaps the most interesting of these, since it is related to the path integral in a quite obvious way, is that of Klemm and Storer (32).This essentially is an iterative method based on (4.6). These authors, and others since, (see eg. 33), have dealt with a two body problem, involving only 1-dimensional integrals, and extended the results to N-body problems by defining an effective potential V_{eff}:

$$g(r) = \exp -\beta V_{eff}(r,\beta)$$

where g(r) is the density-independent part of the pair correlation function. The results obtained are comparable with those given in this work. Given such an effective potential, the problem becomes equivalent to a classical one, and can be solved by simulation, or by use of the various integral equation methods (34) in precisely the same fashion as a classical problem. In (33) g(r) is taken as the two body Slater sum.

The solution of the two-body problem reduces to a series of matrix squaring operations, each halving the temperature. The method cannot be generalised to more particles, as the repeated numerical integration implicit in (4.6) is then impossible. The relationship between this method and path integrals is discussed in (35), where the method is applied to the two-body Coulomb problem.

Given the potential, whether effective or not, the thermodynamic properties can be obtained by the use of various approximate integral equation theories, as well as computer simulation. The approximations made in these theories can only be tested by comparison with the exact (in principle, at least!) simulations. There are two main integral equations, Percus-Yevick and Hypernetted-chain . These will be referred to as the PY and HNC equations. Both relate the radial distribution function $g(r)$ to the pair potential $u(r)$, but involve another unknown function as well. The Ornstein-Zernicke equation also relates these three functions:-

$$h(r_{12}) = c(r_{12}) + \rho \int h(r_{13}) c(r_{23}) \, d\underline{r}_3 \qquad (6.1)$$

where $h(r) = g(r) - 1$, and this equation defines $c(r)$, the direct correlation function. Before this equation can be used to find $h(r)$, a second expression is needed, to give two equations in two unknowns. The PY equation supplies such a closure:-

$$c(r) = (1 - \exp -\beta u(r)) \, g(r) \qquad (6.2)$$

and the HNC equation supplies an alternative:-

$$c(r) = -\beta u(r) + g(r) - 1 - \log g(r) \qquad (6.3)$$

These two equations can then be solved by a variety of methods to obtain approximate $g(r)$ from $u(r)$. Once $g(r)$ is known, thermodynamic properties can be estimated by using the appropriate integrals over $g(r)$, (such as (3.6)). Dynamical properties cannot be obtained by these methods. There are extensions of this work to more accurate closures, and the two described above are not unique.

A great deal of work has been done for the ground state of both bose and fermi fluids, using these integral equations or Monte Carlo techniques identical to those in use for classical fluids. The wavefunction of the system is taken as

$$\Psi = \prod_{i<j} f_{ij}(r_{ij}) \qquad \text{bosons}$$

$$= D \prod_{i<j} f_{ij}(r_{ij}) \qquad \text{fermions}$$

where D is a Slater determinant, (of plane waves, for instance), and $f_{ij}(r_{ij})$ is a function such that the wavefunction vanishes if any two particles overlap, and tends to a constant if the particles become widely separated. The form of f is usually decided by considering the asymptotic form of the two-body wavefunction, and by requiring that the energy expectation values exist. The earliest use of the form can be traced back to Jastrow, Bijl, and Dingle, and it is frequently referred to as a Jastrow wavefunction. Usually f has an exponential form,

$$f(r) = \exp -u(r)$$

with u(r) being called the pseudopotential. The expression for quantum-mechanical expectation values is then very similar to the classical form (2.2):-

$$\langle A \rangle = \int A \exp - \Sigma u(r_{ij}) / \int \exp - \Sigma u(r_{ij}) \qquad (6.4)$$

The pseudopotential is written with a number of parameters, and the variational theorem is then used to determine the parameters which minimise the energy. The method is therefore limited to the ground state.

The integral equations can be used with little change, (36), apart from requiring the energy to be a minimum.

Monte Carlo techniques precisely as described for classical fluids can be applied to this problem. There is little point in using molecular dynamics, since the dynamical information that is so desirable classically is without meaning in this case. A recent review is given in (28, 37).

Since the variational theorem is used, the results obtainable by this method are limited to the ground state, that is zero temperature. The method also assumes the form of the pseudopotential, which is a serious problem. It has in fact been shown that the form commonly used gives results 10-15% above the true experimental ground state, and that if the wavefunction includes three-body terms, better agreement is obtained, at greater cost! A Monte Carlo method that is not restricted to the zero temperature case, and which does not assume a form for the wavefunction, has been developed over the last 20 years by M.H.Kalos, and co-workers, (38), under the name "Green's function Monte Carlo", which will be abbreviated to GFMC here. This is a general method of obtaining the solution of a certain class of integral equation, the integral representation of the Schrodinger equation being a member of this class. The Bloch equation is also a member. Consider a system of N particles, with coordinates $(\underline{x}_1,\ldots,\underline{x}_N) = \underline{X}$. Then the Schrodinger equation is

$$-\sum_i \frac{\hbar^2}{2m_i}\nabla_i^2 \Psi(\underline{X}) + V(\underline{X})\ \Psi(\underline{X}) = E\ \Psi(\underline{X}) \qquad (6.5)$$

Suppose that E is known, and negative, say -B. Write $\underline{R} = (2mB)^{\frac{1}{2}}/\hbar\ \underline{X}$,

$$V(\underline{X}) = -\lambda B W(\underline{R})$$

and thus

$$(-\nabla^2 + 1) \Psi(\underline{R}) = \lambda W(\underline{R}) \Psi(\underline{R}) \qquad (6.6)$$

(The Laplacian is 3N dimensional here). This can be transformed into an integral equation by the Green's function $G(R,R')$, which can be expressed in terms of certain Bessel functions. The Schrodinger equation then becomes, in an iterative form and for any λ_o

$$\Psi_{n+1}(\underline{R}) = \lambda_o \int G(\underline{R},\underline{R}') \; W(\underline{R}') \Psi_n(\underline{R}') \; d\underline{R}' \qquad (6.8)$$

It can be shown that this iteration is stable only if λ_o is the correct value, and that the normalisation of the Ψ_n will increase or decrease as λ_o is above or below this value. An improved estimate of λ_o can be obtained from the change in normalisation, and thus the value of B need not be known a priori. More seriously, $G(\underline{R},\underline{R}')$ may not be known explicitly. It is still possible to devise a Monte Carlo scheme to sample it, however, by relating it to the known solution of the same problem in a subdomain of the domain of the main problem. Full details are given in (28).

The extension to non-zero temperatures, (32) follows from the Bloch equation, and the finding of a suitable Green's function for it. As of 1979, the method had been implemented for two hard spheres, for which analytical answers can also be obtained. This paper includes a full description of the algorithm employed.

The method is not restricted to the systems of atoms which have been the main focus of this work.

Kalos has used a form of GFMC to calculate the ground state of the helium atom, (40). Very similar methods have been described by Anderson, (41), in application to the helium atom and H_3^+. The calculation for this last required 6-30 hours of computing on an IBM 370-3033, so the use of this method for larger systems seems unlikely, at least in the immediate future.

6.3 Conclusions:-

In this work we have shown that it is possible to include quantum mechanical effects into the computer simulation of very simple liquids and solids, using a variety of methods. With the exception of the Wigner expansion, none of these methods has been applied to many body problems previously. All agree fairly well.

The quantum corrections obtained are significant in neon, and large in helium, and can be seen to vary with both temperature and density. There are small, but still significant, differences between the corrections from the Gaussian and Lennard-Jones potentials, at a given state point, and these differences are in accord with the slightly narrower minimum of the gaussian potential giving slightly larger quantum effects.

Less work has been done for diatomic systems, with Fluorine the main system studied. The quantum effects here were again significant, although it was not possible to apply all of the methods, or to perform least squares fits of the free energy corrections.

All of the methods can be extended, more or less simply, to deal with more general potentials, such as Coulomb interactions, or more complicated systems, diatomics for instance. The wavepacket methods also offer the possibility of using different forms for the wave-function, and of obtaining time-dependent properties.

Appendix I:- Useful Integrals.

(All integrals are over $(-\infty,\infty)$, unless otherwise stated).

$$\int \exp(-\alpha r^2)\, dr = (\pi/\alpha)^{\frac{1}{2}} \tag{A.1}$$

$$\int \exp(-\{\alpha r^2 + \beta r + \gamma\})dr$$

$$= (\pi/\alpha)^{\frac{1}{2}} \exp(\beta^2/4\alpha - \gamma)$$

$$\int r^2 \exp(-\alpha r^2)\, dr = (\pi/\alpha)^{\frac{1}{2}} (2\alpha)^{-1}$$

differentiating (A.1) w.r.t α.

$$\int \exp(-\underline{r}^T \underline{\underline{\Delta}}\ \underline{r})\, d\underline{r} = (\pi^n/\det \underline{\underline{\Delta}})^{\frac{1}{2}}$$

where $\underline{\underline{\Delta}}$ is an $n \times n$ matrix. Note that this reduces to (A.1) if n=1, and to a product of such integrals if $\underline{\underline{\Delta}}$ is diagonal. $\underline{\underline{\Delta}}$ is required to be positive definite, as is the case in all applications in this work.

$$\int \exp(-\{\underline{r}^T \underline{\underline{\Delta}}\ \underline{r} + \underline{p}.\underline{r}\})\, d\underline{r}$$

$$= (\pi^n/\det \underline{\underline{\Delta}})^{\frac{1}{2}} \exp(\underline{p}^T \underline{\underline{\Delta}}^{-1}\ \underline{p}/4) \tag{A.2}$$

Note that this reduces to the forms above if n=1, or $\underline{p} = \underline{0}$. Other integrals required can easily be derived from this result by differentiating w.r.t. elements of $\underline{p}$ or $\underline{\underline{\Delta}}$.

Appendix II:- Monte Carlo Algorithms.

The usual algorithm employed in the Monte Carlo simulation of liquids, etc, is due to Metropolis et.al., (5). In recent years several alternatives have been proposed. One of these, known as "Smart" Monte Carlo, (29), has been used in some of the simulations reported above, and is here descibed briefly, along with results relating to its performance.

Consider a system of N particles, 1,...,j,...,k,...,N, interacting via a pair potential $u_{jk}(r_{jk})$. The Metropolis algorithm uses 4 random numbers, uniformly distributed in (0,1), to move one particle, j, say, and proceeds as follows:-

i) calculate $\sum_{k\neq j} u_{jk} = U$

ii) use 3 random numbers to form a displacement vector $\underline{\Delta r}$, with components uniform in $(-\mathbb{L},\mathbb{L})$, and displace j by this vector.

iii) Again calculate $\sum_{k\neq j} u_{jk} = U'$

iv) Choose a random number R in (0,1), and goto (vi) if $R < \exp(U - U')/kT$

v) restore j to its previous position.

vi) calculate the current configurational properties, and include in averages.

vii) goto (i), after changing j, appropriately.

This procedure continues until each particle has been moved many times,(typically 1000-10000 times). $\mathbb{L}$ is a parameter, and is chosen such that about ½ of the moves are accepted at step (iv).

The "Smart" method uses the forces acting on the particle being moved, and also uses normally distributed random numbers. Let the force acting on particle j be $\underline{F}$.

Then proceed as follows:-

i) Calculate U and $\underline{F}$

ii) Calculate $\underline{\Delta r} = \beta A \underline{F} + \underline{R}$

where the $\underline{R}$ is distributed according to

$$w(\underline{R}) = (4A\pi)^{-3/2} \exp(-\underline{R}.\underline{R}/4A)$$

and displace particle j by this amount.

iii) Calculate U' and F'.

iv) Choose a random number R in (0,1), and goto (vi) if

$$R < \exp(U - U')/kT \; . \; \exp(\underline{\Delta r} - \beta A \underline{F})^2/4A \; . \; \exp(-(\underline{\Delta r} - \beta A \underline{F}')^2/4A)$$

v) restore j to its previous position.

vi) change j, and goto (i).

Again the whole procedure is repeated until all particles have been moved many times. A is a parameter which is chosen to optimise the performance of the algorithm. This algorithm clearly requires a greater computational effort than the Metropolis method,(about 30% more cp time per move), but is hoped to give a more efficient sampling of phase space. If the mean square displacement $\langle \underline{\Delta r}.\underline{\Delta r} \rangle$ is used as a measure of the efficiency, then it is found that the "Smart" method is about 30% more efficient than the Metropolis algorithm, under optimum conditions, for the atomic fluids described in chapter 2. This gain almost exactly offsets the extra computing needed.

REFERENCES:-

1.-Singer,K, Nature 181,262,(1958)

2.-Hansen,J.P., McDonald,I.R., "Theory of simple liquids", Academic Press,1976, p.68

.-Brown,J.S., Proc.Phys.Soc.(London) 89,987,(1966)

3.-Binder,K, (ed) "Monte Carlo methods in statistical physics", Topics in Current Physics 7,Springer, 1979, ch. 2.

-ref. 2, p 45

4.-Hammersley,J.M.,Handscomb,D.C., "Monte Carlo methods", Methuen,1965

5.-Metropolis, et. al., J.Chem.Phys.,21,1087,(1953)

6.-Fincham,D.,Comp.Phys.Comm., 21,247,(1980)

7.-Wigner,E.,Phys.Rev.,40,749,(1932)

8.-Band,W.,Mayer,J.E.,J.Chem.Phys.,15,141,(1947)

9.-Green,H.S.,J.Chem.Phys.,19,255,(1951)

10.-Landau,L.D.,Lifshitz,E.M.,"Statistical Physics", Pergamon,1978

11.-ref 2, pp 200-206

12.-Powles,J.G.,Rickayzen,G., Mol.Phys. 38,1875,(1979)

13.-Hansen,J.P.,Weis,J-J,Phys.Rev.188,314,(1969)

14.-Glandt,E.B.,J.Chem.Phys.,74,1321,(1981)

15.-Singer,K.,et.al.,Mol.Phys. 13,1757,(1977)

16.-Feynman,R.P.,Hibbs,A.R.,"Quantum mechanics and Path Integrals",McGraw,1965

17.-Feynman,R.P.,"Statistical Mechanics",Benjamin,1972

18.-Marinov,M.S.,Phys.Rep.60(1),(1980)

19.-Young,R.A.,Phys.Rev.Lett.,45,638,(1980)

" ,Phys.Rev.23A,1498,(1981)

20.-Stratt,R.M.,Miller,W.H.,J.Chem.Phys.,67,5894,(1977)

21.-Chandler,D.,Wolynes,P.G. " 74,4078,(1981)

. Chandler, et.al. " 75,1347,(1981)

22.-Barker,J.A., " 70,2914,(1979)

23.-Heller,E.J., " 62,1544,(1975)

24.-Heller,E.J., " 64, 63 ,(1976)

25.-Furry,W.H., in "Lecture notes in Theoretical Physics", V,(1962)

26.-Hansen,J.P.,Phys.Rev.,172,919,(1968)

27.-ter Haar,D.,"Selected problems in Quantum Mechanics", London,1962

28.-Binder,K. (ed.), ref.3 above, ch.4

29.-Berne,B.J.,Rao,M.,J.Chem.Phys.,71,129,(1979)

Doll,J.D.,Friedman,H.L.,Rossky,P.J., J.Chem.Phys.,69,4628,(1978)

30.-Hirschfelder,J.O.,Curtiss,C.F.,Bird,R.B.,"Molecular theory of gases and liquids",Wiley,1954.

31.-McClachlan,A.D.,Mol.Phys.8,39,(1964)

32.-Klemm,A.D.,Storer,R.G.,Aust.J.Phys.,26,43,(1973)

33.-Bruch,L.W.,et.al.,J.Low.T.Phys.,35,185

. Weres,O.,J.Chem.Phys.,64,840,(1976)

34.-Andersen,H.C.,Ann.Rev.Phys.Chem.,(1975),145

Barker,J.A.,Henderson,D.,Rev.Mod.Phys.,48(4),(1976)

35.-Storer,R.G.,J.Math.Phys.,9,964,(1968)

36.-Campbell,C.E., in "Progress in liquid Physics", Croxton,(ed),Wiley,1978, pp 213-308

37.-Kalos,M.H.,Nucl.Phys.,A328,153,(1979)

38.-Whitlock,P.A.,Kalos,M.H.,et.al.,Phys.Rev.,B19,5598,(1979)

39.-Whitlock,P.A.,Kalos,M.H.,et.al.,J.Comp.Phys.,30,361,(1979)

40.-Kalos,M.H. " 2,257,(1967)

41.-Anderson,J.B.,J.Chem.Phys.,73,3897,(1980)